INFLAMMATORY MEDIATORS PROMOTE THE DEVELOPMENT AND PROGRESSION OF METAPLASIA IN THE STOMACH

By

Christine Pope Petersen

Dissertation

Submitted to the Faculty of the

Graduate School of Vanderbilt University

In partial fulfillment of the requirements

For the degree of

DOCTOR OF PHILOSOPHY

in

Cell and Developmental Biology

May 2016

Nashville, TN

Approved:

James R. Goldenring, MD, PhD

David Bader, PhD

Robert Coffey, MD

Barbara Finglton, PhD

Chin Chiang, PhD

TABLE OF CONTENTS

Page

ACKNOWLEDGEMENTS v

LIST OF TABLES viii

LIST OF FIGURES ix

Chapter

I. MODELS OF GASTRIC FUNDIC NEOPLASIA AND INFLAMMATION 11
Definition of hyperplastic, metaplastic and pre-neoplastic lineages in mouse stomach models 11
Oxyntic atrophy 12
Foveolar hyperplasia 12
Mucus neck cell hyperplasia 13
Spasmolytic polypeptide expressing metaplasia 13
Intestinal metaplasia 14
Invasive submucosal glands 15
Dysplasia 15
Adenocarcinoma 15
Human Disease inception and progression 18
Murine models of gastric neoplasia 19
Helicobacter infection 19
Acute drug induced models of SPEM 20
DMP-777 20
Tamoxifen 21
L635 21
Gastrin genetic models 22
INS-GAS 22
Gastrin KO 22
Genetic models of parietal cell loss 23
Claudin 18 KO 23
KLF4 KO 24
H/K-Cholera Toxin 24
Models of signaling pathway activation 25
MAPK/ERK 25
TGFb and BMP 26
H/K Noggin 27
EGFR 27
Immune-mediated pre-neoplastic mouse models 28
H/K-ATPase-IFNg Transgenic 28
Hip1r and IFNg Double KO 29
TxA23 29
H/K-ATPase Il1b Transgenic 30
SDF1 Transgenic 30
K19-C2mE 31
Gan 32

Exogenous IL-11 32
Exogenous IL-33 33
Conclusions 33
Aims 35

II. MACROPHAGES PROMOTE THE PROGRESSION OF SPASMOLYTIC POLYPEPTIDE EXPRESSING METAPLASIA (SPEM) AFTER ACUTE PARIETAL CELL LOSS 36
Introduction 36
Methods 39
Treatment of Animals 39
L635 Treatment 39
DMP-777 Treatment 40
Immunohistochemistry 40
Quantitative real-time PCR 41
Quantitation of proliferative SPEM and immune cells 42
Results 43
Rag1 and IFNg knockout mice develop acute proliferative SPEM 43
Neutrophil-depleted mice develop acute proliferative SPEM 47
Macrophages are involved in the development of acute L635-induced SPEM 51
DMP-777-induced SPEM does not recruit macrophages 57
Macrophages in L635-treated mice express M2 polarization markers 57
M2 macrophages increase in human SPEM and intestinal metaplasia 61
Discussion 63

IL-33 REGULATES METAPLASIA AND MACROPHAGE POLARIZATION IN THE STOMACH. 70
Introduction 70
Methods 73
Mice 73
Drug treatment 73
Macrophage isolation and fluorescence-activated cell sorting (FACS) 73
Quantitative real-time PCR analysis 74
RNA sequencing 75
Immunocytochemistry 77
Image Quantitation 78
Cytokine Array 78
Results 78
Analysis of macrophage transcriptome from acute SPEM models 78
IL-33 is necessary for SPEM induction 84
Loss of M2-polarized macrophages in L635-treated IL33KO mice 89
IL-33-positive macrophages in human SPEM and intestinal metaplasia 94
Discussion 96

I. CONCLUSIONS AND FUTURE DIRECTIONS 101
Conclusions 101
Future Directions 105
IL-33-related studies 106
Th2 cytokines in the induction and intestinalization of SPEM 107
IL-25 and Innate lymphoid cells (ILCs) 109

REFERENCES 111

ACKNOWLEDGEMENTS

I first must thank my mentor for the past five years, Dr. James R. Goldenring. I am forever grateful for Jim's guidance, training, support, and friendship. He provided insights and alternatives when I was lost, and gave me space when I found my stride. Quite literally, Jim was the best mentor I could have possibly imagined. I can honestly say these past five years have been the most fun I've had in science, ever. As a result of his leadership, I feel that I possess the tools, courage, confidence and knowledge to be successful. I will always follow your lead to embrace big questions and think big ideas. Thank you Jim for an amazing PhD experience, and helping me fall deeper in love with discovery.

I would also like to thank my committee members: Dr. Barbara Fingleton, Dr. Robert Coffey, Dr. Chin Chiang, and my chair, Dr. David Bader. Since the Qualifying Exam when I brought parietal cells, chief cells, and SPEM cell cookies (many thanks to Dr. Victoria Weis) and Dr. Coffey said, "shouldn't we eat the Parietal Cells first?", we have had wonderful rapport. Thank you for your insights, constructive criticisms, and reflections. I would not be the scientist I am today without your guidance. I must further thank Dr. Barbara Fingleton for your collaboration on my first paper. Barbara, you so patiently helped me work through data, tailor methods and approaches, and always made sure my reasoning was sound! I was also very fortunate to have Dr. Robert Coffey in the lab next door and part of the Epithelial Biology Center (EBC). Bob, thank you for your feedback and guidance throughout the years!

Not only have I been so fortunate with having wonderful mentors around, but also a wonderful lab environment. Coming to work each day in the Goldenring Lab was amazing. Every person, past and present, was always willing to help out, aide in a new experiment, find that missing tube, or be an extra pair of hands when time was tight. The Gastric Group in particular was instrumental in my education. To the past members: Dr. Victoria Weis, Dr. Josane Sousa and Dr. Ki Taek Nam. Tori, thank you for entrusting me to take the project over!

Your friendship from science to children is very dear to my heart. Josane, I will never look at quantitative PCR in the same light again! You taught me how to be a shrewd scientist and to always be objective. Ki Taek, learning mouse gastric pathology from the maestro was an honor! I am especially grateful to the current Gastric Group members: Dr. Eunyoung Choi and Dr. Takahiro Shimitzu. Eunyoung, you are such a wonderful mentor! From sitting around dreaming up the next great experiment, to finding out ways to optimize the current experiment, I know I am a much better scientist because of you influence. I cannot wait to collaborate in the future. Thank you for keeping me optimistic when things looked down and laughing when things seem impossible! I would also like to thank Cathy Caldwell and Lynne Lapierre. Cathy, you have always been there to help me troubleshoot uncompromising SPEM or Chief cell lines, and to talk to about everything under the sun. Lynne, thank you for your never-ending support and good nature around lab! I must also thank Dr. Joseph Roland. Joe, I appreciate the never ending chocolate, assistance in getting the best pictures (ever), and for pushing me harder than most. Thank you to MSTP student Dr. Byron Knowles for your amazing friendship and laughter that always brightened my day. Thank you to new members Dr. Cameron Schlegel and Dr. Amy Engevic, I am so happy that we were able to have our time cross over even for the little bit that it has. You two ladies inspire me and I have thoroughly enjoyed our conversations. Finally, I have had wonderful friends along the way! Thank you to Dr. Emily Poulin, Alina Starchenko, Elizabeth Ennis, and Dr. Yuping Yang. And a thank you to all members of the Goldenring Lab to whom I will always hold in such a dear place.

And most importantly, the biggest thank you to my family. To my dearest husband Alec, I could not have made it through these past 9 years without you. Through your deployment in Afghanistan, starting our family with sweet Penny, beginning medical school, and to the birth of our son Kellan- life is full and wondrous with you and I would not change a single minute. I cannot wait for our next adventure, wherever that may be. I love you the mostest. To my son Kellan, thank you for making me a mother and showing me a deeper love than I ever imagined.

Your smiles, laughs, and kisses each day bring a deeper meaning to everything in my life. To Penny, for being my therapy dog more times then I can count! To my in-laws, Ron and Diane, thank you for always supporting the family and being there for me. To my parents, for always knowing I would get here one day, in my own time, in my own way, and believing in me all along the way. I love you mom and dad. To my siblings, Jennifer and Brenton, you guys are everything to me. I am forever grateful for the experiences and mentorship during my time here, and I feel that the Vanderbilt culture has truly shaped the kind of scientist I have become.

Finally, I would like to acknowledge the funding sources. My studies were supported by grants from the Department of Veterans Affairs Merit Review Award, NIH Grant RO1 DK10332, and my F31 NRSA DK104600. Furthermore the shared resources provided by the Vanderbilt-Ingram Cancer Center and the Vanderbilt Digestive Disease Center has been an immense help, including the Vanderbilt Flow Cytometry Core (Dave Flaherty) and TPSR.

LIST OF TABLES

Table Page

1. Markers used to define different stages of metaplasia in the gastric corpus 16

LIST OF FIGURES

Figure Page

1. The progression of gastric neoplasia in mice 17
2. Effective parietal cell loss after L635 administration in wild type, Rag1KO and IFNγKO mice 44
3. Wild type, Rag1KO and IFNγKO mice have similar recruitment of neutrophils and macrophages after L635-treatment 45
4. Wild type, Rag1KO and IFNγKO mice develop acute proliferative SPEM after L635-treatment 46
5. Effective neutrophil depletion did not significantly alter macrophage recruitment 49
6. Neutrophil-depletion in mice does not alter the development acute advanced proliferative SPEM after L635 treatment 50
7. Clodronate treatment reduced the influx of macrophages into the fundic mucosa after L635 treatment 52
8. Macrophage depletion inhibits the development of proliferative SPEM following L635 treatment 54
9. Macrophage depletion does not affect SPEM cell proliferation or F4/80-positive cells in DMP-777-treated mice 56
10. Macrophages are M2 polarized in L635-treated mice, but not in DMP-777-treated mice 59
11. M2 marker transcripts are markedly increased in L635-treated mice. 60
12. M2 macrophage infiltration in human SPEM and IM. 62
13. F4/80 positive cells isolated from acute SPEM models. 80
14. RNA sequencing of F4/80 positive cells in L635 and DMP-777-treated mice show a macrophage-enriched population 81
15. Transcriptome analysis of macrophages associated with SPEM and intestinalized SPEM 82
16. Transcriptome analysis of macrophages associated SPEM 83
17. IL-33 is necessary for SPEM induction 86

18. Mist1 expression is still present in L635-treated IL33KO mice that do not develop SPEM 88

19. IL33KO mice treated with L635 do not develop proliferative or intestinalized SPEM after acute parietal cell loss 90

20. IL33 is required for macrophage M2 polarization after acute parietal cell loss ... 92

21. IL33 is required for M2a macrophage polarization and the production of Th2 cytokines 94

22. Macrophages associated with human SPEM and intestinal metaplasia are IL-33 positive 95

Chapter I
MODELS OF GASTRIC CORPUS NEOPLASIA AND INFLAMMATION

Adapted From: Petersen, C. P., Mills, J.C. and Goldenring J.R. Murine models of gastric fundic neoplasia and inflammation.

Gastric adenocarcinoma leads in worldwide cancer-related deaths. Poor clinical outcomes result from the lack of early clinical indicators. Insights into the progression of pre-neoplastic processes that promote gastric cancer are therefore a necessity. Murine models are currently used to understand the molecular mechanisms driving metaplasia in the stomach towards cancer. At the outset however, it should be noted that no mouse models have produced true tumor masses in the body of the stomach that lead to local or distal metastasis. Therefore, the general utility of mouse models lies in the evolution of precancerous lesions and the analysis of mechanisms that are responsible for the induction and presence of metaplasia. The following discussion will examine models of gastric neoplasia in mice and the insights provided into the origin and progression of human disease.

1. Definition of hyperplastic, metaplastic and pre-neoplastic lineages in mouse stomach models:

There is considerable variability in the nomenclature used to assign pathology changes observed in the gastric mucosa. This has resulted in poor understanding of the cellular processes that lead to adenocarcinoma. Therefore in effort to standardize the nomenclature, we impart specific biomarkers that positively identifies key epithelial changes that occur during the progression of metaplasia. This adoption of terminology that specifies certain pathology features is necessary to then accurately classify cellular changes at key stages. Described below are terms used to describe different observed states in the metaplastic process. Figure

1 illustrates these specific changes in the gastric mucosa during the development and progression of metaplasia. Furthermore, Table 1 provides specific biomarkers that differentiate the different stages of metaplasia.

Oxyntic atrophy.

The loss of parietal cells, also known as oxyntic atrophy, is considered the *sine qua non* for the development of metaplasia in the human stomach (Eidt et al., 1996). In humans and mice, chronic *Helicobacter* infection leads to loss of parietal cells in the corpus of the stomach (Fox et al., 1996; Fox et al., 2003; Wang et al., 2000b; Wang et al., 1998). Oxyntic atrophy can be diagnosed on hematoxylin and eosin staining based on the loss of eosinophilic parietal cells as well as hematoxylin-positive chief cells (Figure 1 A*ii*). More definitive analysis of these lineages can be made using specific markers for these lineages including H/K-ATPase antibodies for parietal cells and antibodies against either intrinsic factor or the transcription factor Mist1 for chief cells (Figure 1 B*ii)*.

Foveolar hyperplasia.

Foveolar hyperplasia represents an expansion of the surface mucous cell compartment. It is usually associated with an increase in proliferation in the normal neck progenitor cells (Nomura et al., 2005b) (Figure 1 *ii*). Increases in foveolar hyperplasia are associated with elevations in gastrin (Poynter et al., 1986), or TGF-alpha (as observed in human Menetrier's disease) (Dempsey et al., 1992a). Oxyntic atrophy and resulting loss of acid secretion is usually associated with varying levels of foveolar hyperplasia commensurate with the level of hypochlorhydria.

Mucus neck cell hyperplasia.

Mucous neck cell hyperplasia or mucous metaplasia connotes and expansion of the mucous neck cells in the middle region of corpus glands in the stomach (Figure 1 *ii*). Mucous metaplasia has been reported in a number of settings with alterations of ion channels or endocrine cell influences (Lee et al., 2000). The expansion of mucous neck cells is not associated with proliferation within the mucous neck cell population, but rather appears to reflect either an increased production of mucous neck cells from progenitors or a slowing of differentiation of mucous neck cells into chief cells. Proliferative (Ki67 positive) GSII–lectin positive cells is indicative of mucus neck cell hyperplasia (Figure 1B*ii*).

Spasmolytic Polypeptide-expressing Metaplasia (SPEM).

Loss of parietal cells in the stomach leads to transdifferentiation of chief cells into SPEM (Figure 1*iii*). This lineage was originally characterized by its expression of spasmolytic polypeptide, now designated TFF2 (Schmidt et al., 1999b). This lineage can often be identified by pink staining in Diastase-resistant-PAS staining, compared with the purple staining in surface mucous cells (Goldenring and Nomura, 2006). This lineage appears to overlap with previously-described pathologies including pseudopyloric metaplasia (Hattori et al., 1982) and Ulcer-associated lineages (UACL) (Wright et al., 1990). Several markers of SPEM have been characterized that are not present in the normal stomach, including HE-4 (WFDC2) (Nozaki et al., 2008b) and CD44variant (Wada et al., 2013). Some studies have noted the identification of proliferative cells expressing both gastric intrinsic factor and TFF2 along with Ki-67 as reflective of SPEM induction (Weis et al., 2013b) (Figure 1B*iii*). Nevertheless, it is clear in a number of models that morphological apparent SPEM lineages can often show varying levels of intestinalizing transcripts including MAL2, CFTR and Muc4 (Weis et al., 2014; Weis et al., 2013b). This intestinalized SPEM is morphologically identical to other SPEM lineages and can

only be recognized by immunostaining with specific intestinal markers or Ki67 positive SPEM cells (Figure 1 *iv*) (Weis et al., 2013b).

Intestinal Metaplasia.

While both SPEM and intestinal metaplasia are present in the stomachs of humans with atrophic gastritis secondary to *H. pylori* infection (Lennerz et al., 2010), few instances of documented intestinal metaplasia exist in mouse models. In human stomach, Alcian blue staining of intestinal type goblet cells is often used to define intestinal metaplasia. However, in mice, deep antral mucous cells are strongly Alcian blue positive and SPEM is often Alcian blue positive (Goldenring and Nomura, 2006). Thus, more specific markers are required. MUC2 and TFF3 labeling of cells with specific goblet cell morphology provides the most specific indication of intestinal metaplasia (Choi et al., 2015; Goldenring et al., 2010). Notably, expression of TFF3 and Muc2 has been reported in lineages with immunocytochemical evidence of SPEM, so there may be intermediates of intestinalized SPEM that reflect evolution of metaplastic phenotypes (Varon et al., 2012; Weis et al., 2013b). Expression of nuclear Cdx1 and Cdx2 has been noted in human intestinal metaplasia (Kang et al., 2011), but has been less apparent in mouse models.

Invasive submucosal glands.

The presence of glands penetrating into the submucosa (sometimes referred to as gastritis cystica profunda), is usually considered a dysplastic morphology in humans, where the presence of GCP has been noted decades after gastrojejunostomy for ulcer disease and is considered a pre-neoplastic lesion (Yamaguchi et al., 2001). Intermediate levels of penetrating or invasive glands can also be observed. While this morphology has been reported in *H. pylori* infected Mongolian gerbils, recent investigations have suggested that invasive glands are reversible after eradication (Tatematsu et al., 2007). These findings place some of neoplastic

implications of invasive submucosal glands in doubt. In addition, most invasive glands are associated with TFF2 expressing mucous cells and often have less proliferation than lesions within the mucosa.

Dysplasia.

Dysplastic phenotypes are defined my cellular and glandular morphologies on hematoxylin and eosin staining. No specific markers of dysplasia exist. The interpretation of dysplasia is therefore fraught with controversy even among human pathologists. The situation is even more uncertain in mouse models where correlations with cancerous outcomes are difficult to assess since there are few instances of cancerous tumors. Thus it is difficult to build key connections between putative dysplastic morphologies and progression to cancer.

Adenocarcinoma.

In humans, cells with aberrant, invasive and metastatic characteristics are defined as adenocarcinoma. The aberrant morphologies are generally defined by patterns in hematoxylin and eosin staining including multilayered cell patterns (cribiforming) along with altered nuclear morphology and positioning. Proliferative rates are expected to be high, but metaplastic lineages also show high proliferative rates. No present studies have defined specific mutations that might define a transition to cancer.

Table 1. Markers used to define different stages of metaplasia in the gastric corpus.

MARKER	Normal Stomach	Foveolar Hyperplasia	SPEM	Intestinalized SPEM	Intestinal Metaplasia
Muc5AC	Surface Cell	Positive	Negative	Positive	Positive
UEA1	Surface Cell	Positive	Negative	Negative	Negative
Muc6	Mucous Neck Cell	Negative	Positive	Positive	Negative
GSII	Mucous Neck Cell	Negative	Positive	Positive	Negative
Intrinsic Factor	Chief Cell	Negative	Positive	Positive	Negative
Chromogranin A	Enteroendocrine Cells	Negative	Negative	Negative	Negative
HE4	Not detected	Negative	Positive	Positive	Positive
Phospho-ERK	Progenitor Cells	Progenitor Cells	Positive	Positive	Positive
CD44variant	Not detected	Negative	Positive	Positive	Positive
$Ki67^{+}$ SPEM cells	Progenitor Zone	Negative	Negative	Positive	Negative
Muc2	Not detected	Negative	Negative	Negative	Positive
TFF3	Not detected	Negative	Negative	Negative	Positive
Cdx1	Not detected	Negative	Negative	Negative	Positive
CFTR	Not detected	Negative	Positive	Positive	Positive
Villin	Not detected	Negative	Negative	Negative	Positive

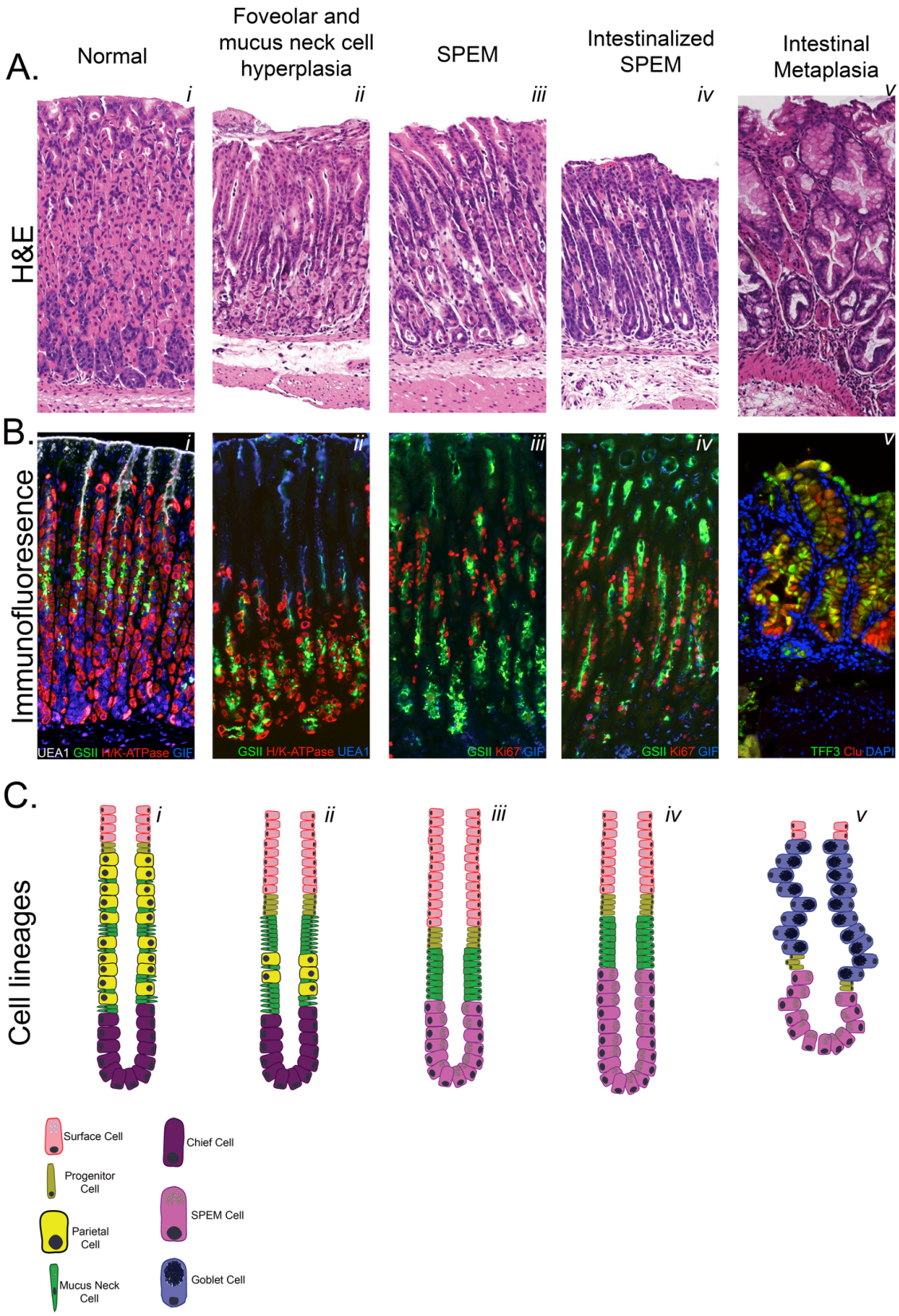
A.
Normal
Foveolar and mucus neck cell hyperplasia
SPEM
Intestinalized SPEM
Intestinal Metaplasia
i
ii
iii
iv
v
H&E
B.
Immunofluoresence
UEA1 GSII H/K-ATPase GIF
GSII H/K-ATPase UEA1
GSII Ki67 GIF
GSII Ki67 GIF
TFF3 Clu DAPI
C.
Cell lineages
Surface Cell
Progenitor Cell
Parietal Cell
Mucus Neck Cell
Chief Cell
SPEM Cell
Goblet Cell

Figure 1. The progression of gastric neoplasia in mice. Gastric corpus cell lineage changes observed in the atrophic stomach, with an emphasis on different pathology features and cell-specific markers used to distinguish stages of metaplasia. Parietal cell loss disrupts normal corpus gland hierarchy and results in the transdifferentiation of chief cells into SPEM. SPEM can further progress to intestinalized SPEM and intestinal metaplasia. **A.** Hematoxylin and Eosin images of A*i*. Normal gland lineages, A*ii*. Parietal cell loss and the development of foveolar and mucus neck cell hyperplasia, A*iii*. Chief cell transdifferentiation into SPEM, A*iv*. Intestinalized SPEM, A*v*. intestinal metaplasia. **B.** Immunofluorescence of different cell-specific markers that distinguish pathology features. B*i*. normal corpus glands have surface cells (UEA1), parietal cells (H/K-ATPase), mucus neck cells (GSII-lectin), and chief cells (gastric intrinsic factor, GIF). B*ii*. Loss of parietal cells is shown through parietal cell marker H/K-ATPase. The epithelial cells respond through an expansion of mucus neck cells (GSII-lectin) and surface cells (UEA1). B*iii*. SPEM is detected at the base of the glands through double-positive GSII-lectin and GIF. The proliferative zone expands throughout the isthmus, however SPEM is not proliferative at this stage. B*iv*. Intestinalized-SPEM is similar to SPEM when observed via H&E. However intestinalized SPEM is highly proliferative, and therefore triple-positive for GIF, GSII-lectin and Ki67. B*v*. Intestinal metaplasia is indicated through TFF3 positive enterocytes (shown) and Muc2 positive goblet cells (not shown) with Clusterin (Clu) positive cells at the base of glands, indicative of SPEM. **C.** Cell lineage diagrams highlighting pathology features representative of the different stages of metaplasia. C*i*. Normal gastric corpus oxyntic gland, with the majority of the epithelial cells types represented: surface cells, progenitor cells, parietal cells, mucus neck cells, and chief cells. C*ii*. The loss of parietal cells results in the expansion of surface cells (foveolar hyperplasia) and mucus neck cells (mucus neck cell hyperplasia). C*iii*. Shortly after parietal cell loss, chief cells transdifferentiate into SPEM cells. C*iv*. Intestinalized SPEM is proliferative and therefore the number of SPEM cells expands upwards into the isthmus. The visual characteristic of intestinalized SPEM is identical to SPEM cells except for the presence of Ki67. Transcriptome analysis is required to indicate intestinalization at this stage. C*v*. Intestinal metaplasia is characterized by the presence of intestinal cell lineages (enterocytes, goblet cells) interspersed with intestinalized SPEM and SPEM cells.

2. Human Disease inception and progression

The proximate cause of most intestinal type gastric cancer is referable to chronic infection with virulent *Helicobacter pylori* (*H. pylori)* strains (Correa and Piazuelo, 2012). *H. pylori* is a gram-negative bacteria that inhabits two-thirds of the global population (CDC). Chronic *H. pylori* infection leads to changes in the corpus mucosa that can predispose individuals to gastric adenocarcinoma. These changes result from oxyntic atrophy and chronic inflammation. The effect of parietal cell loss is the transdifferentiation of mature zymogen-secreting chief cells at the base of the fundic glands into spasmolytic-polypeptide expressing metaplasia (SPEM). Work over the past several years by our group and others in both humans

(Halldorsdottir et al., 2003; Minegishi et al., 2007; Yamaguchi et al., 2001) and rodents (Goldenring et al., 2000b; Weis et al., 2013b) has established that SPEM is a common metaplastic phenotype observed in the atrophic human and rodent stomach. In the setting of inflammation, SPEM is thought to progress into intestinal metaplasia in humans. Pelayo Correa originally described the association of intestinal metaplasia with the development of intestinal type gastric cancer (Correa, 1988). Thus, metaplastic cell lineages in the stomach are recognized as precursors of neoplasia. In addition, intestinal-type gastric cancer, the most predominant type of gastric adenocarcinoma, is frequently associated with both SPEM and intestinal metaplasia. Whether SPEM or IM gives rise to cancer has yet to be established.

3. Murine models of gastric neoplasia

An in depth review of studies over the past 20 years that display SPEM phenotypes in association with varying degrees of gastric neoplasia is detailed below:

Helicobacter infection

Mice infected with *Helicobacter felis* recapitulate the pathology associated with *Helicobacter pylori* infection observed in humans, complete with parietal cell loss, inflammation, and metaplasia. The mechanism by which *Helicobacter* causes parietal cell loss actually requires the host's inflammatory response. Roth et al identified that T-cells were necessary for *Helicobacter* associated parietal cell loss, as T-cell deficient mice infected with *Helicobacter* did not develop oxyntic atrophy or metaplasia (Roth et al., 1999). Further studies mouse models observed an expansion in TFF2-expressing mucus metaplasia in response to oxyntic atrophy (Fox et al., 1996; Wang et al., 1998). The mucus cell lineage expansion was identified as SPEM (Schmidt et al., 1999a), which is derived from the transdifferentiation of mature chief cells (Nam et al., 2010b). While SPEM in *H. felis*-infected mice is highly proliferative throughout the metaplastic lineages (Weis et al. 2013), goblet cell intestinal metaplasia is

notably absent from mice. However, there is evidence for intestinalization of SPEM during chronic *H. felis* and *H. pylori* infection (Nomura et al., 2004; Varon et al., 2012; Weis et al., 2013a).

Acute drug induced models of SPEM

A caveat of using *Helicobacter* infection for studying metaplasia is that alterations, especially to the immune system, may affect the competency of *Helicobacter* to induce oxyntic atrophy, a prerequisite for metaplasia development. Therefore acute drug treatment models that induce parietal cell death provides an essential tool to study the inflammatory process in metaplasia progression.

Oral administration of DMP-777.

Treatment with the parietal-cell specific protonophore drug DMP-777, initially developed by Merck, leads to rapid loss of parietal cells within 3 days followed by induction of SPEM after 10-14 days of treatment (Goldenring et al., 2000b; Nomura et al., 2005b). All of the metaplasia is reversible within 7-14 days following cessation of DMP-777 treatment. Interestingly in both mice and rats, administration of DMP-777 for up to 2 years led to prominent continuous metaplasia, but never resulted in any dysplastic or neoplastic lesions (Goldenring et al., 2000b). The absence of dysplastic lesions in the face of chronic metaplasia appears to be due to a lack of inflammation, likely because of the other action of DMP-777 as a cell-permeate elastase inhibitor (Goldenring et al., 2000b; Nomura et al., 2005b; Weis et al., 2013a).

3.2.2 Intraperitoneal injections of high doses of tamoxifen.

Mice given three consecutive daily doses of 5 mg of tamoxifen have a 90% reduction in parietal cell mass in the stomach. High dose tamoxifen-treated mice develop non-proliferative SPEM within 3 days of treatment. The effect can be reversed after 2-3 weeks following drug

withdraw (Huh et al., 2012). The pattern of SPEM induction by high dose tamoxifen resembles that induced by DMP-777, although there is evidence for increased levels of inflammation.

Oral administration of L635.

L635 is a chiral molecular cousin of DMP-777, which retains parietal cell protonophore activity, but lacks the elastase inhibitory capacity (Goldenring et al., 2000b). L635 treatment causes rapid induction of parietal cell loss and SPEM in the presence of a prominent inflammatory milieu. The quick oxyntic atrophy combined with a strong inflammatory infiltrate in the gastric mucosa leads to accelerated development of a proliferative and intestinalized SPEM lineage within 3 days of treatment (Nam et al., 2010a) that is remarkably similar to SPEM observed in *H. felis* (Weis et al., 2013a). M2 macrophages drive the proliferation and intestinalization of SPEM in L635-treated mice (Petersen et al., 2014). Therefore L635 treatment provides a rapid model for the development of proliferative intestinalizing SPEM.

Gastrin Genetic Models

Located in the antrum, G cells produce gastrin to promote gland homeostasis by regulating acid secretion from parietal cells. Gastrin also functions as a growth factor for ECL cells, invasion, angiogenesis, and anti-apoptotic activity at the transcriptional level (Dockray et al., 2001). In the stomach, endogenous gastrin levels increase in response to parietal cell loss in order to maximize gastric acid secretion and increase epithelial cell proliferation (Ray et al., 1996).

Insulin-gastrin (INS-GAS) transgenic mice.

The INS-GAS mouse model uses the mouse insulin promoter to drive expression of a human gastrin transgene, producing moderate elevations in circulating gastrin levels. The INS-GAS mice on the FVB background develop SPEM and dysplasia, that lead to invasive

lesions in the gastric corpus by 20 months of age (Wang et al., 2000b). Metaplastic changes are accelerated in the setting of *Helicobacter* infection, and inhibited by using an H2-histamine receptor inhibitor (CITE). These findings suggest that the induction of parietal cell loss resulted from a chronic state of acid hyper-secretion.

Gastrin Knockout mice.

Gastrin knockout mice develop antral tumors by 12 months of age. In the corpus, the mucosa is generally thinner with fewer parietal cells present. DMP-777 treatment in gastrin knock out mice causes an accelerated induction of SPEM in one to three days, as compared to 10 days in wild type mice. (Nomura et al., 2005b; Nozaki et al., 2008b). Gastrin knock out however do not develop foveolar hyperplasia that typically occurs as a result of oxyntic atrophy, consistent with the concept that gastrin is a major driver of foveolar hyperplasia.

Genetic mouse models of parietal cell loss

Several mouse models induce changes spontaneously consistent with the development of SPEM in the corpus of the stomach. These models may initiate with a normal mucosa and then develop increasing levels of atrophy and metaplasia.

Claudin 18 knockout mice.

Claudin-18 levels are high in the normal stomach but are prominently reduced in the metaplastic stomach (Hayashi et al., 2012). Tsukita and colleagues examined the impact of claudin-18 loss in the stomachs of claudin-18 knockout mice (Hayashi et al., 2012). These mice displayed few parietal cells at birth and never progressed to normal of parietal cell lineages during the postnatal period. Instead claudin-18 knockout mice demonstrated proliferative SPEM that was associated with a significant neutrophil infiltrate and elevations in IL-1b expression. The claudin-18 stomachs also demonstrated high levels of the SPEM

marker, HE4. While the metaplastic SPEM lineages in the claudin-18 knockout mice were highly proliferative, these mice were only studied up to 16 weeks of age, where no invasive or dysplastic lesions were reported. Thus Claudin 18 is necessary for normal parietal cell development and therefore gland homeostasis.

KLF4 knockout mice.

KLF4 is down-regulated in gastric cancers and loss of KLF4 is associated with poor prognosis (Hsu et al., 2013; Wei et al., 2005). In the KLF4 knockout mouse, the stomach shows marked oxyntic atrophy from birth and an expansion of both foveolar hyperplasia and mucus cell metaplasia (Katz et al., 2005). Some intrinsic factor-expressing cells do remain at the bases of corpus glands that are dominated by a TFF2-expressing mucus cell lineage. While no dual labeling for intrinsic factor and TFF2 was performed, the staining for TFF2 appears at the base of the glands, consistent with the suggestion that these glands represent SPEM. Interestingly however, the authors note that there is very little proliferation among the SPEM lineages and with observation of mice up to one-year, no intestinal metaplasia, dysplasia or invasive lesions developed. They also noted that no inflammation was appreciated. Thus, this model confirms that concept that SPEM can exist as a stable benign metaplasia as was observed in long term administration of DMP-777 (Goldenring et al., 2000b).

H/K-Cholera Toxin mouse.

Increased cAMP is the major driver of parietal cell acid secretion mediated through activation of the H2-histamine receptor. Samuelson and colleagues examined a model of chronic acid over-production in the H/K-Cholera Toxin mouse (Lopez-Diaz et al., 2006). This mouse showed increased acid secretion from an early age, as would be expected for parietal cells with increased expression of cholera toxin and cAMP production. While the mice show a normal compendium of cell lineages in the gastric corpus at 2 months of age, by 7 months of

age the mice develop increasing levels of parietal cell loss and show severe parietal cell loss by 15-16 months of age. The parietal cells loss at the later time points is associated with the presence of SPEM. The loss of parietal cells appears to relate to the development of auto-antibodies against parietal cell antigens, especially H/K-ATPase. This model therefore mimics the pathogenesis of autoimmune gastritis. No invasive glands were noted in these mice at the later stages although measures of proliferation were not determined.

Models of signaling pathway activation

Several studies conducted on characterizing gene and protein expression of metaplasia in the murine and human stomach has yet to identify a dominant signaling pathway driving neoplasia (Nozaki et al., 2008a; Sousa et al., 2012; Weis et al., 2013a). However different signaling pathways aberrations in gastric cancer has been characterized, identifying KRAS, FGFR2, EGFR, ERBB2 and MET using single nucleotide polymorphism arrays (Deng et al., 2012). These and other signaling pathways have been investigated for their role in the development of metaplasia and adenocarcinoma.

MAPK/ERK.

Up-regulation of phospho-ERK in metaplasia has been noted in both humans and mice. However, Ras mutations have only been observed in approximately 9% of gastric cancers. Nevertheless, recent gene profiling studies have noted a signature for up-regulation of Kras activity in greater than 40% of intestinal type human gastric cancers (Cancer Genome Atlas Research, 2014; Tan et al., 2011). Choi, et al. have recently examined the induction of metaplasia in Mist1-CreERT2; LSL-KRas (G12E) mice (Choi et al., 2015). Following tamoxifen induction, these mice express activated Kras in gastric chief cells, and after 4 weeks developed proliferative metaplasia. Two months after induction intestinal goblet cells expressing Muc2 are evident, progressing to invasive glands 4 months post induction.

Importantly, treatment of the mice with a MEK inhibitor, Selumetinib, caused arrest of the metaplasia and allowed recrudescence of normal gastric lineages. These normal lineages were derived from a normal progenitor cell and not the metaplastic lineages. The normal gastric lineages appeared to cause extrusion of the metaplastic glands from the gastric mucosa into the lumen. These findings indicate that activation of Ras is involved at all of the key steps in the development of metaplasia, from transdifferentiation of chief cells into SPEM, to further differentiation of intestinal metaplasia and the promotion of invasive changes.

TGFb and BMP.

Smad3 is a critical signaling protein downstream of TGFb receptor activation. Smad3 KO mice were first extensively characterized for the spontaneous development of colonic adenocarcinoma (Zhu et al., 1998). While development of colon cancers required colonization of animals with *Helicobacter hepaticus*, observations at the Jackson Laboratories indicated that gastric tumors evolved in the absence of any infection. Detailed analysis of these mice subsequently demonstrated that these mice developed SPEM by 6 months of age and invasive lesions in the proximal corpus by 10 months of age (Nam et al., 2012). Invasive lesion, thought to be derived from the first gland of the corpus, generally showed TFF2-positive cells along with large numbers of DCLK1-positive tuft cells. These results suggested that loss of Smad3 could lead to development of proximal gastric neoplasia.

H/K-Noggin mouse.

Todisco and colleagues sought to evaluate the role of BMP signaling in the differentiation of gastric lineages in the H/K-Noggin mouse (Shinohara et al., 2010). Inhibition of BMP signaling through over-expression of Noggin resulted in reduction of parietal cell numbers and expansion of SPEM lineages expressing TFF2. While there was increased proliferation in the mucosa, most of this proliferation was abolished when the transgenic mice

were crossed onto gastrin knockout, a finding consistent with a role for proliferation in foveolar hyperplasia in these mice rather than SPEM (Todisco et al., 2015). Importantly, the over-expression of Noggin in the stomach caused an augmentation of metaplastic changes after infection with *H. felis* or *H. pylori* (Takabayashi et al., 2014). These findings suggest that BMP signaling is generally anti-inflammatory and that loss of this signaling may promote metaplasia development.

EGFR.

The role of EGFR and its ligands in alterations in gastric mucosal lineage differentiation has been well established. Over-expression of TGF-alpha in the gastric corpus is associated with severe foveolar hyperplasia in Menetrier's disease in humans (Dempsey et al., 1992b; Nomura et al., 2005a). Over-expression of TGF-alpha in the stomachs of MT-TGF-alpha mice leads to a similar phenotype (Goldenring et al., 1996). These studies all suggested that over-expression of TGF-alpha altered the differentiation of gastric progenitors to the production of surface mucus cells over gland cells (e.g. parietal, mucus neck and chief cells).

Nevertheless, other studies have suggested that alterations in EGFR activation can influence the induction of metaplasia. Waved-2 mice, which have an attenuating mutation of the EGFR, demonstrated enhanced development of SPEM after loss of parietal cells induced by DMP-777 (Ogawa et al., 2006). These effects seemed to be specific to particular EGFR ligands since although TGF-alpha KO mice showed no alteration in SPEM induction, amphiregulin KO mice showed an enhanced induction of SPEM after DMP-777 treatment, similar to that observed in *waved-2* mice (Nam et al., 2007). Just as interestingly, amphiregulin deficient mice over one year of age developed SPEM spontaneously (Nam et al., 2009). By 18 months of age, over 40% of amphiregulin knockout mice showed parietal cell loss and both SPEM as well as goblet cell intestinal metaplasia. The goblet cell intestinal metaplasia evolved in glands also containing SPEM and cells with intermediate morphology

with dual expression of TFF2 and MUC2 observed at the interface between SPEM and intestinal metaplasia lineages (Nam et al., 2009). These findings demonstrated that EGFR-mediated signaling was involved in the evolution of gastric lineages.

Immune-mediated pre-neoplastic mouse models

Inflammation accompanies most models of metaplasia in the gastric mucosa. Insights into different aspects of the inflammatory response reveal the impact of immune cells in the progression of metaplasia.

H/K-ATPase-IFNg transgenic mice.

The expression of the pro-inflammatory cytokine IFNg, typically expressed by Th1 polarized T-cells, is increased in *Helicobacter* infected mice. Transgenic overexpression of IFNg by the parietal cell specific driver H/K-ATPase b promoter causes a prominent inflammatory infiltrate, oxyntic atrophy, epithelial cell proliferation and SPEM after 3.5 months. SPEM and immune infiltration is still present in Tg- IFNg mice crossed to Rag 1 knock out mice that lack T and B cells (Syu et al., 2012). Therefore IFNg alone can drive gastric metaplastic changes without the assistance of polarized T or B cells.

Hip1r and IFNg double knockout mice.

Huntington interacting protein 1 is required for normal parietal cell maturation (Jain et al., 2008). Parietal cells undergo apoptosis in Hip1r knock out mice and develop a robust inflammatory response and SPEM by 12 months of age. Double Hip1R and IFNg knock out mice have delayed metaplasia development, but mice 12 months of age appear to have similar phenotypic SPEM as control Hip1R knock out mice. Therefore, IFNg is not required for SPEM induction after parietal cell loss (Liu et al., 2012).

TxA23 mice.

Human autoimmune gastritis occurs when T-cells target parietal cells for apoptosis in the stomach, causing robust metaplasia that predisposes affected individuals to endocrine carcinoids (Solcia et al., 1992). Transgenic mice engineered with CD4+ T-cells that recognize the parietal specific antigen H/K-ATPase crossed on to the BALB/c background develop SPEM by 2-4 months of age. By 12 months of age, TxA23 mice have extensive inflammation with areas of aberrant gland morphology and penetrating submucosal glands (Nguyen et al., 2013). The severity of phenotype observed in this model may be attributed to the BALB/c background, which is considered a Th2 dominant background (Hsieh et al., 1995; Watanabe et al., 2004). Specifically, T-cells in BALB/c mice express higher levels of IL-4 than IFNg that drives a Th2 response. Most investigations in the stomach use C57Bl/6 mice, which is considered a Th1 dominant background where T cells express higher levels IFNg. Therefore the severity of metaplasia in the TxA23 atrophic gastritis model is perhaps indicative of a Th2 driven environment paired with parietal cell loss.

H/K-ATPase IL-1b transgenic mice.

Polymorphisms in the IL-1 beta gene are observed in a variety of human, including gastric adenocarcinoma. Il-1b is part of the IL-1 family of cytokines that function as alarmins by promoting the inflammatory response. Il-1b expression increases in *Helicobacter* infections and is also associated with myeloid cell infiltration. Transgenic mice expressing human Il-1b by parietal cells using the H/K-ATPase promoter develop spontaneous inflammation, oxyntic atrophy, and SPEM with dysplastic lesions at late time points. *Helicobacter* increases the susceptibility and speed at which gastric pathology develops in Tg Il-1b mice (Tu et al., 2008). Conversely, IL-1 receptor antagonist treatment can inhibit the progression of metaplasia and inflammatory cell infiltration. Together these findings support Il-1b as a major driver of inflammatory cell recruitment that promotes the progression of metaplasia.

Sdf1 Transgenic mice.

Stromal derived factor 1 (SDF1) is typically expressed by cancer-associated fibroblasts and found upregulated in *Helicobacter*-infected gastric mucosa. Transgenic mice expressing SDF-1 from parietal cells using the H/K ATPase driver do not have recruitment of inflammatory cells, however display hyper-proliferative gastric epithelial cells and focal areas of SPEM with dilated glands at late time points (18 months). *H. felis* infected SDF1-Tg mice develop accelerated pathology. And similarly when Tg-SDF1 mice are crossed to pro-inflammatory Tg-IL1b mice there is increased epithelial cell proliferation and accelerated SPEM development in the corpus (Shibata et al., 2013). These data indicates that while SDF1 does not drive recruitment of inflammatory cells, it does appear to promote epithelial changes and promote SPEM, especially in the setting of atrophic gastritis.

K19-C2mE mice.

Cox2 is frequently overexpressed in gastric cancer. Oshima et al developed transgenic mice expressing Cox-2 and mPGES-1 in progenitor cells, driven by the cytokeratin 19 promoter (CITE). These effects cause M2 polarized macrophages to be recruited into the mucosa, subsequently causing the development of SPEM. After 80 weeks, these mice progress to develop hyperplastic tumors. Treatment using the non-steroidal anti-inflammatory drug meloxicam ameliorates the inflammation and reverses the metaplastic gland morphology. In an effort to determine the role of specific cytokines in this process, TNFa and IL1r1 knock out mice were crossed on to the K19-C2mE. Mice null for TNFa had decreased inflammation, reducing metaplasia overall. However no overt change in inflammation or metaplasia was observed in IL1r1 null mice. Therefore Cox2 and PGE2 can drive metaplastic changes in the stomach through the recruitment of M2 polarized macrophages in a TNFa-dependent pathway (Oshima et al., 2005).

Gan mice.

Activated b-catenin activity, however not mutations in APC, is observed in 51% of human intestinal type gastric cancers (Oshima et al 2006). K19 progenitor cells driving Wnt1 expression cause suppression of normal gastric epithelial cell differentiation that is accompanied with increased proliferation and TFF2 positive cells. By 7 to 18 weeks mice develop small preneoplastic lesions in the corpus. The Gan mice were developed by crossing K19-Wnt1 mice to K19-C2mE mice (described above), thereby activating Wnt signaling in progenitor cells with a coordinated immune cell infiltration. This results in exacerbated metaplasia that drives the rapid development of gastric dysplasia and tumors in the corpus. Furthermore, amelioration of the inflammatory response using a CCL2 chemokine inhibitor or clodronate treatment to deplete macrophages causes tumor regression in Gan mice (Oshima et al., 2011a). Thus activation of the Wnt signaling pathway can drive metaplasia formation but inflammation is necessary for metaplasia progression.

Exogenous IL-11 treatment.

IL-11 belongs to the IL-6 family of cytokines that induces signal transduction through the IL-11Ra. IL-11 is not expressed during the early stages of an inflammatory response associated with *Helicobacter* infection, but gradually increases during chronic inflammation and intestinal metaplasia. While IL-11 expression is normally localized to parietal cells, this is subsequently lost in the setting of oxyntic atrophy in response to *Helicobacter* infection. Therefore the source of increased IL-11 expression in chronic *Helicobacter* infection originates elsewhere. Nevertheless, exogenous treatment of IL-11 in wild-type mice leads to parietal cell loss within 24 hours, an infiltration of polymorphonuclear cells, and the emergence of SPEM (Howlett et al., 2012). Thus, it is hypothesized that IL-11 is released by dying parietal cells to recruit inflammatory cell into the stomach and promote the development of SPEM.

Exogenous IL33 treatment.

A member of the IL-1 family of cytokines, IL-33 is expressed normally in the gastric mucosa, localizing to cells in the surface cell zone. IL-33 synergizes to promote a Th2 inflammatory response that activates innate and adaptive immune cells. Several studies refer to IL-33 as an alarmin due to its release into the extracellular environment by necrotic or apoptotic cells. IL-33-treated mice develop mucus metaplasia and a robust inflammatory response in the lungs, intestine and stomach, indicating that IL-33 is sufficient to recruit inflammatory cells and drive mucus production within respiratory and gut epithelial tissue (Buzzelli, 2015; Pastorelli et al., 2013). However, IL-33 is only expressed in the normal stomach by cells in the surface cell zone in the corpus, which do not undergo cell death during *Helicobacter* infection. Therefore while administration of IL-33 is capable of recruiting inflammatory cells and inducing SPEM, it is remains to be seen if endogenous IL-33 functions in this capacity.

5. Conclusions

Data from mouse models indicates that the induction of metaplasia involves at least two phases. Induction of metaplasia first requires the loss of parietal cells. Parietal cell loss induced by *Helicobacter* infection requires the action of specific lymphocytic populations and specific immune modulatory molecules. In a second phase, following the loss of parietal cells, SPEM develops from transdifferentiation of chief cells. However, expansion of the metaplasia requires the chronic influence of M2-macrophage subclasses. The utilization of a number of drug-induced methods to ablate parietal cells acutely can bypass the first chronic phase required for parietal cell loss. Similarly, genetic models, such as directed activation of Ras in chief cells, directly induced transdifferentiation of chief cells and promote inflammatory regulators required for expansion of metaplasia. Mouse models of immune modulator over-

expression can similarly induce both parietal cell loss and SPEM induction. It seems evident that inflammatory mediators and/or MDSCs are required for induction of more aggressive and proliferative metaplasia that can progress to dysplasia.

What remains unclear from mouse models is a clear connection with the latter stages of carcinogenesis. Most models interrogate the initiation of metaplasia and none of the models can induce clear metastatic or even regionally invasive adenocarcinoma. Indeed, many of the lesions that are labeled as "dysplastic" seem over-interpretations of metaplastic or reactive lesions. With the exception of the Mist1-Ras mouse and some older amphiregulin KO mice, mouse models of metaplasia have not faithfully recapitulated the induction of goblet cell-containing intestinal metaplasia. Given the presence of invasive lesions derived from SPEM in a number of the mouse models, this may suggest that intestinal metaplasia may represent an adaptive response to chronic injury rather than a true preneoplastic lesion. Further studies are therefore needed to discern the molecular mediators of key transition points along the metaplasia to carcinoma sequence: at the point of transdifferentiation of chief cells into SPEM, at the transition of SPEM into intestinal metaplasia and at the point of true dysplastic transition from metaplasia (SPEM or intestinal metaplasia).

4. Aims

Recent studies have thus allowed the proposal of a paradigm that unifies our knowledge of metaplasia in mice and humans. It seems likely that the initiating event in metaplastic induction in both mice and humans is a loss, either acutely or chronically, of acid-secreting parietal cells. The loss of parietal cells triggers the transdifferentiation of chief cells into SPEM (Nam et al., 2010a). In the setting of local injury to the mucosa, this type of response would provide a mechanism for local repair of mucosal defects. Thus, induction of SPEM as a primary metaplasia may be inherently reparative and reversible. Nevertheless, in both human and mouse SPEM, the presence of inflammatory infiltrates appears to lead to an increasingly

proliferative metaplasia as well as progression towards more intestinalized metaplastic phenotypes. While in humans this process culminates in the development of a fully intestinalized mucus cell phenotype (intestinal metaplasia), SPEM in mice acquires intestinalizing characteristics under the influence of inflammation without complete phenotypic changes characteristic of goblet cell intestinal phenotypes (Varon et al., 2012; Weis et al., 2013b). Intestinalized proliferative SPEM in mice is emblematic of the progression to an advanced metaplastic phenotype. Nevertheless, the influences responsible for the expansion of this metaplasia to a more proliferative phenotype and its further differentiation into a more intestinalized metaplasia remain obscure. Previous data suggest that inflammation is driving this process forward. The following chapters will provide definitive data implicating M2a macrophages producing IL-33 as the driving force behind metaplasia development and progression.

Chapter II

MACROPHAGES PROMOTE PROGRESSION OF SPASMOLYTIC POLYPEPTIDE EXPRESSING METAPLASIA (SPEM) FOLLOWING ACUTE PARIETAL CELL LOSS

Appear as: Christine P. Petersen, Victoria G. Weis, Ki Taek Nam, Josane F. Sousa, Barbara Fingleton and James R. Goldenring. Macrophages promote progression of spasmolytic polypeptide expressing metaplasia (SPEM) following acute parietal cell loss. *Gastroenterology*. 146(7):1727-38. 2014

Introduction

Gastric adenocarcinoma is the second highest cause of cancer-related death in the world (de Martel et al., 2012). Due to a lack of early clinical manifestations, gastric cancer frequently presents as late stage disease. *Helicobacter pylori* (*H. pylori*) infection is the major predisposing factor for gastric cancer, causing chronic inflammation and oxyntic atrophy in the gastric mucosa (Blaser and Parsonnet, 1994). The parietal cell loss disrupts the homeostatic glandular environment and chief cells transdifferentiate into spasmolytic polypeptide expressing metaplasia (SPEM) (Nam et al., 2010b; Weis et al., 2013a). Increasing data suggest that intestinal metaplasia (IM) arises from SPEM in humans, supporting the hypothesis that SPEM is the critical initial pre-neoplastic metaplasia predisposing to gastric adenocarcinoma (Goldenring et al., 2010; Nam et al., 2009; Yoshizawa et al., 2007).

Helicobacter felis (*H. felis*) infection in mice recapitulates the inflammatory and pre-neoplastic cascade of human *H. pylori* infection (Nam et al., 2010b). In the murine *Helicobacter* infection model, SPEM develops after 6 to 12 months of infection. As in human infection with *H. pylori*, there appear to be two phases in the development of metaplasia. First, the infection induces parietal cell loss or oxyntic atrophy. Oxyntic atrophy is required for the induction of metaplasia

in humans (El-Zimaity et al., 2002; Meining et al., 2001). In the presence of on-going inflammation, metaplasia then evolves and expands. Given the long latency for SPEM development in *H. felis*-infected mice, our group developed two acute SPEM models. The administration of either drugs DMP-777 or L635 induces SPEM by selectively ablating parietal cells (Goldenring et al., 2000a; Nomura et al., 2005b). Mice treated with DMP-777 for 14 days develop SPEM without the presence of significant inflammation, likely due to the ability of DMP-777 to also inhibit elastase activity (Goldenring et al., 2000a). In contrast, L635-treated mice develop an advanced proliferative SPEM with intestinal characteristics (previously designated as SPEM-IC) in just 3 days of treatment which is associated with both loss of parietal cells and a prominent inflammatory infiltrate (Nam et al., 2010b; Weis et al., 2013a). The phenotype of mice treated L635 for 3 days is similar to that for mice infected with *H. felis* for 6 months or more (Weis et al., 2013a). Thus, the L635 model appears to bypass the initial phases of *H. felis* infection that leads to oxyntic atrophy by directly inducing parietal cell loss acutely. While mice do not develop typical goblet cell intestinal metaplasia in either the L635-treatment or *Helicobacter* infection models, they do develop advanced proliferative SPEM that is characterized by the expression of specific upregulated intestinal transcripts (*Cftr*, *Dmbt1* and *Gpx2*) and an increase in proliferative SPEM cells (Houghton et al., 2004; Wang et al., 2000a; Weis et al., 2013a). Similarly, Varon et al. observed an increase in intestinal characteristics in murine metaplasia associated with long-term *Helicobacter* infection (Varon et al., 2012). Studies with DMP-777 treatment demonstrate that loss of parietal cells even without inflammation leads to the development of SPEM from transdifferentiation of chief cells; however, the presence of inflammation in L635-treated mice leads to more rapid SPEM induction as well as promotion of both increased proliferation and a more intestinalized phenotype . Thus, inflammation is a key factor in the advancement of SPEM to a more aggressive metaplastic phenotype. Nevertheless, the precise immune cell populations responsible for the progression of metaplasia are not known.

Four distinct inflammatory cell populations are most frequently associated with *Helicobacter* infection in the stomach: B-cells, interferon-γ (IFNγ) secreting T-cells, neutrophils, and macrophages (Fox et al., 1993). Through the manipulation of specific immune cells, previous studies have shown that T-cells contribute to parietal cell loss and the development of metaplasia in *Helicobacter* infection (Roth et al., 1999). However, chronic inflammation associated with *Helicobacter* infection is predominately made up of neutrophils and macrophages. These phagocytic cells migrate into the mucosa to engulf debris and propagate the inflammatory response (Chow et al., 2011). Similarly, during acute induction of SPEM with L635, there is a significant influx of T-cells, B-cells, neutrophils and macrophages that migrate into the mucosa (Nam et al., 2010b). Still, little is known about which immune cells promote the advancement of SPEM.

In the present studies, we have sought to assess the influence of specific immune cell populations on the advancement of SPEM following the induction of parietal cell loss. To address the specific immune components, we evaluated the presence and characteristics of L635-induced SPEM in various mouse models of depleted immune cells. Rag1 knockout mice (Rag1KO) deficient in T- and B-cells, IFNγ knockout mice (IFNγKO), neutrophil-depleted mice (Ly6G antibody-treated), and macrophage-depleted mice (clodronate-treated) were each administered L635 to induce acute parietal cell loss and SPEM. Our findings indicated that M2 macrophages are the critical immune cell driver of the induction of metaplasia following loss of parietal cells.

Methods

Treatment of Animals

L635 treatment

Each experimental group consisted of three male mice. L635 (synthesized by the Chemical Synthesis Core of the Vanderbilt Institute of Chemical Biology), dissolved in deionized DNA

and RNA-free water, was administered by oral gavage (350 mg/kg) once a day for three consecutive days. Neutrophils were depleted through intraperitoneal injection of anti-Ly6G antibody (Leaf, BioLegend, San Diego, CA) (100 µg) two days prior to and throughout the three day L635 administration. Control mice received intraperitoneal injections of a non-specific isotype-matched IgG antibody. Macrophages were depleted by intraperitoneal injection of clodronate-containing liposomes (Encapsula NanoSciences, Brentwood, TN) (10 mg/kg) two days prior to and throughout the three days of L635 administration. Control mice received liposomes alone (10 mg/kg). Mice were sacrificed on the third day of L635 administration.

DMP-777 treatment

Three male mice were used for each experimental group. DMP-777 (a gift from DuPont-Merck Co.) dissolved in 1% methylcellulose was administered by oral gavage (350mg/kg) once a day for 8 consecutive days. Macrophages were depleted using four intraperitoneal injections of clodronate-containing liposomes (10 mg/kg) every other day of DMP-777 treatment. Control mice received liposomes (10 mg/kg) with or without DMP-777-treatment. Mice were sacrificed the ninth day.

Immunohistochemistry

Stomachs from mice were fixed in 4% paraformaldehyde overnight and transferred into 70% ethanol for subsequent paraffin embedding. Five µm sections were used for all immunohistochemistry studies. Sections were deparaffinized and rehydrated. Target Retrieval Solution (DakoCytomation, Glostrup, Denmark) was used for antigen retrieval in a pressure cooker. Slides were blocked using Protein Block Serum-free (DakoCyomation) for one hour at room temperature. The following primary antibodies were incubated at 4°C overnight in Antibody Diluent with Background Reducing Components (DakoCyomation): goat

anti-intrinsic factor (1:1000, a gift from Dr. David Alpers, Washington University, St. Louis, MO), rat immunoglobulin G (IgG) anti-Ki-67 (1:500; Dako), rat anti-F4/80 (1:500; Invitrogen, Grand Island, NY), rat anti-mouse Ly6B.2 (1:500; AbD Serotec, Oxford, UK), goat anti-Arginase II (1:100; Santa Cruz, Dallas, TX), rabbit anti-CD68 (1:200; Abbiotec, San Diego, CA), mouse anti-iNos (1:300; Abcam, Cambridge, MA), mouse anti-CD163 (1:200; NeoMarkers, Fremont, CA), mouse anti-human CD68 (1:5,000; Dako). Fluorescent secondary antibodies (1:500) and Alexa 488 and 647-conjugated *Griffonia simplicifolia* lectin II (GSII-lectin) (1:1500; Molecular Probes, Eugene, OR) were incubated for one hour at room temperature for detection. Sections were analyzed using a Zeiss Axiophot microscope equipped with an Axiovision digital imaging system (Zeiss, Jena GmBH, Germany) or an Ariol SL-50 automated slide scanner (Leica Biosystems, Buffalo Grove, IL, USA) in the Vanderbilt Digital Histology Shared Resource.

Quantitative real-time PCR

Total RNA from the fundus was extracted from paraformaldehyde-fixed paraffin-embedded (FFPE) tissue of three male mice per group to examine the expression of intestinal transcripts (*Cftr, Dmbt1, Gpx2*). Five µm sections were taken for H&E stain to identify fundic areas in the tissue blocks. A 2 mm biopsy punch was then used to extract fundic tissue. The standard Qiagen RNeasy FFPE kit protocol was used for purification of total RNA and DNAse treatment. A *mir*Vana PARIS kit (Ambion) was used to extract total RNA from fresh whole fundus to assess M1 and M2 macrophage transcript expression. One µg of RNA was DNAse-treated (Promega) and used for cDNA synthesis using Superscript III Reverse Trascriptase (Invitrogen). Quantitative real-time polymerase chain reaction (qRT-PCR) was performed with EXPRESS SYBR GreenER qPCR SuperMix (Invitrogen) and specific primers in an ABI StepOnePlus Real-Time PCR System (Applied Biosystems, Foster City, CA). All samples were run in triplicate following the SYBR Green Supermix manufacturer's protocol. The expression of TATA-box binding protein (TBP) was used as an endogenous control for

normalization and the $2^{-\Delta\Delta}$ method was used to compare samples when assessing the expression of the intestinal transcripts *Cftr, Dmbt1, Gpx2*. Statistical significance ($p<0.05$) between the groups was determined using the Mann-Whitney *U* one-tailed or two-tailed test. The primer sequences used have been previously reported (*Cftr*, *Dmbt1*, *Gpx2*, *Tbp, TNFα, IL10, IL4, IFNγ*).(Nam et al., 2009; Weis et al., 2012) Additionally specific IL-1b primers were used: forward AAATGCCACCTTTTGACAGTG and reverse GGCAGTATCACTCATTGTGGC. Primers for M1 and M2 macrophage marker primers: *Ym1* (Chi3L3), *Fizz1* (Resistin-like alpha, Retnla), *Argl*, *Nos2*, *Cd3*, and *Cxcl10* (QuantiTect Primer Assay, Qiagen), were used per the manufacturer's protocol with EXPRESS SYBR GreenER qPCR mix on the ABI StepOnePlus Real-Time PCR System. The expression of the M1 and M2 markers was normalized to *GAPDH* expression (QuantiTect Primer, Qiagen) and displayed as expression levels ($2^{-\Delta Ct}$), multiplied by a 1000.

Quantitation of proliferative SPEM and immune cells

Images were analyzed using CellProfiler or manually counted.(Jones et al., 2008) Each experimental group contained three mice. Five representative images were taken for each mouse at 20X, and the cells of interest in each image were counted. SPEM cells were identified as gastric intrinsic factor and GSII-lectin co-positive cells. Ki67 was used to identify proliferative cells. SPEM proliferation was identified through Ki67, intrinsic factor, and GSII-lectin triple-positive cells, and quantitated by counting the number of triple-positive cells on each 20X field image. Neutrophils and macrophages were labeled using specific markers and both counted in five images per mouse in a 20X field image. For all cells counted, nuclei were present as detected by DAPI. The Mann Whitney *U* one tailed Test was used to calculate statistical significance ($p<0.05$). The inflammatory infiltrate in human metaplasia was assessed using sections from a tissue array(Leys et al., 2007) containing normal and metaplastic gastric tissue. Samples were stained for macrophage markers CD68 (general macrophage) or CD163

(M2 macrophage) in serial sections and co-labeled with GSII-lectin. Each core was scanned using an Ariol SL-50 automated slide scanner at 20X, and the cells of interest were counted using Cell Profiler. At minimum, three cores from each group were counted.

Results

Rag1 and IFNγ knockout mice develop acute proliferative SPEM

To determine the role of the adaptive immune system in the development of proliferative SPEM, wild type, Rag1KO and IFNγKO mice were administered L635 for three days and stomach cell lineages were analyzed. Histologic examination revealed parietal cell loss and significant inflammatory infiltration in the fundus of the stomach in all L635-treated mice (Figure 1). Upon L635 treatment, neutrophils increased by 6-fold in wild type mice, with no significant difference observed in L635-treated Rag1KO or IFNγKO mice (Figure 2A and C). F4/80 positive cells increased three to five-fold in wild type, Rag1KO, and IFNγKO L635-treated mice compared to untreated mice (Figure 2B and C). L635-treated Rag1KO and IFNγKO mice did not have a significant change in F4/80 positive cells compared to wild-type L635-treated mice (Figure 2C). L635-treated Rag1KO and IFNγKO mice developed SPEM (as defined by intrinsic factor and GSII-lectin co-positive cells),(Liu et al., 2012) similar to L635-treated wild-type mice (Figure 3A and C). Furthermore, L635-treated Rag1KO and IFNγKO mice showed a 40 to 50-fold increase in SPEM cell proliferation similar to wild-type L635-treated mice (as

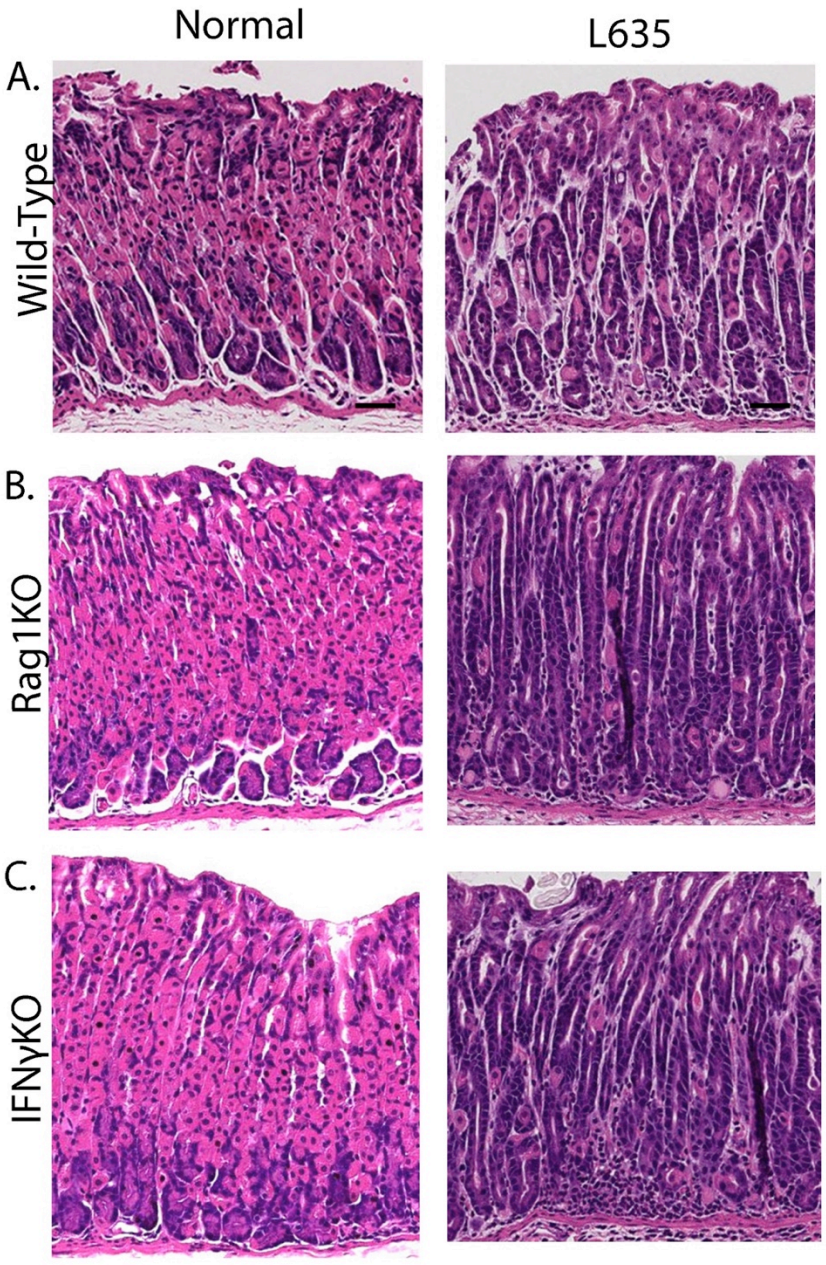

Figure 2: Effective parietal cell loss after L635 administration in wild type, Rag1KO and IFNγKO mice. A. Hematoxylin and eosin staining of untreated and L635-treated wild-type fundus. B. Staining of normal and L635-treated Rag1KO fundus. C. Staining of normal and L635-treated IFNγKO mice. Scale bars: 50 μm.

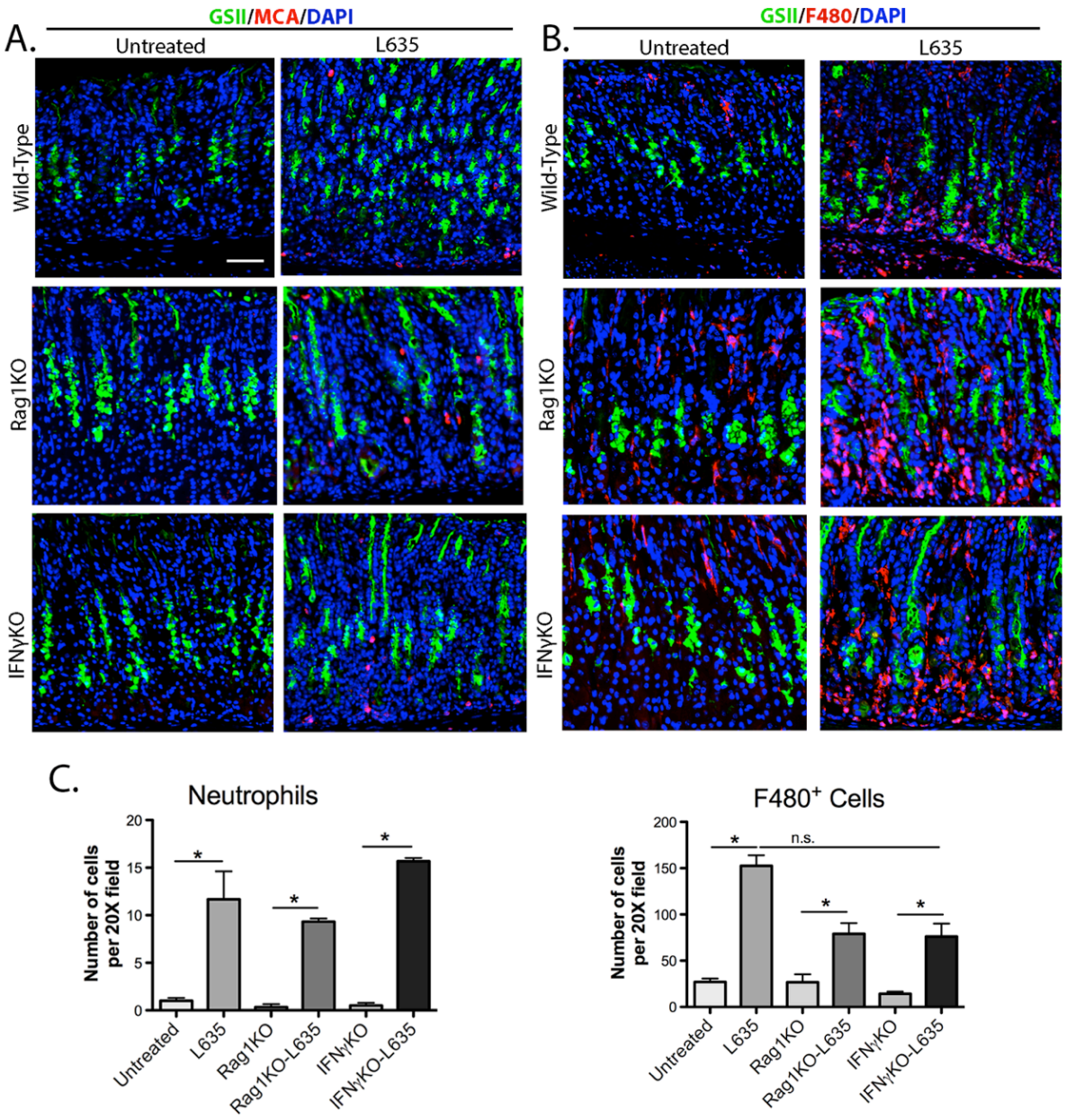

Figure 3: Wild type, Rag1KO and IFNγKO mice have similar recruitment of neutrophils and macrophages after L635-treatment. A. Immunofluorescence staining with antibodies against Ly6B.2 (red) to label neutrophils co-labeled with GSII-lectin (green) and DAPI (blue) staining in untreated and L635-treated wild type, Rag1KO and IFNγKO mice. B. Immunofluorescence staining with antibodies against F4/80 (red) to label macrophages and dendritic cells co-labeled with GSII-lectin (green) and DAPI (blue) staining. C. Quantitation of the total number of neutrophils and F4/80 positive cells counted per 20X field. L635-treated wild type, Rag1KO and IFNγKO mice all showed a significant increase in neutrophils and macrophages (*p=0.05) compared to untreated controls. There was no significant difference in neutrophil or F4/80 positive cell numbers between wild type mice compared to either Rag1KO or IFNγKO treated with L635 (Mann Whitney *U* two-tailed Test). Scale bars: 50 μm.

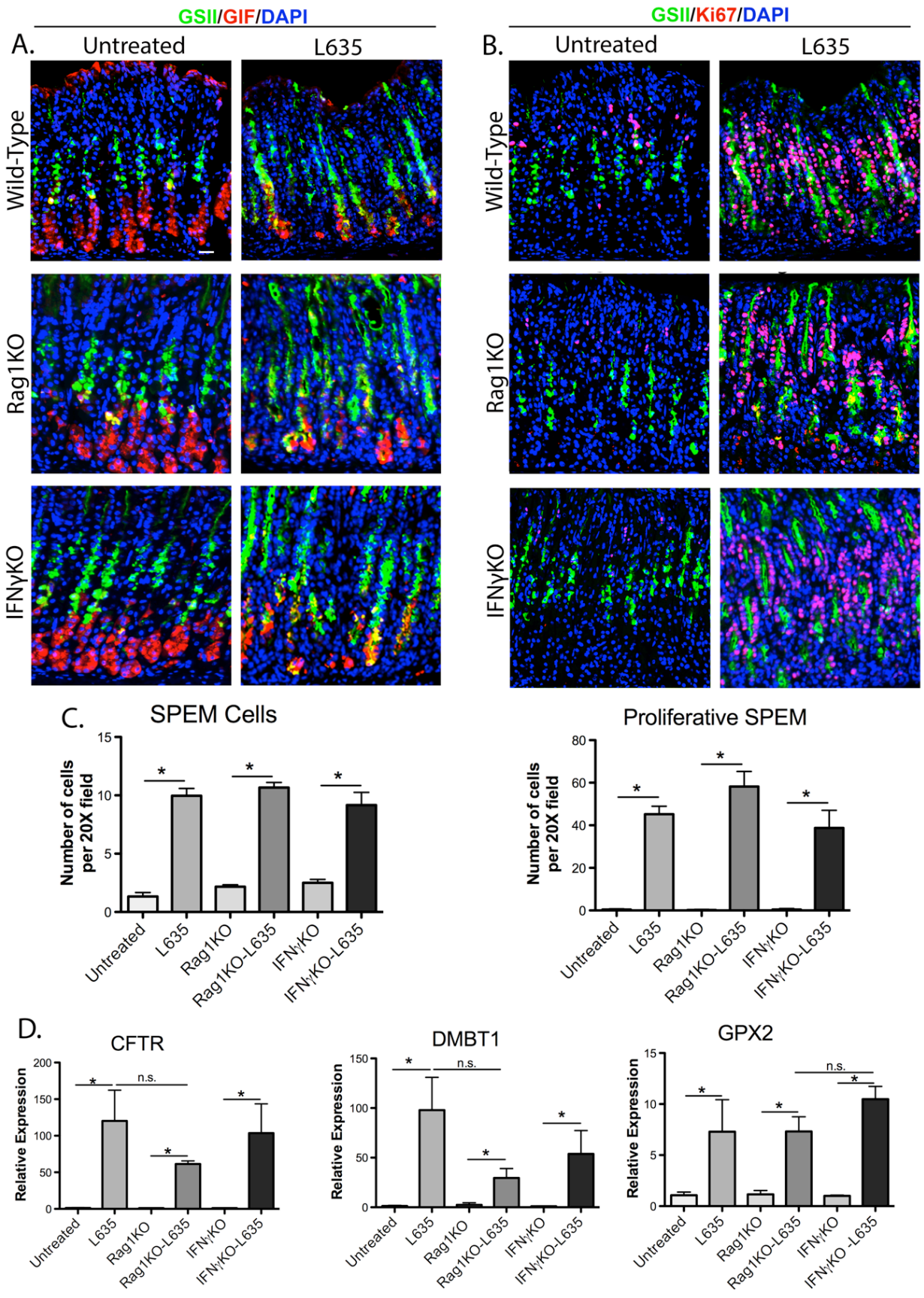
GSII/GIF/DAPI
A.
Untreated
L635
Wild-Type
Rag1KO
IFNγKO
GSII/Ki67/DAPI
B.
Untreated
L635
Wild-Type
Rag1KO
IFNγKO
C.
SPEM Cells
Number of cells per 20X field
Untreated
L635
Rag1KO
Rag1KO-L635
IFNγKO
IFNγKO-L635
Proliferative SPEM
Number of cells per 20X field
Untreated
L635
Rag1KO
Rag1KO-L635
IFNγKO
IFNγKO-L635
D.
CFTR
Relative Expression
n.s.
DMBT1
Relative Expression
n.s.
GPX2
Relative Expression
n.s.
IFNγKO -L635

Figure 4: Wild type, Rag1KO and IFNγKO mice develop acute proliferative SPEM after L635-treatment. A. Immunofluorescence staining for SPEM using gastric intrinsic factor (GIF) in red co-labeled with GSII-lectin (green) and DAPI (blue). GSII-lectin and GIF co-positive cells at the base of the glands were considered SPEM. B. Immunofluorescence staining for proliferation using Ki67 (red) co-labeled with GSII-lectin (green) and DAPI (blue) to determine the presence of SPEM cell proliferation before and after L635 administration in wild type, Rag1KO and IFNγKO mice. Ki67, GIF, and GSII-lectin triple-positive cells were considered proliferative SPEM. C. Quantitation of $GSII^+$ and GIF^+ cells (SPEM) and proliferative SPEM cells in wild type, Rag1KO and IFNγKO mice, (*p=0.05). D. qPCR of advanced proliferative SPEM markers. All L635-treated mice showed significant increases in the expression in intestinal transcript markers *Cftr*, *Dmbt1* and *Gpx2* (*p=0.05). Scale bars: 50 μm.

defined by Ki67, gastric intrinsic factor, and GSII-lectin triple-positive cells) (Figure 3B and 1C). To determine whether Rag1KO or IFNγKO mice develop advanced proliferative SPEM, the expression of SPEM-associated intestinal transcripts was analyzed by qRT-PCR (Figure 3D). *Cftr, Dmbt1,* and *Gpx2* expression was significantly upregulated (55-fold, 30-fold, and 7-fold, respectively) in L635-treated Rag1KO mice (Figure 3D). L635-treated IFNγKO mice showed similar changes in *Cftr*, *Dmbt1* and *Gpx2* expression comparable to changes observed in L635-treated wild type (Figure 3D). These results all indicate that the presence of T- and B-cells or IFNγ is not necessary for the development of advanced proliferative SPEM after acute parietal cell loss.

Neutrophil-depleted mice develop acute proliferative SPEM

Neutrophils are potent phagocytic cells that are recruited to the gastric fundus in L635-treated mice (Nam et al., 2010b). Neutrophils were depleted in mice using an anti-Ly6G antibody to determine the role of neutrophils in the development of SPEM (Daley et al., 2008). Control mice were dosed with a matched anti-IgG, and L635 was administered to both groups of mice. Prominent parietal cell loss and inflammation were observed by H&E within the fundic mucosa of all mice (Figure 4A). Immunostaining for Ly6B.2, a neutrophil and polymorphonuclear cell marker, confirmed effective depletion of neutrophils in L653-Ly6G-treated mice compared to control L635-IgG-treated mice (Figure 4B and D). Macrophage and dendritic cells labeled by

F4/80 antibody were not significantly altered by neutrophil depletion (Figure 4C and D). The number of SPEM cells increased five-fold, while SPEM cell proliferation increased 40 to 50-fold, in both neutrophil-depleted and control L635-treated mice (Figure 5A, B, and C). Quantitative PCR for intestinal transcripts revealed a significant upregulation of *Cftr*, *Dmbt1* and *Gpx2* in both neutrophil-depleted and control L635-treated mice (Figure 5D). These results indicate that neutrophils are not necessary for the development of acute advanced proliferative SPEM.

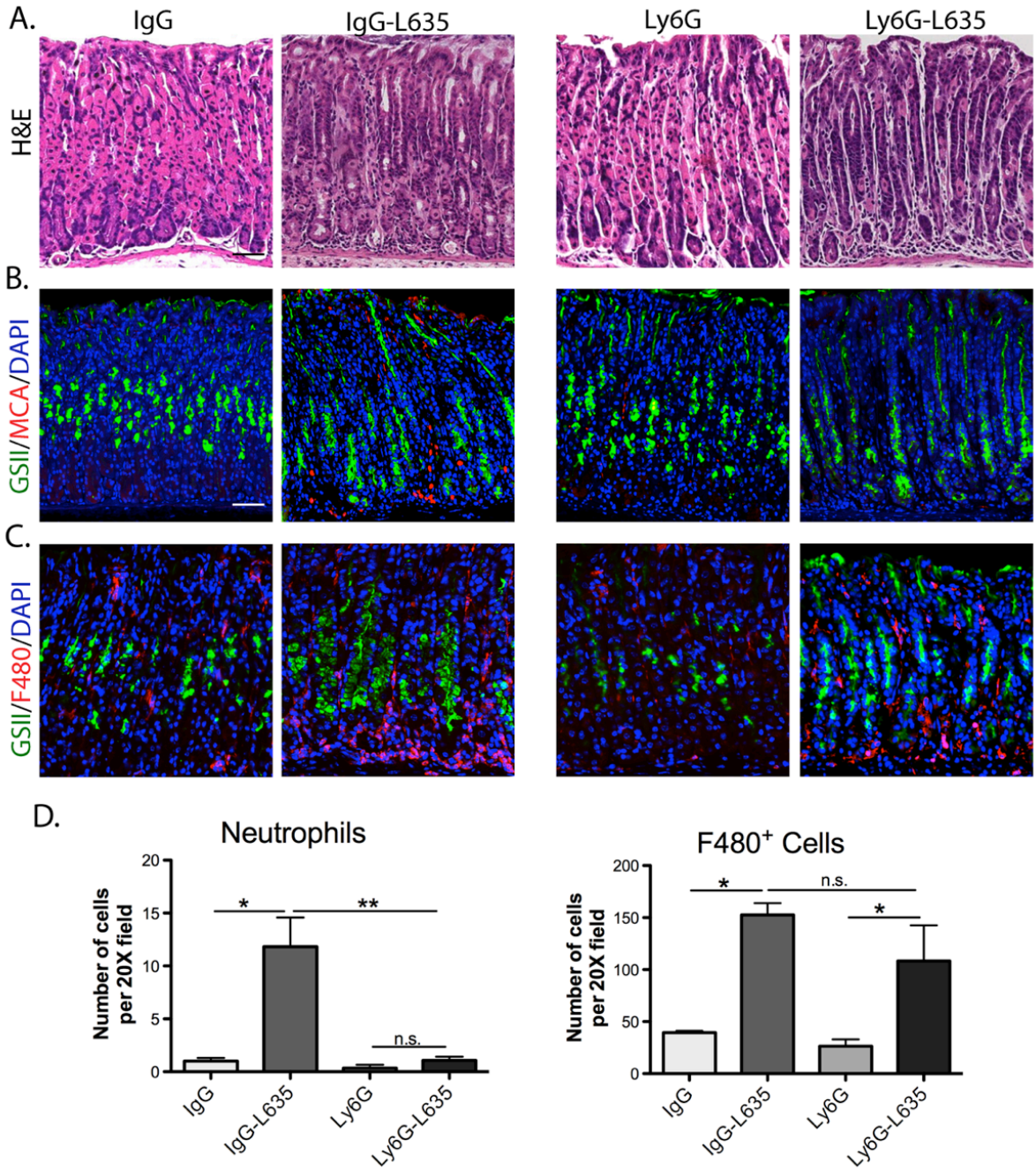

Figure 5: Effective neutrophil depletion did not significantly alter macrophage recruitment. A. Hematoxylin and eosin staining of control and neutrophil-depleted mice. B. Immunofluorescence staining of neutrophils with antibodies against Ly6B.2 (red) co-labeled with GSII-lectin (green) and DAPI (blue) in mice treated with either control IgG or anti-Ly6G to deplete neutrophils. Note the effective depletion of neutrophils with anti-Ly6G treatment. C. Immunofluorescence staining of macrophages and dendritic cells with F4/80 (red) antibody co-labeled with GSII-lectin (green) and DAPI (blue) in mice treated with either control IgG or anti-Ly6G. D. Quantitation of the total number of neutrophils and macrophages counted per 20X field. IgG-L635-treated mice had a significant increase in neutrophils (*p=0.05) compared to controls. Neutrophils were decreased significantly in mice treated with both anti-Ly6G and L635 (*p=0.05) compared to anti-IgG-L635-treated mice. Macrophages significantly increased in all L635-treated mice (*p=0.05). Macrophage recruitment following L635 treatment was not significantly altered after neutrophil depletion. Scale bars: 50 μm

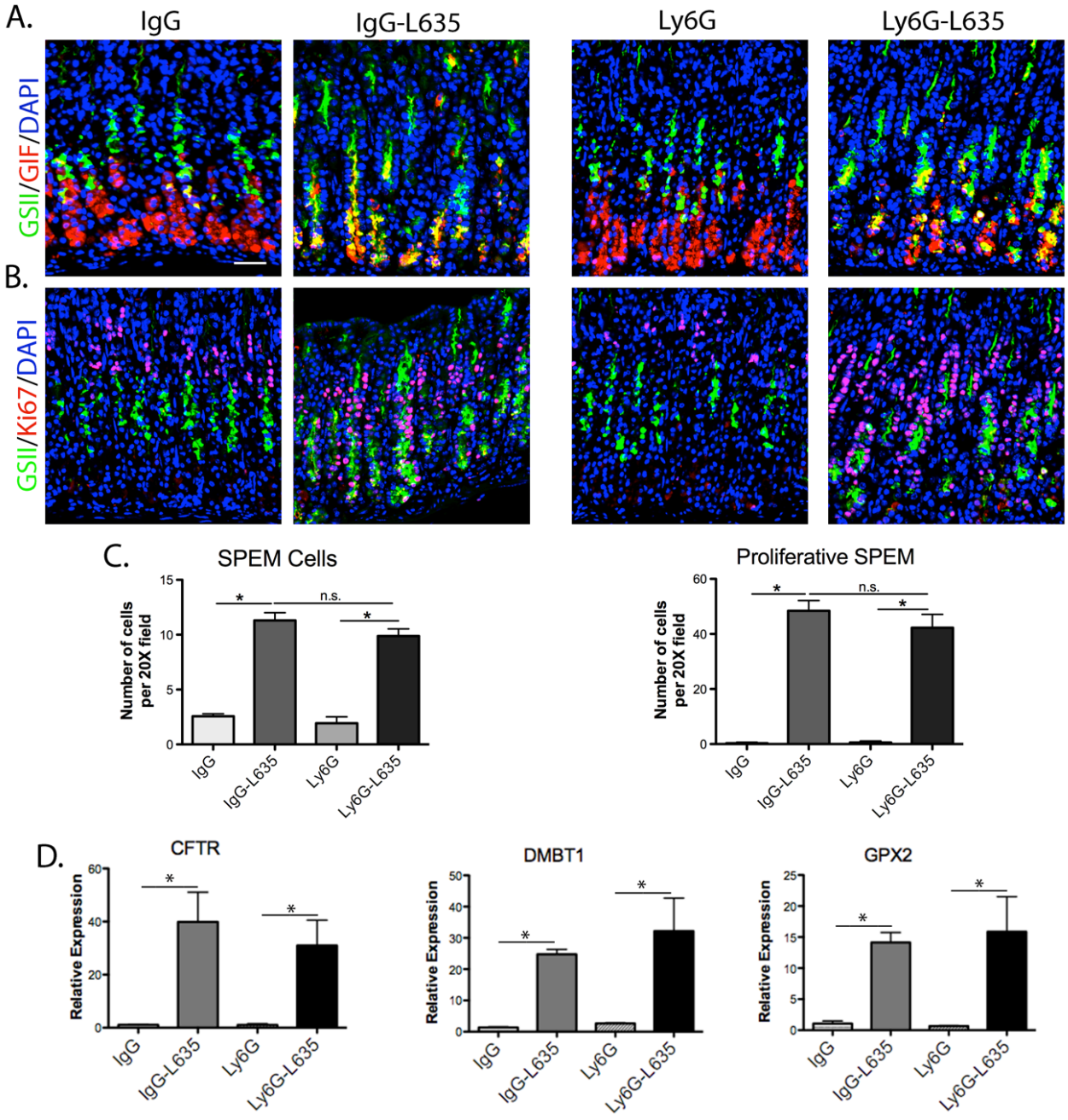

Figure 6: Neutrophil-depletion in mice does not alter the development acute advanced proliferative SPEM after L635 treatment. A. Immunofluorescence staining of SPEM cells with antibodies against GIF (red) co-labeled with GSII-lectin (green) and DAPI (blue) in mice treated with either control anti-IgG or anti-Ly6G. B. Immunofluorescence staining of proliferating cells with antibodies against Ki67 (red) co-labeled with GSII-lectin (green) and DAPI (blue), in untreated or L635-treated mice administered either control anti-IgG or anti-Ly6G to deplete neutrophils. C. Quantitation of $GSII^+$ and GIF^+ cells (SPEM) and proliferative SPEM cells per 20X field. IgG-L635-treated mice had a significant increase in SPEM cells and proliferative SPEM cells (*p=0.05) compared to anti-IgG untreated mice. In mice treated with anti-Ly6G and L635 we observed significant increases in SPEM cells and proliferative SPEM cells (*p=0.05) compared to anti-Ly6G untreated mice. D. qPCR of intestinal transcript markers. All L635-treated mice showed similar increases in *Cftr*, *Dmbt1* or *Gpx2* expression (*p=0.05). Scale bars: 50 μm.

Macrophages are involved in the development of acute L635-induced SPEM

Macrophages make up a significant portion of the inflammatory infiltrate in L635-treated mice (Nam et al., 2010b). Therefore, we evaluated the impact of macrophage depletion using clodronate on the development of SPEM induced by L635. Mice were treated with either clodronate-containing liposomes or control liposomes without clodronate for two days prior to and throughout the three days of L635 administration. All L635-treated mice showed significant parietal cell loss (Figure 6A). Mice treated with L635 and either control liposomes or clodronate demonstrated a 10 to 15-fold increase in neutrophils (Figure 6B and D). Therefore neutrophil recruitment was not significantly affected by macrophage depletion (Figure 6D).

The antibody F4/80 was utilized to identify macrophages and dendritic cells to confirm macrophage depletion by clodronate treatment. In untreated mice an average of 50 tissue-resident macrophages and/or dendritic cells was observed per 20X field (Figure 6C). These resident immune cells serve to alert the host to invading pathogens and to clear dead cells (Chow et al., 2011). After L635 administration, F4/80 positive cells increased three-fold in control mice; however, the number of F4/80 positive cells in the gastric fundic mucosa of clodronate-L635-treated mice remained unchanged and similar to untreated mice (Figure 6C and D). These findings suggest that clodronate-containing liposomes depleted systemic macrophages, but not tissue-resident macrophages or dendritic cells in the stomach.

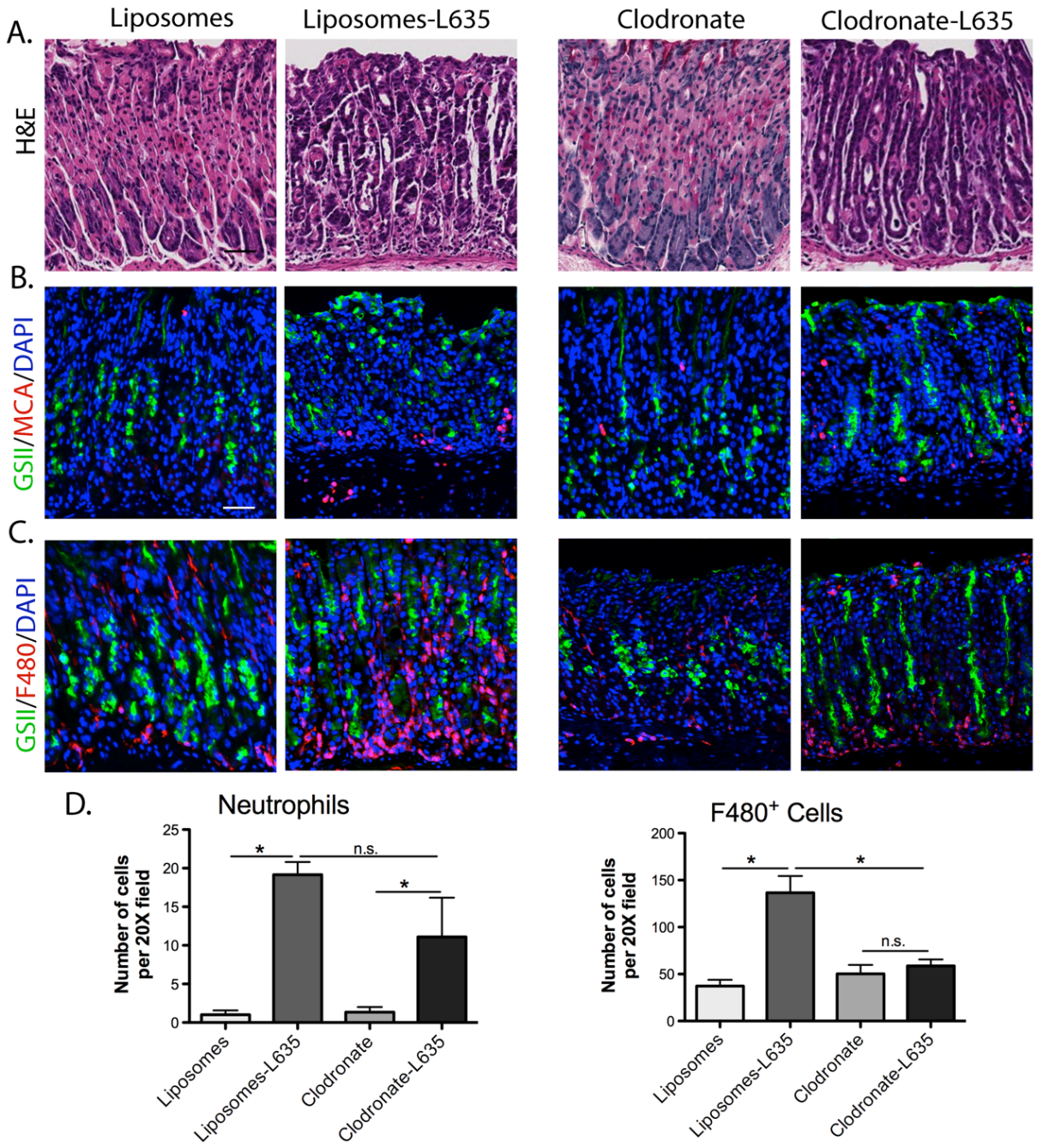

Figure 7: Clodronate treatment reduced the influx of macrophages into the fundic mucosa after L635 treatment. A. Hematoxylin and eosin staining of control (liposome-treated) and macrophage-depleted (clodronate-treated) mice. B. Immunofluorescence staining of neutrophils with antibodies against Ly6B.2 (red) co-labeled with GSII-lectin (green) and DAPI (blue) in mice treated with either control liposomes or clodronate to deplete macrophages. C. Immunofluorescence staining of macrophages with antibodies against F4/80 (red) co-labeled with GSII-lectin and DAPI in mice treated with either control liposomes or clodronate. D. Quantitation of total numbers of neutrophils and macrophages counted per 20X field. Neutrophils increased significantly in both control and macrophage-depleted L635-treated mice (*p=0.05). Neutrophil numbers were not significantly affected in mice treated with both clodronate and L635. Note that macrophage recruitment into the fundic mucosa was inhibited in mice treated with both clodronate and L635 (*p=0.05). Scale bars: 50 μm.

After L635 administration, control mice showed a five-fold increase in SPEM cells, while clodronate-treated mice L635 elicited only a two-fold increase in the number of SPEM cells (Figure 7A and C). Furthermore, SPEM cell proliferation increased 40-fold in control L635-treated mice, but only 10-fold in mice treated with both clodronate and L635 (Figure 7B and C). Therefore, macrophage depletion significantly attenuated the number of SPEM cells per gland and the proliferative response in SPEM following L635 administration (Figure 7A, B, and C). Notably, mice treated with both clodronate and L635 demonstrated significantly lower levels of intestinal transcripts for *Cftr*, *Dmbt1* and *Gpx2* compared to the L635-treated control mice (Figure 7D).

We have previously shown that IL-1β and IL10 expression significantly increases in SPEM associated with inflammation (Nam et al., 2010b). Thus, we sought to evaluate how depletion of macrophages might affect these specific cytokine levels. As previously noted (Nam et al., 2010b), control mice demonstrated a significant increase in IL-1β following L635 administration (Figure 7E). However, IL-1β cytokine expression was significantly reduced in clodronate-L635-treated mice compared to L635-treated mice (Figure 7E). In contrast, clodronate treatment had no significant effect on TNFα or IL10 expression, which can be produced by other cells besides macrophages. IFNγ and IL4 were undetectable in all samples (data not shown).

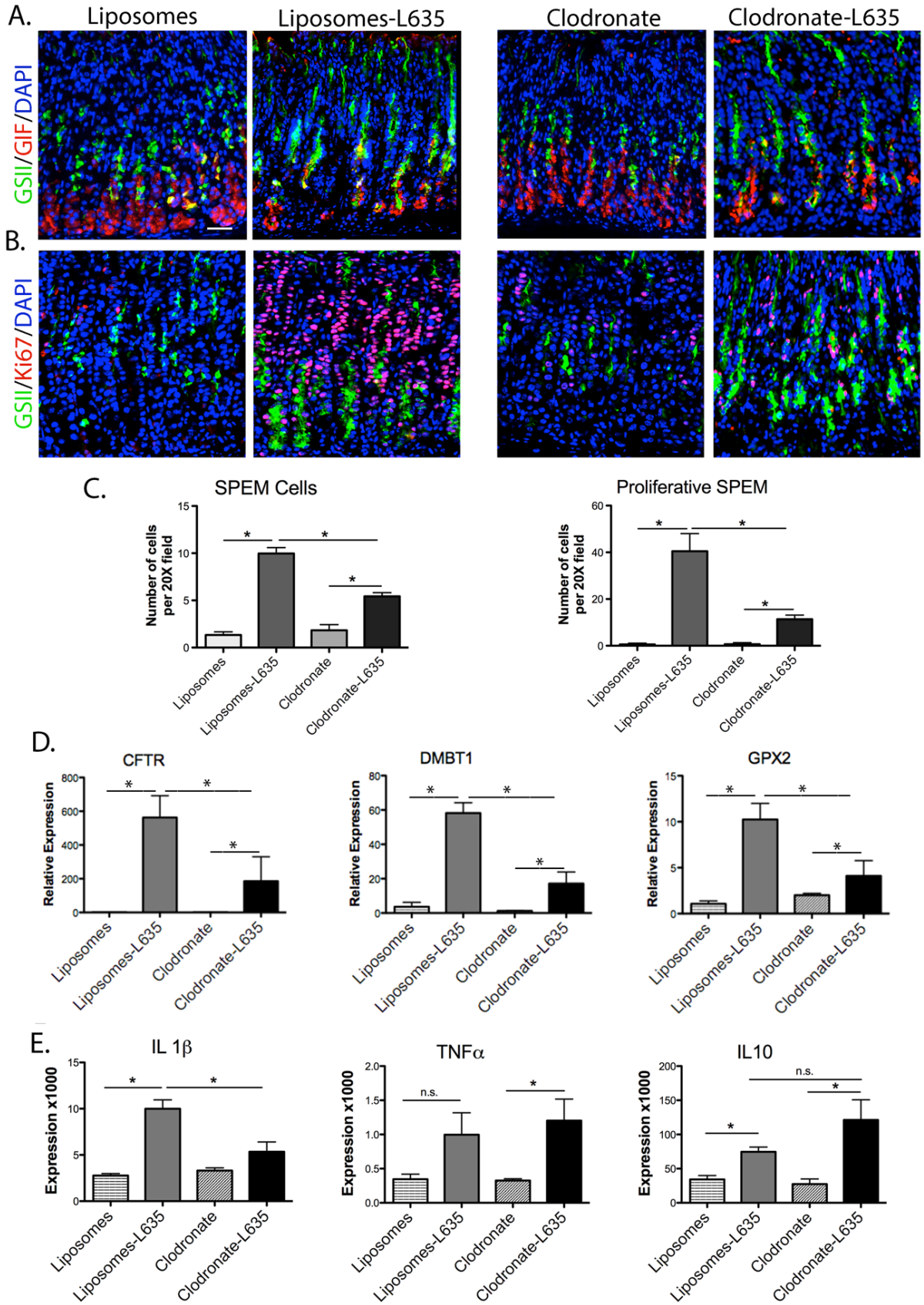
A.
Liposomes
Liposomes-L635
Clodronate
Clodronate-L635
GSII/GIF/DAPI
B.
GSII/Ki67/DAPI
C.
SPEM Cells
Number of cells per 20X field
Proliferative SPEM
Liposomes
Liposomes-L635
Clodronate
Clodronate-L635
D.
CFTR
DMBT1
GPX2
Relative Expression
E.
IL 1β
TNFα
IL10
Expression x1000
n.s.

Figure 8: Macrophage depletion inhibits the development of proliferative SPEM following L635 treatment. A. Immunofluorescence staining of SPEM cells with antibodies against GIF (red) co-labeled with GSII-lectin (green) and DAPI (blue) in mice treated with either control liposomes or clodronate-containing liposomes, with or without L635-treatment. B. Immunofluorescence staining of proliferating SPEM cells with antibodies against Ki67 (red) co-labeled with GSII-lectin (green) and DAPI (blue). C. Quantitation of the number of $GSII^+$ and GIF^+ cells (SPEM) and proliferative SPEM cells. Mice treated with both clodronate and L635 had significantly reduced SPEM cell numbers and SPEM cell proliferation (*p=0.05) compared to mice treated with liposomes and L635. D. qPCR showing relative expression of intestinal transcript markers. Clodronate treatment significantly reduced the expression of *Cftr*, *Dmbt1* and *Gpx2* in L635-treated mice (*p=0.05). E. qPCR for *IL1b*, *TNFa* and *IL10* cytokines. Clodronate treatment only significantly reduced *IL1b* expression (*p=0.05). Scale bars: 50 μm.

DMP-777 induced SPEM does not recruit macrophages

DMP-777 drug treatment induces SPEM over an 8-day treatment without appreciable inflammation (Goldenring et al., 2000a). In contrast with SPEM induced by L635 treatment, DMP-777-induced SPEM demonstrates only a low proliferative rate. Furthermore, DMP-777-Other groups have noted that clodronate treatment does not influence tissue resident macrophage or dendritic cell populations in some organs (Ferenbach et al., 2012; van Amerongen et al., 2007). Importantly, we observed a lack of immunostaining for the macrophage marker CD68 and only a rare Arginase II positive cell in DMP-777 treated mice, indicating neither M2 macrophages nor macrophages were recruited into the gastric mucosa during DMP-777 treatment (Figure 8D and 5E). A previous study showed local expansion of tissue resident macrophages in association with tissue maintenance or inflammation (Jenkins et al., 2011). Thus, the increase in F4/80+ cells in DMP-777 treated mice likely reflects the expansion of tissue resident dendritic cells within the gastric mucosa. The lack of an effect of macrophage depletion on SPEM development induced by DMP-777 supports the concept that infiltration by macrophages promotes the progression to an advanced proliferative metaplasia.

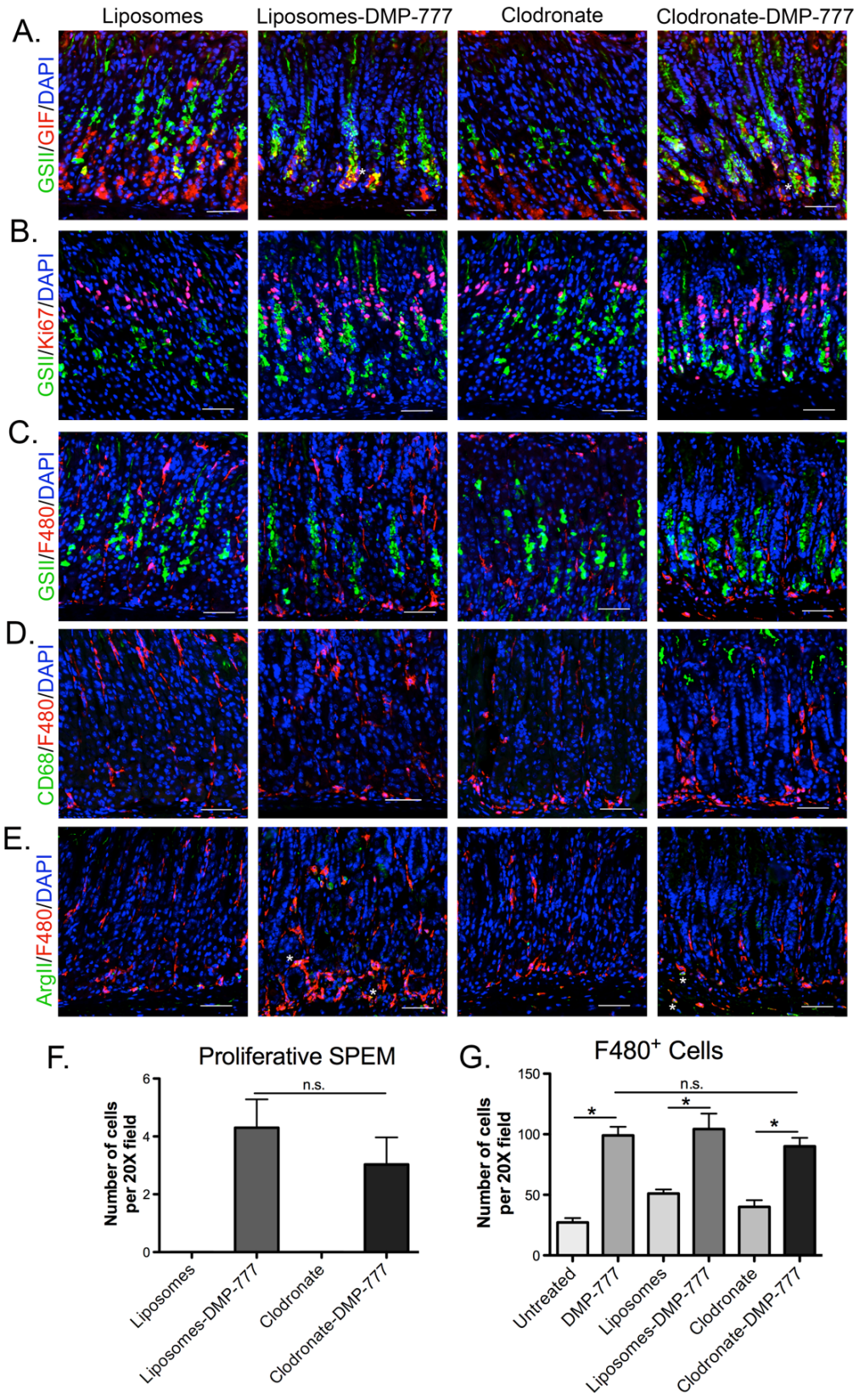
Liposomes
Liposomes-DMP-777
Clodronate
Clodronate-DMP-777
A.
GSII/GIF/DAPI
B.
GSII/Ki67/DAPI
C.
GSII/F480/DAPI
D.
CD68/F480/DAPI
E.
ArgII/F480/DAPI
F.
Proliferative SPEM
Number of cells per 20X field
n.s.
Liposomes
Liposomes-DMP-777
Clodronate
Clodronate-DMP-777
G.
F480+ Cells
Number of cells per 20X field
n.s.
Untreated
DMP-777
Liposomes
Liposomes-DMP-777
Clodronate
Clodronate-DMP-777

Figure 9: Macrophage depletion does not affect SPEM cell proliferation or F4/80 positive cells in DMP-777-treated mice. Immunofluorescence of fundus in control liposome and liposome-DMP-777-treated mice compared to clodronate and clodronate-DMP-777-treated mice. A. Immunolabeling for SPEM cells using GSII-lectin (green), gastric intrinsic factor (GIF) (red), and DAPI (blue). Eight days of DMP-777 treatment induced SPEM in both liposome and clodronate-treated mice. An asterisk denotes co-positive GSII and gastric intrinsic factor staining SPEM cells. B. Immunolabeling to identify proliferative SPEM. Ki67 (red) used to mark proliferating cells with GSII-lectin (green). Unlike L635-treatment, DMP-777-treatment does not induce highly proliferative SPEM. C. Immunolabeling for macrophages and dendritic cells using F4/80 antibody (red). D. Immunolabeling for macrophages using CD68 antibody (green). DMP-777 treatment does not recruit CD68 positive macrophages to the mucosa, indicating that the F4/80 positive cells present are likely dendritic cells. E. Immunolabeling for M2 marker, Arginase II. There were very few M2 positive cells in DMP-777 treated mice, and labeling was unaffected by clodronate treatment. F. Quantitation of proliferative SPEM Cells (identified as cells triple-labeled for GSII, Ki67 and gastric intrinsic factor 20X field). There was no change in the number of proliferating SPEM cells between control and macrophage-depleted DMP-777-treated mice. Of note, there were few proliferating SPEM cells in DMP-777 treated mice. G. Quantitation of F4/80 positive cells per 20X field. F4/80 positive cells significantly increased (*p=0.05) after DMP-777 treatment in all mouse models, indicating an expansion of dendritic cells during DMP-777 treatment that is unaffected by clodronate administration. Scale bars: 50 μm.

Macrophages in L635-treated mice express M2 polarization markers

Macrophage activation is typically described as either "classical" (M1) or "alternative" (M2) (Stoger et al., 2012). M1 polarized macrophages are considered pro-inflammatory and are associated with iNos expression (Quiding-Jarbrink et al., 2010). In contract, M2 macrophages are associated with wound healing and are anti-inflammatory, but are also known to promote neoplasia (Murray and Wynn, 2011). We assessed the characteristics of the infiltrating macrophages after L635 treatment to determine M1 or M2 polarization. The F4/80^{+} cells at the base of glands after L635-treatment were identified as macrophages through co-staining with CD68 (Figure 9A). The macrophages present in L635-treated mice were also positive for the M2 marker and hemoglobin-scavenger receptor CD163, but were negative for the M1 marker iNos (Figure 9B and C) (Heusinkveld and van der Burg, 2011; Verreck et al., 2006). Furthermore, L635-treated mice displayed a predominance of Arginase II (ArgII) positive macrophages, likely an M2 marker as Arginase II competes for similar substrates as iNos

(Figure 9D) (Bronte and Zanovello, 2005). In contrast, as noted above, F4/80$^+$ cells in DMP-777-treated mice were negative for macrophage markers (Figure 9) with the exception of rare ArgII$^+$ cells in the submucosa (Figure 9D).

To further characterize macrophage polarization, M1 and M2 transcript expression was analyzed using RNA from fresh whole fundic tissue for qRT-PCR (Figure 10). M1 markers *Cxcl10*, *Cd3* and *Nos2* were all significantly upregulated after DMP-777 and L635 administration, but both the absolute expression levels and the magnitude of expression changes were small (Figure 10A). In contrast, the expression of the M2 marker *Ym1* increased 75-fold and *ArgII* expression increased 5-fold (Figure 10B) in L635-treated mice. M2 macrophages produce high levels of Ym1, which is proposed to deposit extracellular matrix for wound healing (Chang et al., 2001; Nair et al., 2005). *Fizz1* increased to equal levels with both DMP-777 and L635 treatment, which may be reflective of *Fizz1* expression in both macrophages and dendritic cells (Nair et al., 2005). Therefore, while a few iNos (protein expression of *Nos2*) positive M1 cells can be detected, the majority of macrophages infiltrating into the mucosa after L635-treatment were M2 polarized.

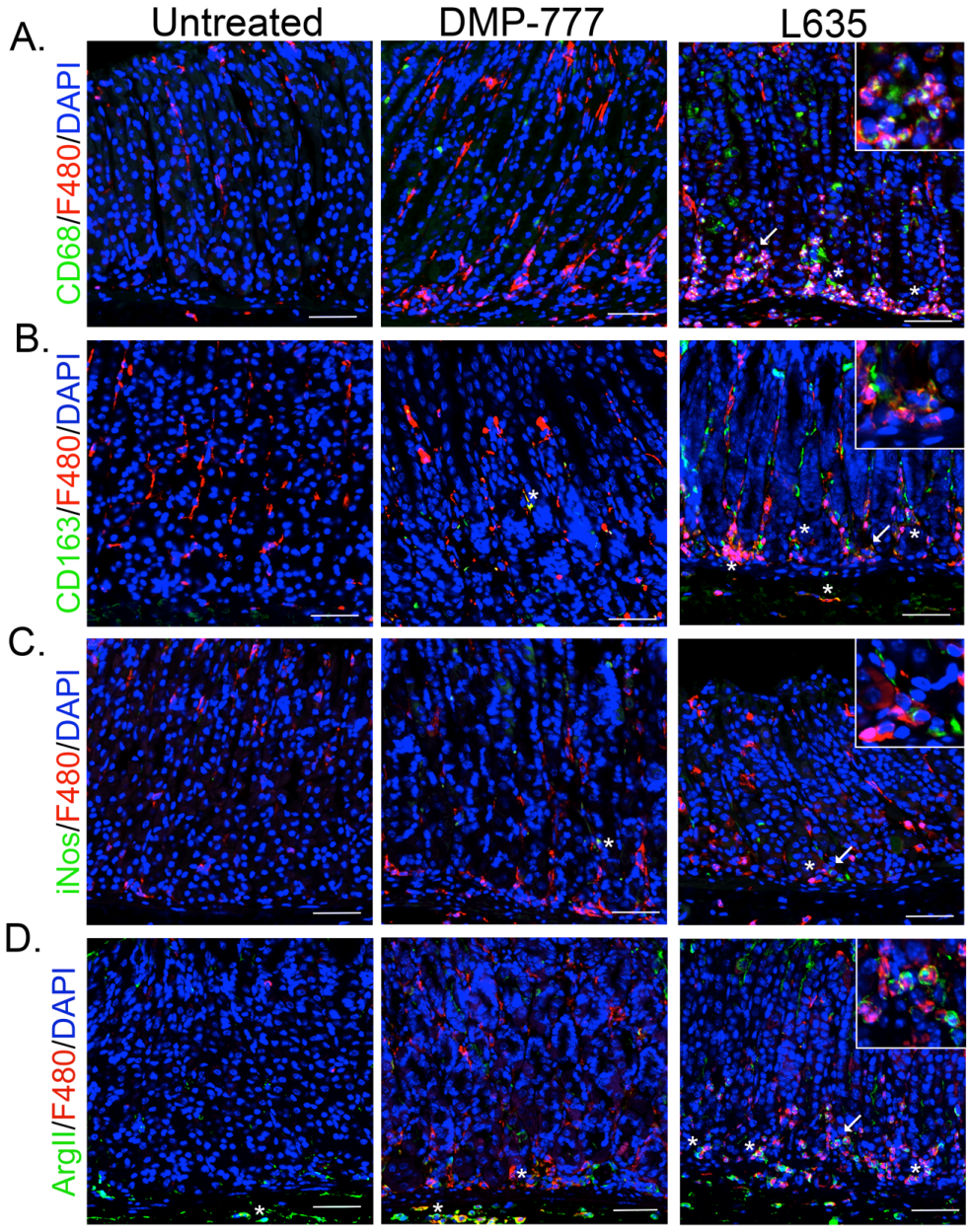

Figure 10: Macrophages are M2 polarized in L635-treated mice, but not in DMP-777-treated mice. Immunofluorescence of fundic mucosa from untreated, DMP-777 and L635-treated mice. A. Identification of macrophages by co-positive CD68 (green) and F4/80 (red) cells. F4/80 positive cells, negative for CD68 staining were considered dendritic cells. F4/80 positive cells at the base of glands in L635-treated mice were also CD68 positive. Inset in L635 panel illustrating dual-positive F4/80 and CD68 cells. B. Immunofluorescence staining of CD163 (green) marked M2 polarized macrophages. Several CD163 positive M2 polarized macrophages co-labeling with F4/80 are present in L635-treated mice. Inset showing CD163 and F4/80 co-positive cells. C. Immunofluorescence staining of the M1 marker iNos (green), F4/80 (red) and DAPI (blue). Inset in L635 showing rare iNos and F4/80 positive cells. D. Immunofluorescence of Arginase II (green), an M2 marker, with F4/80 (red) and DAPI (blue). DMP-777-treated mice had a few Arginase II and F4/80 co-positive cells, mostly localized to the submucosa. L635-treated mice have several Arginase II and F4/80 co-positive cells within the mucosa. Scale bars: 50 μm. All insets show enlarged view of area marked by arrow. All co-positive cells marked by asterisk.

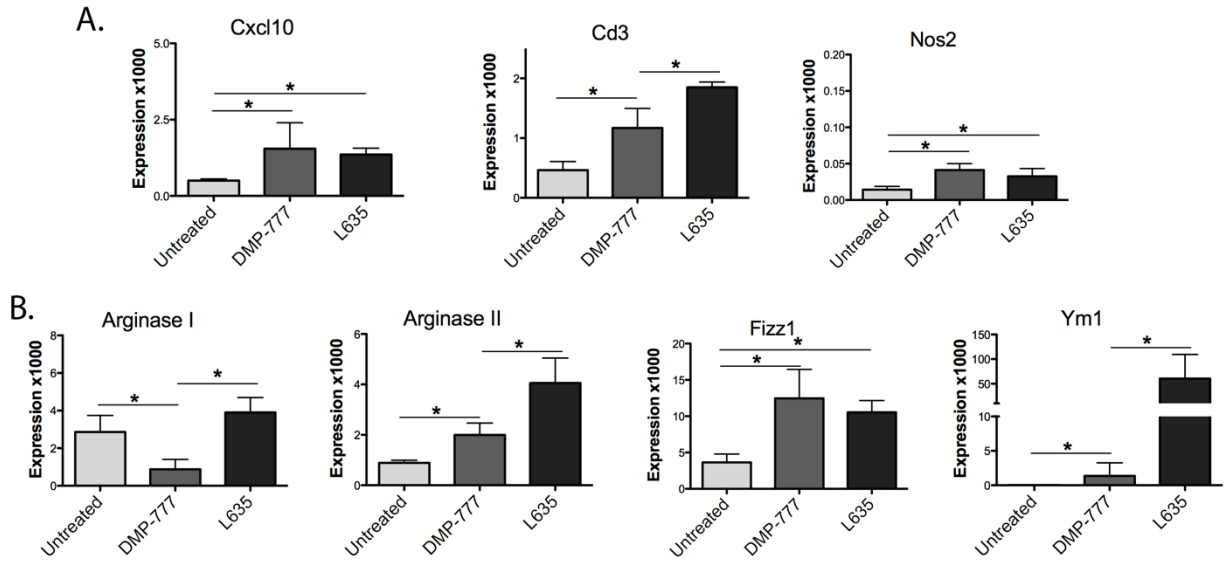

Figure 11: M2 marker transcripts are markedly increased in L635-treated mice. Quantitative PCR showing mRNA expression from whole fresh fundus of M1 and M2 markers normalized to *GAPDH*, shown as expression level multiplied by 1000 for scale. A. M1 markers *Cxcl10*, *Cd3*, and *Nos2* all significantly increase (*p=0.05) in DMP-777 and L635-treated mice. However, the expression levels overall of the M1 markers are very low. B. M2 markers *Arginase I*, *Arginase II*, *Fizz1*, and *Ym1* all significantly increase in L635-treated mice (*p=0.05).

M2 macrophages increase in human SPEM and intestinal metaplasia

Based on the characteristics of macrophages found in the murine model, we examined macrophages associated with stomach metaplasia in humans. Normal human fundic mucosa contained $CD68^+$ macrophages (Figure 11A and D). However, in mucosa with SPEM and intestinal metaplasia (IM), the number of $CD68^+$ macrophages significantly increased two to three-fold (Figure 11B, C and D). Typically macrophages were dispersed throughout the SPEM area, while in IM the macrophages clustered together in regions around blood vessel-like structures (Figure 11B and C inset). Normal gastric tissue demonstrated only a few M2 polarized macrophages labeled with CD163 (Figure 11A and E), which increased two to three-fold SPEM and IM (Figure 11B, C and E).

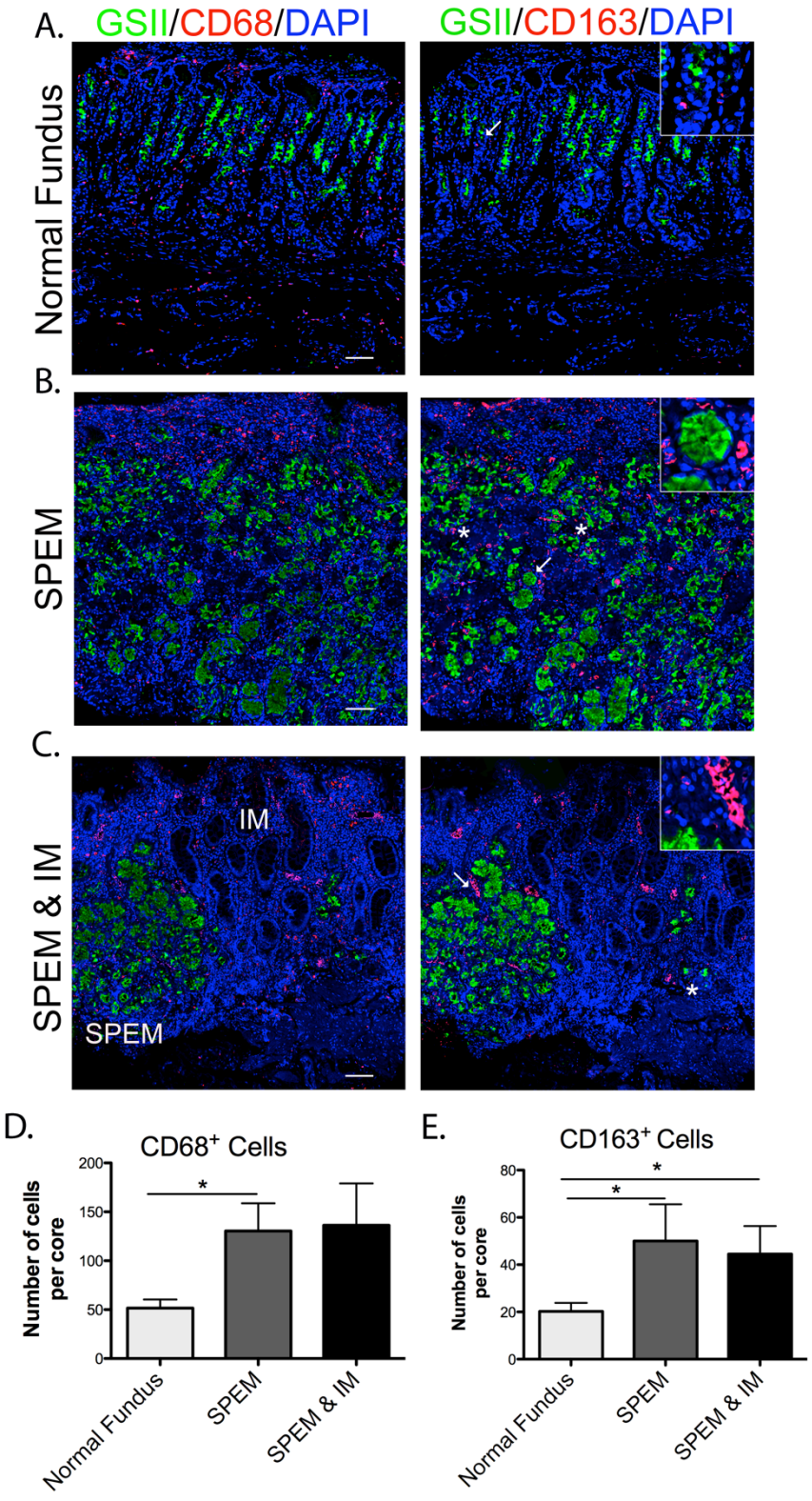
A.
GSII/CD68/DAPI
GSII/CD163/DAPI
Normal Fundus
B.
SPEM
C.
SPEM & IM
IM
SPEM
D.
CD68+ Cells
Number of cells per core
200
150
100
50
0
*
Normal Fundus
SPEM
SPEM & IM
E.
CD163+ Cells
Number of cells per core
80
60
40
20
0
*
*
Normal Fundus
SPEM
SPEM & IM

Figure 12: M2 macrophage infiltration in human SPEM and IM.
A. Left panel: Normal human mucosa labeled with GSII-Lectin (green) marking mucus neck cells and CD68 (red) for macrophages. Right panel shows CD163 (red) antibody labeling for M2 macrophages, GSII-Lectin (green) and DAPI (blue) in a serial section. B. Left panel: SPEM in human tissue immunolabeled with GSII-Lectin (green), CD68 (red) and DAPI (blue), showing an increased number of CD68+ macrophages. Right panel shows an increase in CD163 (red) M2 marker staining cells in a serial section. Inset in right panel is showing SPEM surrounded by CD163+ macrophages C. Left panel: SPEM (GSII-Lectin in green) and IM show increased CD68+ (red) macrophages clustered around vessel-like structures. Right panel: CD163 staining in a serial section demonstrates macrophages were M2 polarized in SPEM and IM. Inset showing M2 macrophages cluster around vessel-like structures. D. Quantitation of $CD68^+$ macrophages per core in normal, SPEM and IM. CD68 positive cells significantly increase (*p=0.05) from normal fundus to SPEM, and SPEM/IM. D. Quantitation of CD163 positive cells per core. The number of M2 polarized macrophages significantly increased (*p=0.05) from normal to SPEM and SPEM/IM tissue. Scale bars: 50 μm. All insets show enlarged view of area marked by arrow.

Discussion

The loss of parietal cells, also known as oxyntic atrophy, is considered an absolute requirement for the development of both metaplasia and intestinal-type gastric cancer (El-Zimaity et al., 2002; Goldenring et al., 2010; Meining et al., 2001). Nevertheless, the exact cause of parietal cell loss during chronic *Helicobacter* infection remains unclear. Previous studies have investigated the role of immune factors during *Helicobacter* infection and their impact on parietal cell loss and the development of metaplasia. Severe combined immune deficient (SCID) mice do not undergo parietal cell loss following *H. pylori* infection, implicating the adaptive immune system in the development of *Helicobacter*-associated oxyntic atrophy (Smythies et al., 2000). Roth et al. found that Rag1 knockout mice, deficient in mature T and B lymphocytes, do not lose parietal cells when infected with *H. pylori* (Mombaerts et al., 1992; Roth et al., 1999). In further studies, they found that T-cells were necessary for parietal cell loss during *H. pylori* infection (Roth et al., 1999). Therefore, the T-cell-mediated response to *H. pylori* infection results in oxyntic atrophy, a prerequisite for induction of metaplasia (Appelmelk et al., 1996; Roth et al., 1999).

While the loss of parietal cells during *Helicobacter* infection requires the influence of T-cells, the development of metaplasia appears to relate directly to parietal cell loss. Our recent investigations have demonstrated that SPEM is derived from transdifferentiation of chief cells in mice (Goldenring et al., 2010; Nam et al., 2010b; Weis et al., 2012; Yoshizawa et al., 2007). In the present studies, L635-treated Rag1KO mice developed proliferative SPEM and upregulated intestinal transcripts similar to wild type L635-treated mice. Thus, while T-cells are necessary for parietal cell loss in chronic *Helicobacter* models to facilitate the development of SPEM (Roth et al., 1999), T-cells are not necessary for the development of SPEM in the acute L635 treatment model. It is important to note that DMP-777 and L635 treatments directly induce parietal cell loss bypassing the mechanisms that require T-cell influences to induce oxyntic atrophy in association with *Helicobacter* infection. These models can be used to decouple the immune influences required to induce oxyntic atrophy from the mechanisms of chief cell transdifferentiation into metaplasia. Furthermore, studies using the drugs DMP-777 and L635 have demonstrated that SPEM does not progress to an advanced proliferative metaplasia without the presence of inflammation (Goldenring et al., 2000a; Weis et al., 2012). Thus, the present study addresses the role of different immune factors in the development of advanced SPEM after parietal cell loss using the drug L635.

Previous studies have evaluated the role of specific cytokines secreted by T-cells such as IFNγ in oxyntic atrophy and SPEM (Liu et al., 2012; Tu et al., 2011). IFNγ secreted by T-cells drives several different immune processes, including the activation of macrophages and upregulation of IFNγ target genes in epithelial cells (Houghton et al., 2004; Kang et al., 2005). Liu et al. used a knockout of Hip1r, a model of parietal cell loss through apoptosis, crossed to IFNγ knockout mice to show reduced metaplasia initially; but over a longer time course, loss of IFNγ did not impair the development of SPEM (Liu et al., 2012; Mueller et al., 2004). In contrast, *Helicobacter*-infected mice overexpressing IFNγ through the H^+/K^+-ATPase promoter develop less *Helicobacter*-associated gastric pathology due to increased epithelial autophagy

and decreased parietal cell loss, indicating that IFNγ may also have a cytoprotective role (Tu et al., 2011). Using a similar model to overexpress IFNγ, Syu et al. reported IFNγ induced metaplasia (Syu et al., 2012). In the present study, L635-treated IFNγKO mice developed SPEM similar to wild type mice. The difference in our findings may depend on experimental conditions used to induce parietal cell loss. Furthermore, the mouse models manipulating IFNγ likely focus on mechanisms related to promotion of chronic parietal cell loss, whereas the L635 treatment model causes rapid toxic loss of parietal cells. The L635 treatment model therefore focuses on the regulation of the processes influencing the transdifferentiation of chief cells into SPEM and their development to more advanced proliferative metaplasia. Our present data indicate that IFNγ is not a requisite mediator in the development of acute advanced SPEM.

While shorter lived than macrophages, neutrophils are a highly effective phagocytic cells that are tightly controlled due to their high cytotoxicity (Silva, 2010). Neutrophil-associated tissue damage caused by extravasation, increased vascular permeability, neutrophil-derived destructive enzymes and reactive oxygen species is well documented (Kozol et al., 1991; Silva, 2010). Nevertheless, neutrophils play an essential role in clearing *Helicobacter* infection (Ismail et al., 2003). Typically, phagocytic neutrophils are scarce in the normal stomach mucosa and enter during infection or injury (Fox et al., 1993; Roth et al., 1999), driven in part by chemokines released by epithelial cells (Kozol et al., 1991) and tissue-resident macrophages and dendritic cells (Blaser, 1992; Evans et al., 1995; Mai et al., 1991; Wroblewski et al., 2010). After L635 administration, there is increased neutrophil infiltration, but neutrophil-depleted L635-treated mice developed similar levels of proliferative SPEM and intestinalizing transcript expression as in L635-treated control mice. Therefore, neutrophils are not necessary for the development of advanced SPEM in this model.

Acute injury or infection immediately stimulates antigen-presenting cells, tissue-resident macrophages and dendritic cells, to engulf tissue debris and foreign antigens (Silva, 2010). These cells secrete cytokines that not only influence the adaptive immune system through T-

cell differentiation, but also promote the homeostasis of surrounding epithelial cells, while increasing the inflammatory response (Chow et al., 2011). The short time course of L635 treatment to ablate parietal cells and induce SPEM in just three days facilitated examination of the influence of macrophages on SPEM induction using clodronate treatment, an experimental paradigm that is not practical in conjunction with chronic *Helicobacter* infection models. Clodronate-treated mice demonstrated the same number of F4/80-positive cells with or without L635 treatment. The remaining F4/80-positive cells were likely tissue resident macrophages and dendritic cells that do not label for CD68, and are unaffected by clodronate treatment (Ferenbach et al., 2012). Recently, Hashimoto et al. suggested that tissue-resident macrophages and circulating monocytes are independently maintained at a steady state, and therefore tissue resident macrophages and invading monocytes have varied responses and may not behave similarly (Hashimoto et al., 2013). Indeed, we have observed that DMP-777 treatment increased the number of CD68-negative, F4/80-positive cells, but clodronate had no effect on the induction of SPEM by DMP-777. L635-treated macrophage-depleted mice demonstrated a significant reduction in SPEM cell numbers, SPEM cell proliferation and expression of intestinal transcripts. Therefore, while the discrete role of dendritic cells in SPEM induction remains unclear, the results here indicate that infiltrating macrophages contribute to the advanced metaplastic phenotype in L635-induced SPEM.

Macrophage secretion of several different pro-inflammatory cytokines is well documented (Beuscher et al., 1990; Mai et al., 1991). Cytokine transcript expression for IL-1β, which is secreted by activated macrophages, is increased significantly in L635-treated and *H. felis*-infected mice (Beuscher et al., 1990; Nam et al., 2010b). Notably, macrophage-depleted L635-treated mice have significantly reduced IL-1β transcript expression compared to L635-treated control mice. IL-1β cytokine acts to propagate the inflammatory response and inhibits gastric acid secretion (Beales and Calam, 1998). Transgenic mice that overexpress human IL-1β in the stomach develop spontaneous gastritis and eventually dysplasia after a year (Tu et

al., 2008). However the specific role of IL-1β in the advancement of SPEM is still unknown. Tumor necrosis factor alpha (TNFα) and IL-10, which are secreted by activated macrophages and other inflammatory cell types as well as mucosal cells, increase significantly in *H. felis* mice (Beales and Calam, 1998; Nam et al., 2010b). Nevertheless, since depletion of macrophages did not reduce TNFα or IL-10 levels in L635-treated mice, these cytokines may not contribute to the progression of metaplasia in the acute SPEM model. However, it is likely that specific macrophage cytokines contribute to the advancement of SPEM.

M2 polarized macrophages are attributed to the progression of several reported disease states (Oshima et al., 2011a; Zaynagetdinov et al., 2011). Inhibiting macrophage infiltration using a monocyte chemoattractant protein-1 (MCP-1, CCL2) antagonist led to tumor regression in *Gan* mice, a murine model of gastric cancer (Oshima et al., 2011a). In GAN mice, infiltrating macrophages were M2 polarized, supporting our findings that M2 macrophages are important in the advancement of metaplasia (Oshima et al., 2011b). While we observed a small increase in M1 marker expression, it was minor compared to the dramatic increase observed in M2 marker expression. This finding, coupled with positive staining of CD163 and Arginase II, indicates that macrophages present in L635-treated mice are M2 polarized, but are not present in DMP-777-treated mice. Therefore, while neither $CD68^+$ macrophages nor M2 macrophages are required for the induction of SPEM, M2 macrophages are important for advancing the metaplastic phenotype. This result in mice was supported in human metaplasia, where half of the observed macrophages where M2 polarized. Fehlings et al. reported similar findings of increased $CD163^+$ cells in *H. pylori*-infected patients (Fehlings et al., 2012), supporting the concept that M2 macrophages promote SPEM progression and intestinal metaplasia.

In summary, our data suggest that circulating monocytes invade the gastric mucosa during L635 administration and promote the advancement of SPEM. The macrophages associated with advanced proliferative metaplasia were polarized towards M2, a phenotype

associated with promotion of tumorogenesis in mice and humans (Heusinkveld and van der Burg, 2011; Oshima et al., 2011b). While T-cells and neutrophils may have critical influences on the induction of parietal cell loss in the gastric mucosa during *Helicobacter* infection, these immune cell populations do not appear to have significant direct influences on the emergence of SPEM from transdifferentiation of chief cells or the advancement of SPEM to a more proliferative metaplasia with intestinal characteristics. Further investigations will be required to define the discrete mediators released by M2 macrophages that can promote the process of metaplastic transition.

Chapter III

IL-33 REGULATES METAPLASIA AND MACROPHAGE POLARIZATION IN THE STOMACH

Appear as: Christine P. Petersen, Carlo DeSalvo, Eunyoung Choi, Alec Petersen, Nripesh Prasad, Shawn E. Levy, Theresa T. Pizarro, James R. Goldenring

Introduction

Gastric cancer is a leading cause of cancer-related deaths worldwide (de Martel et al., 2012). Intestinal-type gastric cancer, the most abundant type of gastric adenocarcinoma, is frequently detected at later stages due to poor early clinical indicators. *Helicobacter pylori* is the major risk factor for developing gastric adenocarcinoma by inducing chronic inflammation and loss of acid-secreting parietal cells (oxyntic atrophy) (Blaser and Parsonnet, 1994). Two different types of metaplasia are observed in the atrophic human stomach: spasmolytic polypeptide expressing metaplasia (SPEM) and intestinal metaplasia (Nam et al., 2010b). SPEM arises from the transdifferentiation of mature chief cells and is characterized by antral-type TFF2-expressing mucus cells in the oxyntic body region of the stomach (Nam et al., 2010b). Increasing evidence suggests that intestinal metaplasia, characterized by Muc2-positive goblet cells in the stomach, likely develops from SPEM lesions (Yoshizawa et al., 2007). Both metaplasias are associated with intestinal-type cancer development in the stomach (Goldenring and Nam, 2010; Yoshizawa et al., 2007). However, it remains unclear whether SPEM or intestinal metaplasia is the precursor lineage that gives rise to gastric adenocarcinoma (Goldenring et al., 2010; Nam et al., 2009). Nevertheless, a chronic inflammatory environment promotes the development metaplasia and gastric cancer (Fox and Wang, 2007; Merchant, 2005).

Unlike humans, mice do not typically develop goblet cell intestinal metaplasia. Instead SPEM progresses with increased proliferation and levels of intestinal gene expression, developing into intestinalized SPEM (Weis et al., 2012). Two drugs were previously utilized in our lab to recapitulate the process of oxyntic atrophy and study the progression of SPEM (Goldenring et al., 2000a; Nomura et al., 2005b). DMP-777 is a parietal cell protonophore and neutrophil elastase inhibitor that causes oxyntic atrophy and SPEM with minimal inflammation in the stomach after 10 days of treatment. L635, an analog of DMP-777, causes oxyntic atrophy without inhibiting the inflammatory response. Mice treated with L635 for three days develop a prominent inflammatory infiltrate, that promotes the progression of SPEM into a more proliferative metaplasia with increased expression of intestinal transcripts that resembles lineage changes observed after 6-12 month *Helicobacter felis* infection (Weis et al., 2012; Weis et al., 2013a).

Using clodronate-mediated depletion in L635-treated mice, we recently determined that macrophages were necessary for the development of intestinalized SPEM (Petersen et al., 2014). Macrophage-depleted L635-treated mice had fewer proliferative SPEM cells and a decrease in intestinal transcripts compared to control L635-treated mice. Therefore, macrophage infiltration after acute parietal cell loss drives the advancement of SPEM towards a more proliferative and intestinalized phenotype (Petersen et al., 2014). In addition, macrophages infiltrating into the mucosa after L635 treatment displayed M2-like markers (Petersen et al., 2014). M2 macrophages represent the archetype anti-inflammatory, tumor-associated macrophage driven by Th2 cytokines (Mills et al., 2000). Nevertheless, macrophages specialize in accordance with local environmental stimuli, and therefore are diverse in gene expression and function within different organ systems (Gautier et al., 2012). Furthermore, the generalized M1 and M2 classification that relies solely on a few markers is relatively simplified (Martinez and Gordon, 2014). Thus we sought to characterize macrophages associated with SPEM and intestinalized SPEM to determine the specialized

function of macrophages in the setting of acute injury and to identify factors that contribute to the progression of metaplasia.

Macrophages associated with SPEM (DMP-777-treated mice) or intestinalized SPEM (L635-treated mice) were isolated from the stomach corpus using fluorescent cytometric sorting and RNA was sequenced to generate a profile of metaplasia-associated macrophages. We identified IL-33 as upregulated in macrophages from L635-treated mice compared to DMP-777-treated mice. To investigate the role of IL-33 in the induction and progression in SPEM, IL-33 knock out mice (IL33KO) were treated with L635 and evaluated for SPEM, macrophage infiltration and polarization. Overall our data suggest that IL-33 is required to induce SPEM following parietal cell loss and to promote Th2 cytokines, which are critical to polarize alternatively activated macrophages. These findings reveal a novel inflammatory pathway in the stomach in response to parietal cell loss that resembles the inflammatory environment observed in allergy-associated airway inflammation.

Methods

Mice

C57BL/6J mice were purchased from Jackson Labs (Bar Harbor, ME). IL-33 knock out (IL33KO) mice were generated as previously described and maintained on the C57BL/6J background (Maywald et al., 2015). Regular mouse chow and water *ad libitum* was provided during experiments in a temperature-controlled room with 12-hour light-dark cycles. All treatment maintenance and care of animals in these studies followed protocols approved by the Institutional Animal Care and Use Committees of Vanderbilt University and Case Western Reserve University.

Drug Treatment

Three to four mice were used per group. L635 and DMP-777 treatment and dosage was conducted as previously described (Petersen et al., 2014). Clodronate treatment was performed as previously described (Petersen et al., 2014).

Macrophage Isolation and Fluorescence Activated Cell Sorting (FACS)

Three mice were pooled for each macrophage preparation, and three preparations were used for RNA sequencing. L635 and DMP-777-treated mice were sacrificed on the final day of treatment. The stomach was removed and opened along the greater curvature. Stomach contents were rinsed with PBS. The antrum and forestomach were removed with a razor blade and discarded, and the corpus was diced into pieces roughly one mm^3 in size, and washed with 0.07% DTT in PBS three times for five minutes. Stomach corpus pieces were then enzymatically digested using 1 U/mL of Dispase in DMEM/F-12 (Stem Cell Technologies, Vancouver BC) for 7 min at 37°C and subsequently diluted using an equal volume of macrophage growth media, Iscove's Modified Dulbecco's Medium (ThermoFisher), with 10% FBS. Pieces were sieved through a 100 µm filter (Corning) and crushed with a rubber syringe plunger into a single cell suspension over a 50 mL conical tube. Cells were spun down twice at 500g for 10 minutes at 4°C and resuspended in PBS with 10% FBS to remove excess cell debris and media. Cells were blocked using Mouse BD Fc Block (1:100, BD Pharmingen) for 15 minutes on ice and incubated with rat anti-mouse F4/80 conjugated to PE (1:25, BD Bioscience) for 30 minutes on ice. Prior to cell sorting, cells were washed twice in PBS with 10% FBS and incubated with 4',6-diamidino-2-phenylindol (DAPI) (1:10,000). Cells were sorted using a BD FACS Aria III (BD Biosciences, San Jose, California) and initially segregated from debris using forward scatter (FSC) and side scatter (SSC) properties of the 488 nm laser. Single cells were selected using the voltage pulse geometries of the FSC diode and SSC photomultiplier tube (PMT) detectors. Dead cells were excluded based on their DAPI

staining. Macrophages expressing F4/80 were sorted directly into Trizol (Invitrogen) using a 100 µm nozzle. RNA was extracted from Trizol and DNAse-treated (Promega) using the manufacturer's protocol.

Quantitative Real-time PCR analysis

The stomach corpus was isolated using a razor blade and placed into *RNAlater* or frozen on dry ice. Trizol was used to extract RNA from the tissue. One µg of DNAse-treated (Promega) RNA was transcribed into complementary DNA using Superscript III Reverse Transcriptase (Invitrogen). Quantitative real-time polymerase chain reaction was conducted and analyzed as previously described using SYBR Green Supermix (Petersen et al., 2014). The primer sequences used for *Cftr, Dmbt1, Tbp, He4, Mmp12, Clu* were previously reported, while primers for the M1 and M2 markers (*Fizz1, Ym1, Arg1, Arg2, Cd3, Cxcl10, Nos2*) were obtained from Qiagen (QuantiTect). Results were normalized to *TBP* or *GAPDH* and displayed as expression level ($2^{-\Delta Ct}$) (Petersen et al., 2014). Statistical significance ($p<0.05$) between groups was determined with a Mann-Whitney *U* 1-tailed or 2-tailed test.

RNA sequencing

Only RNA samples that had RNA integrity numbers (RIN) ≥7.0 were used. RNA was amplified using the NuGEN Technologies Ovation RNA-Seq System V2 kit (Part # 7102-08) using manufacturer's instructions. Approximately, 2.5 µg amplified DNA from each sample was sheared on a Covaris S200 focused-ultrasonicator (Woburn, MA, USA) with a target yield of an average 200bp fragment size. The fragmented DNA was taken into standard library preparation protocol using NEBNext® DNA Library Prep Master Mix Set for Illumina® (New England BioLabs Inc., Ipswich, MA, USA) with slight modifications. Briefly, end-repair was done followed by polyA addition and custom adapter ligation. Post-ligated materials were individually barcoded with unique in-house genomics service lab (GSL) primers and amplified

through 8 cycles of PCR using KAPA HiFi HotStart Ready Mix (Kapa Biosystems, Inc., Woburn, MA, USA). The quantity of the libraries were assessed by Qubit® 2.0 Fluorometer, and the quality of the libraries was estimated by utilizing a DNA 1000 chip on an Agilent 2100 Bioanalyzer, respectively. Accurate quantification for sequencing applications was determined using the qPCR-based KAPA Biosystems Library Quantification kit (Kapa Biosystems, Inc., Woburn, MA, USA). Each library was then diluted to a final concentration of 12.5nM and pooled equimolar prior to clustering. Paired End (PE) sequencing was performed on an Illumina HiSeq2500 following the manufacturer's protocols. Raw reads were demultiplexed using a bcl2fastq conversion software v1.8.3 (Illumina, Inc., San Diego, CA, USA) with default settings.

Post processing of the sequencing reads from RNA-seq experiments from each sample was performed as per our unique in-house pipeline. Briefly, quality control checks on raw sequence data from each sample were performed using FastQC (Babraham Bioinformatics, London, UK). Raw reads were mapped to the reference mouse genome mm9 using TopHat v1.4 (Langmead et al., 2009; Trapnell et al., 2009) with two mismatches allowed and other default parameters. The alignment metrics of the mapped reads was estimated using SAMtools (Li et al., 2009). Aligned reads were then imported onto the commercial data analysis platform, Avadis NGS (Strand Scientifics, CA, USA). After quality inspection, the aligned reads were filtered on the basis of read quality metrics where reads with a base quality score less than 30, alignment score less than 95, and mapping quality less than 40 were removed. Remaining reads were then filtered on the basis of their read statistics, where missing mates, translocated, unaligned and flipped reads were removed. The reads list was then filtered to remove duplicates. Samples were then grouped as treatment and control identifiers and quantification of transcript abundance was done on this final read list using Trimmed Means of M-values (TMM) (Robinson and Oshlack, 2010) as the normalization method. Differential expression of genes was calculated on the basis of fold change (using

default cut-off ≥ ±2.0) observed between defined conditions, and the p-value of the differentially expressed gene list was estimated by z-score calculations with Benjamini Hochberg False discovery rate (FDR) correction of 0.05 (Supplemental Table 1) (Benjamini, 1995). Differentially expressed genes underwent gene ontology (GO) analysis and pathway analysis using DAVID and Ingenuity Pathway Analysis tool.

Immunocytochemistry

Mouse stomachs were fixed in 4% paraformaldehyde overnight and transferred into 70% ethanol for paraffin embedding. The protocol for subsequent processing and sectioning was previously reported (Petersen et al., 2014). Tissue sections were blocked in Protein Block Serum-Free (DakoCytomation) for 1 hour at room temperature. The following primary antibodies were incubated overnight at 4°C in Antibody Diluent with Background Reducing Components (DakoCytomation): goat anti-intrinsic factor (1:1000, a gift from Dr. David Alpers, Washington University, St. Louis, MO), rat anti-Ki67 (1:50, BioLegend clone 16A8), rabbit anti-Ki67 (1:500, Cell Signaling), rat anti-F4/80 (1:500; Invitrogen, Grand Island, NY), goat anti-clusterin a (1:1000, Santa Cruz Biotechnology, Santa Cruz, CA), rat anti-Cd44v (1:25,000; Cosmo Bio, Japan), mouse anti-CD163 (1:200, NeoMarkers, Fremont, CA), and goat anti-IL-33 (1:200; R&D Systems). Human metaplasia samples were obtained as previously described and immunolabled with mouse anti-CD68 (1:200; Abbiotec, San Diego, CA) and human specific goat anti-IL-33 (1:200; R&D Systems) (Leys et al., 2007). Fluorescent secondary antibodies (1:500) and Alexa 488 and 647-conjugated *Griffonia simplicifolia* lectin II (GSII-lectin) (1:1000; Molecular Probes, Eugene, OR) were incubated at room temperature for one hour. Zeiss Axio Imager M2 microscope with Axiovision digital imaging system (Zeiss, Jena GmBH, Germany) or an Ariol SL-200 automated slide scanner (Leica Biosystems, Buffalo Grove, IL) in the Vanderbilt Digital Histology Shared Resource was used to analyze sections.

Image Quantitation

Images were analyzed using CellProfiler or manually counted (Jones et al., 2008). Experimental groups contained three or four mice, with three to five representative images taken from each mouse at 20X. SPEM lineages were identified as gastric intrinsic factor and GSII-lectin dual positive cells. Proliferative SPEM was identified as gastric intrinsic factor, GSII lectin, and Ki67 triple positive cells. A Mann Whitney *U* 1-tailed test was used to determine statistically significant differences ($p<0.05$).

Cytokine Array

RNA from whole corpus was used to assess 84 genes in the Qiagen Mouse Cytokines and Chemokines Array (PAMM-150ZC). RNA was transcribed into cDNA using the RT^2 First Strand Kit (Qiagen) for the RT2 Profiler PCR Array (Qiagen) using RT SYBR Green ROX qPCR Mastermix (Qiagen). An ABI StepOnePlus machine was used for the real time PCR experiment and data was uploaded to the Qiagen website at http://www.qiagen.com/geneglobe for analysis.

Results

Analysis of macrophage transcriptome from Acute SPEM models

We have previously determined that M2-like macrophages promote the advancement of SPEM (Petersen et al., 2014). Therefore, we sought to determine the characteristics of the infiltrating macrophage populations in L635-treated mice that could explain the promotion of proliferative and intestinalizing metaplasia. F4/80 positive cells from the corpus of L635-treated mice and DMP-777-treated mice were isolated and RNA sequenced for transcriptome analysis (Figure 1). The purity of the isolate cell populations was established by the normalized expression values from the RNA sequencing (Figure 2). Macrophage-specific genes are enriched in both F4/80 positive cells from L635 and DMP-777-treated mice. Other immune

populations were assessed, such as: T-cells (Cd3e), MDSCs and neutrophils (Ly6C and Ly6G), mast cells (Cma1) and eosinophils (Prg2/MBP). Gastric cell lineages were also assessed for contamination, such as: tuft cells (Dclk1), endocrine cells (Chga), parietal cells (Chrm2, Cckbr), SPEM cells (Cftr, Wfdc2), and chief cells (Mib1, Mist1). After we established the RNA sequencing contained an enriched population of macrophages, F4/80-positive cells from the stomach corpus of DMP-777-treated mice were compared to L635-treated mice (Figure 3 and Figure 4). Genes upregulated in macrophages associated with intestinalized SPEM from L635-treated mice were considered key factors of interest (Figure 3A). Several different classes of genes were upregulated: macrophage-related genes (*Csf1*, *Syk*), Th2 polarizing cytokines (*Il33, Il4*), chemokines (*Ccl24*, *Cxcl3*), matrix remodeling (*Mmp25*, *Mmp9*) and growth factors (*Hgf*, *Areg*, *VegfA*) (Figure 3A). Upregulated genes in macrophages associated with SPEM in DMP-777-treated mice were associated with matrix remodeling (Col14a1, Col6a1), macrophage-related genes (Fcer1a, H2-M2), growth factors (Fgf1, Pdgf), cytokines/chemokines (Tnfrsf9, Ccl12), and angiogenesis (Ephb3, Pdgfb) (Figure 4).

Our analysis concentrated primarily on secreted factors or receptors, as macrophages impact the local environment predominantly through paracrine and juxtacrine signaling (Figure 2A) (Lu et al., 2014; Suganami et al., 2005). Another aspect assessed using the RNA sequencing data was differences in macrophage polarization gene markers from L635-treated mice versus DMP-777-treated mice (Figure 2B).

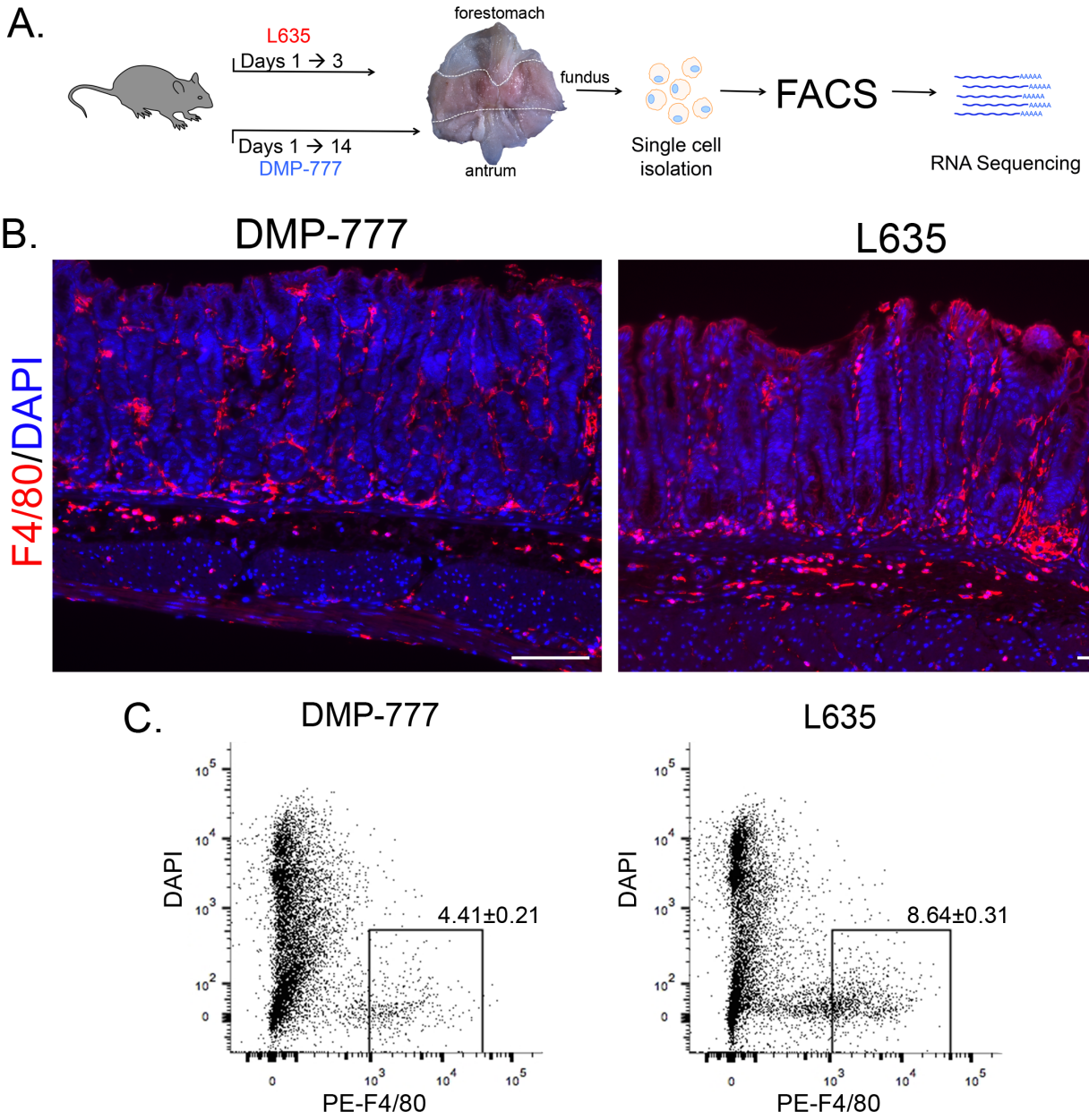

Figure 13. F4/80-positive cells isolated from acute SPEM models. A. Wild-type C57BL/6 mice (n=3 per sample, 3 biological replicate samples) were treated with L635 for 3 days or DMP-777 for 10 days, and were sacrificed on the last day of treatment. The corpus was removed from the stomach and enzymatically digested into a single cell suspension. Macrophages were labeled using the antibody F4/80 and FACS sorted for RNA sequencing, n=3 replicates/each sample**. B.** Immunofluorescence of representative images illustrating the F4/80 positive macrophages sorted from DMP-777 and L635-treated mice. Scale bars 100 mm. **C.** Representative dot plot images of the FACS sorted PE-F4/80 cell population in DMP-777 and L635-treated mice. Macrophages sorted from DMP-777 made up 4.41% (±0.21) of cells, while macrophages sorted from L635-treated mice was 8.64% (±0.31).

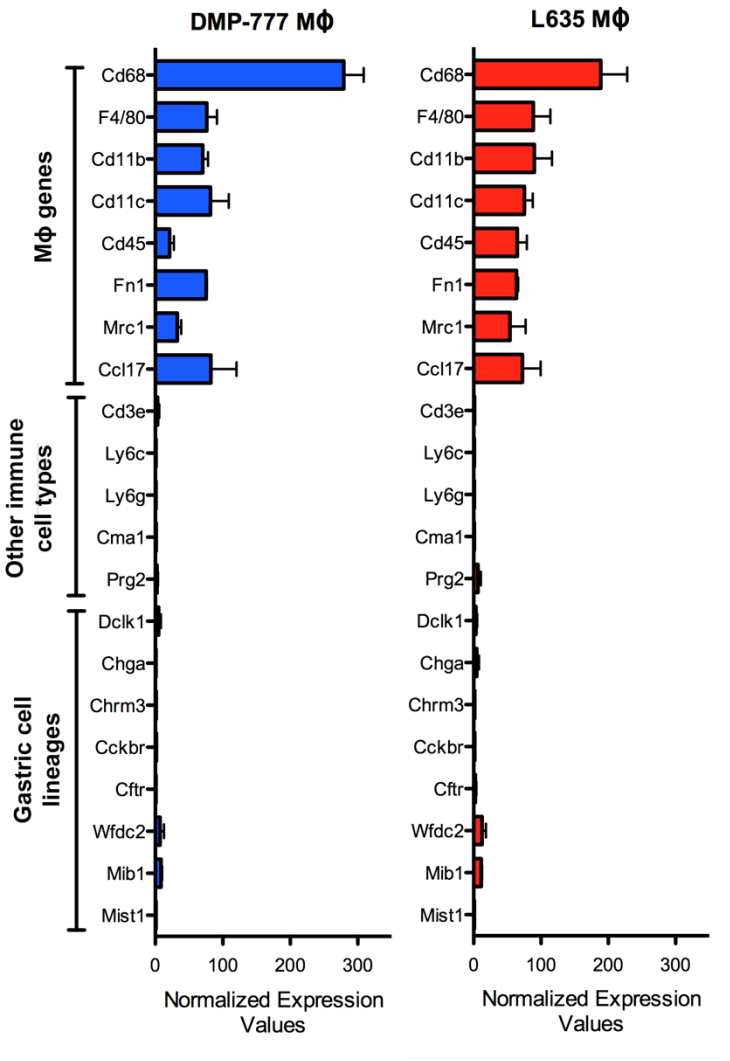

Figure 14. RNA sequencing of F4/80 positive cells in L635 and DMP-777-treated mice show a macrophage-enriched population. Normalized Expression values plotted (n=3) with SEM. Selected genes representing different cell populations are shown. Macrophage specific genes, other immune cell types (T-cell receptor, neutrophils, mast cells, eosinophils), and gastric cell lineages (tuft cells, endocrine cells, parietal cells, SPEM cells, and chief cells). **A.** F4/80+ cells isolated from DMP-777-treated mice **B.** F4/80 positive cells from L635-treated mice. Both data sets show enrichment in genes specific to macrophages compared to other cell types found in the stomach.

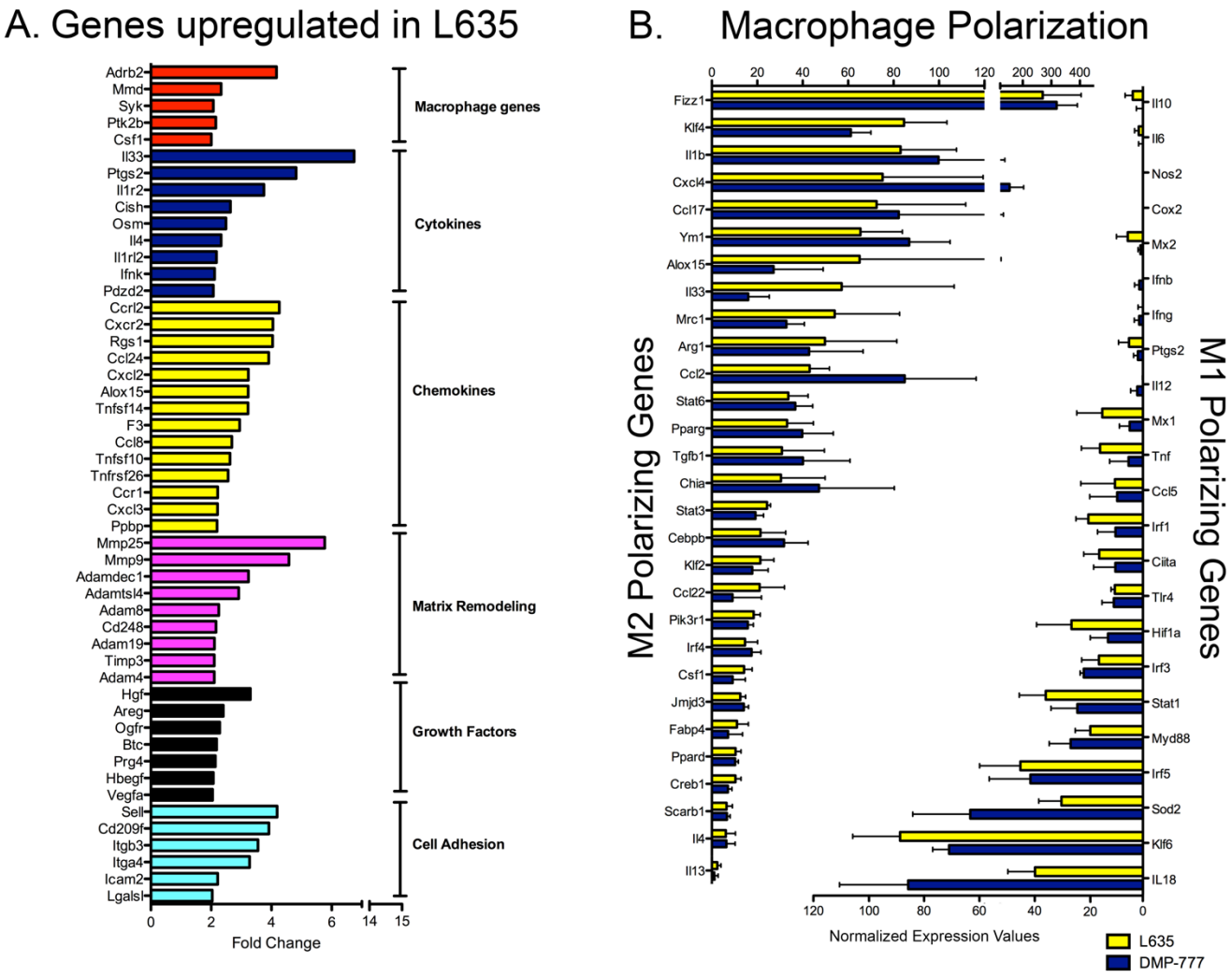

Figure 15. Transcriptome analysis of macrophages associated with SPEM and intestinalized SPEM. Gene expression profile of macrophages from L635-treated mice compared to DMP-777-treated mice; n=3 replicates/each sample. A. Factors significantly upregulated ($p \geq 0.01$; fold change ≥2) in macrophages from L635-treated mice. Representative genes selected were grouped based on function: macrophage genes, cytokines, chemokines, matrix remodeling, growth factors, and cell adhesion. See data also in Figure 3. **B.** Normalized gene expression of M1 and M2-associated genes in macrophages isolated from DMP-777 and L635-treated mice plotted with SEM. Macrophages associated with intestinalized SPEM (L635-treated) express increased M2-like transcripts (*Alox15, Klf4, Il33*) compared to macrophages associated with SPEM (DMP-777 treated) which have increased M1 genes (*Il18, Sod2*).

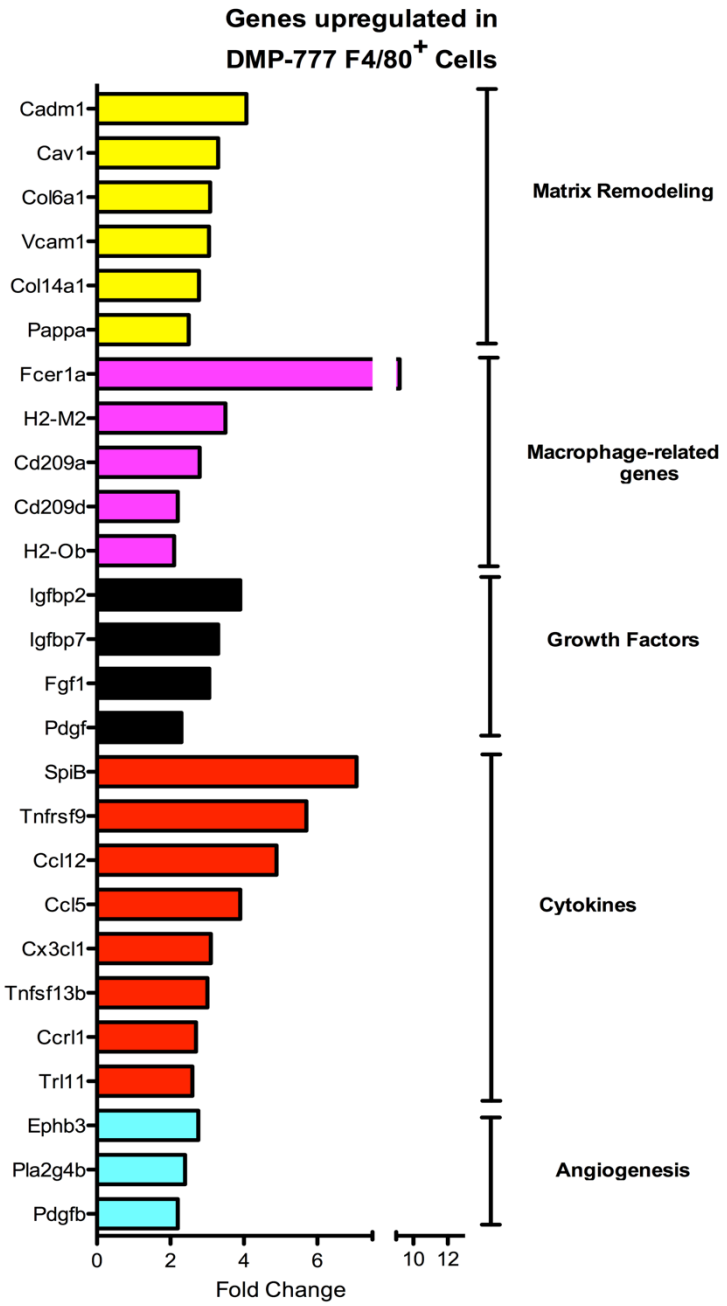

Figure 16. Transcriptome analysis of macrophages associated SPEM. Gene expression profile of transcripts significantly upregulated ($p \geq 0.01$; fold change ≥2) in macrophages associated with SPEM (DMP-777-treated mice), n=3 replicates/each sample. Representative genes selected were grouped based on function: Matrix remodeling, macrophage related genes, growth factors, cytokines, and angiogenic factors.

Controversy exists over M1 and M2 macrophage polarization classification, which is more variable than previously thought (Lawrence and Natoli, 2011; Sica and Mantovani, 2012). We found that macrophages from L635-treated mice and DMP-777-treated mice expressed a variety of M1 and M2-associated genes (Figure 3B). Specifically, macrophages from L635-treated mice expressed higher levels of M2 genes (*Klf4*, *Alox15*, *Il33*, *Mrc1*, *Ccl22*), but other recognized M2 genes such as Fizz1, Ym1 and Arg1 were highly expressed in macrophages from both L635 and DMP-777-treated mice. While macrophages from DMP-777-treated mice expressed higher levels of a sub-group of M1-like genes (*Il18*, *Sod2*), both L635 and DMP-777 isolated macrophages expressed a variety of other M1 genes in similar proportion (*Klf6, Irf5, Irf3, Tlr4*). In addition, both L635 and DMP-777 associated macrophages only expressed low levels of classical M1 markers (*Il6, Il12, Nos2*).

IL-33 is necessary for SPEM induction

The IL-1 family member IL-33 was the most significantly upregulated cytokine in macrophages from L635-treated mice compared DMP-777-treated mice. To investigate the role of IL-33 in the initiation and progression of SPEM, we treated IL-33 knockout mice (IL33KO) with L635 to induce intestinalized SPEM. Untreated IL33KO mice have a normal distribution and assembly of corpus cell lineages similar to wild type mice (Figure 5A). After L635 treatment, IL33KO mice showed parietal cell loss and inflammatory cell infiltration similar to control L635-treated mice (Figure 5A). To determine if IL-33 was required for macrophage recruitment after parietal cell loss, F4/80 positive cells were counted in L635-treated IL33KO mice and control L635-treated mice. Both wild-type control and IL33KO mice demonstrated similar numbers of infiltrating macrophages after L635 treatment (Figure 5B and 5D). Therefore, IL-33 loss did not affect macrophage recruitment into the stomach after acute parietal cell loss.

Oxyntic atrophy causes chief cells located at the base of the glands to transdifferentiate into SPEM, as identified by GSII lectin or CD44 variant co-labeling in gastric intrinsic factor-expressing cells (Wada et al., 2013). However, L635-treated IL33KO mice did not develop SPEM, visualized by the absence of metaplasia markers (GSII lectin or Cd44 variant) in gastric intrinsic factor positive chief cells (Figure 5C and 5E). Another indication of metaplasia development is the loss of Mist1, a transcription factor expressed in mature chief cells (Nozaki et al., 2008a). In L635-treated mice, Mist1 expression was significantly reduced; however, chief cells in L635-treated IL33KO mice do not lose Mist1 expression to the extent observed in control L635-treated mice (Figure 6A and 6B). Therefore, chief cells in L635-treated IL33KO mice do not complete transdifferentiation into SPEM upon acute parietal cell loss.

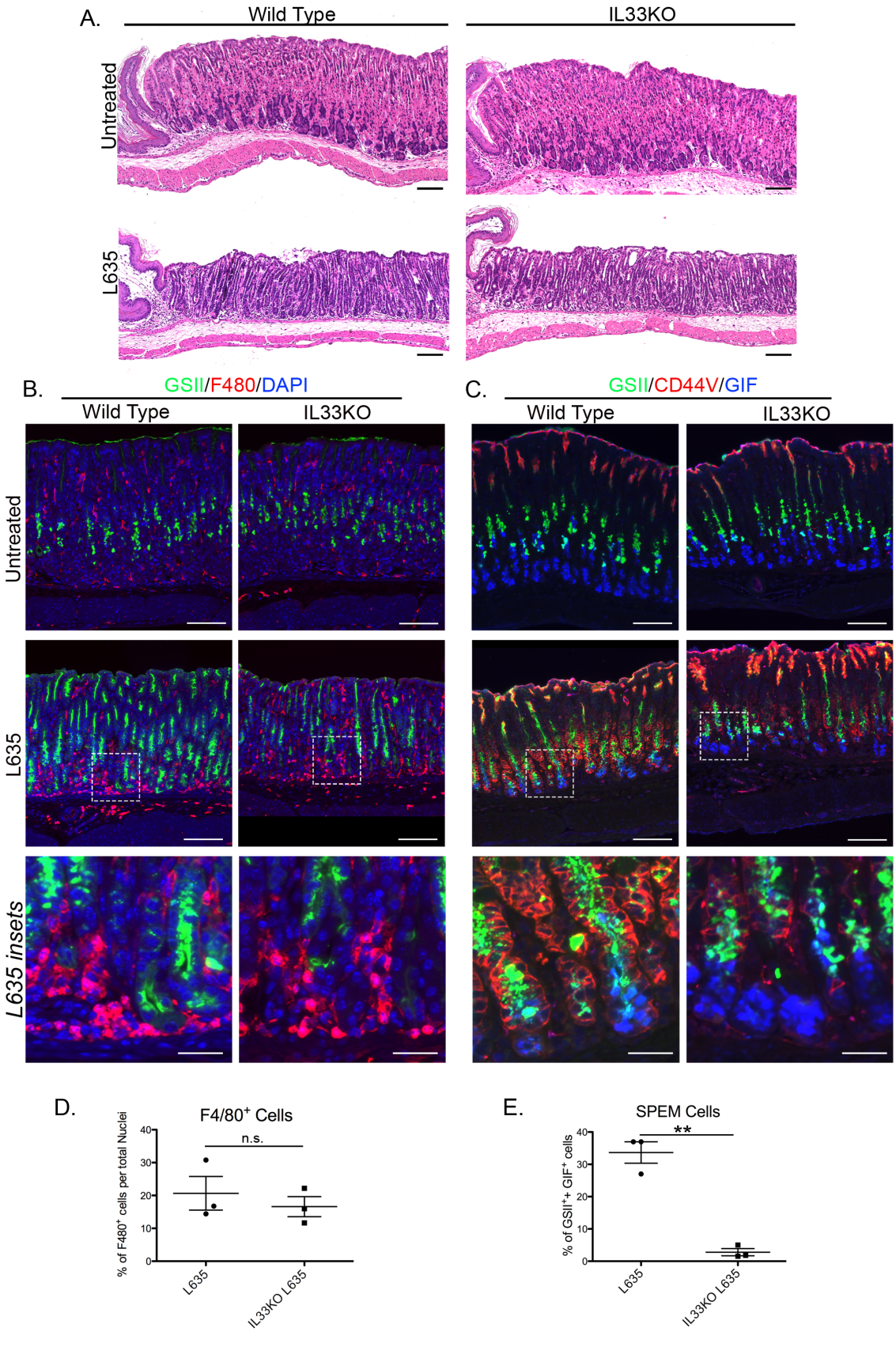
A.
Wild Type
IL33KO
Untreated
L635
B.
GSII/F480/DAPI
Wild Type
IL33KO
Untreated
L635
L635 insets
C.
GSII/CD44V/GIF
Wild Type
IL33KO
D.
F4/80+ Cells
n.s.
% of F480+ cells per total Nuclei
0
10
20
30
40
L635
IL33KO L635
E.
SPEM Cells
**
% of GSII+ GIF+ cells
0
10
20
30
40
L635
IL33KO L635

Figure 17. IL-33 is necessary for SPEM induction. **A.** H&E of wild-type untreated, L635-treated, IL33KO, and L635-treated IL33KO mice (n=3 or 4). Untreated IL33KO mice have normal oxyntic gland morphology and cell lineages. Upon L635-treatment, both wild-type and IL33KO have parietal cell loss accompanied by a significant inflammatory cell infiltrate at the base of glands. **B.** Immunofluorescence of SPEM marker GSII-lectin, macrophage marker F4/80 and DAPI in untreated wild-type and L635-treated control and IL33KO mice. F4/80 positive macrophages infiltrate into the mucosa after L635-treatment in both wild-type and IL33KO mice. **C.** Immunofluorescence of GSII-lectin, metaplasia marker Cd44v and gastric intrinsic factor (GIF) to visualize SPEM. Untreated wild-type and IL33KO mice do not have Cd44v positive cells or double positive GSII-lectin and GIF cells at the base of the gland. After L635 treatment, control mice express double positive GSII and GIF cells at the base that are positive for CD44v, indicative of SPEM. L635-treated IL33KO mice do not have double positive GSII-lectin and GIF or Cd44v positive cells at the base of the gland. Cd44v is positive in the mucus neck cell region only in L635-treated IL33KO mice. **D.** Quantitation of F4/80 positive cells in L635-treated wild-type mice and L635-treated IL33KO mice. No significant change in the number of F4/80 positive macrophages. **E.** The total number of chief cells (GIF positive only) that transdifferentiate into SPEM cells (GSII-lectin and GIF double positive) in a 20x field for n=3 mice. IL33KO mice had a significant reduction of SPEM cell prevalence in response to L635 treatment, $p \geq 0.05$. Mann Whitney *U* 1-tailed test. Scale bars = 100 mm. White boxes depict the magnified insets of L635-treated control and IL33KO mice, inset scale bars = 20 mm.

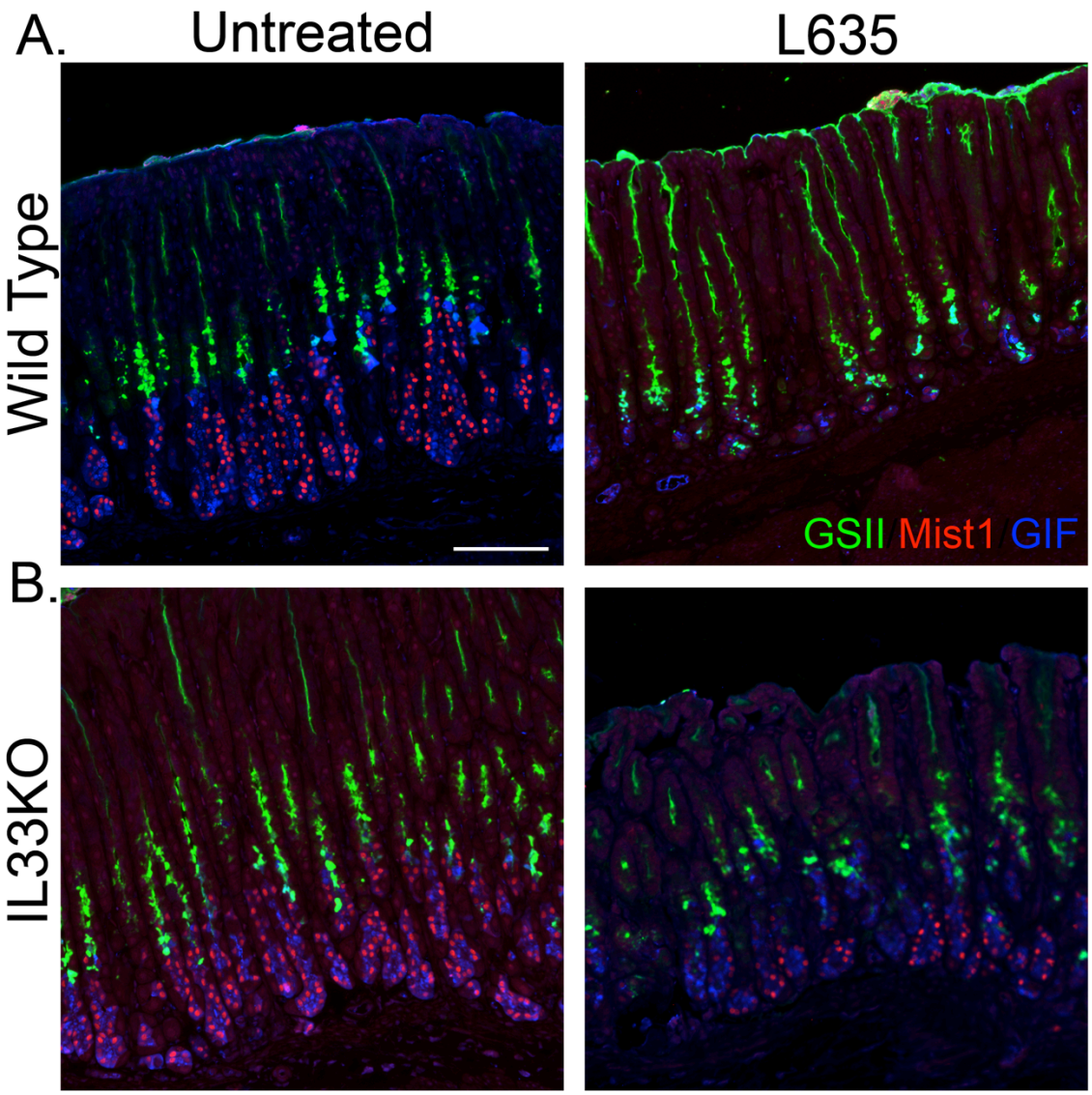

Figure 18. Mist1 expression is still present in L635-treated IL33KO mice that do not develop SPEM. Immunofluorescence of mature chief cell transcription factor Mist1, mucus neck cell and SPEM marker GSII-lectin, and gastric intrinsic factor (GIF) **A.** Mist1expression is present in the nucleus of mature chief cells (GIF positive) in wild-type untreated mice. After L635 treatment, chief cells transdifferentiate into SPEM cells, marked by co-positive GIF and GSII-lectin. Mist1 expression is absent in SPEM cells. **B.** IL33KO mice express Mist1 in chief cells similar to wild-type untreated mice. After L635 treatment, IL33KO mice have fewer observed Mist1 positive GIF cells, however not all Mist1 is lost, indicative of the inability of chief cells to transdifferentiate into SPEM. Scale bars = 100 mm.

A hallmark of inflammation-associated oxyntic atrophy in the stomach is the development of a highly proliferative and intestinalized SPEM, visualized by cells triple-positive for gastric intrinsic factor (GIF), Ki67, and GSII-lectin. L635-treated wild-type mice developed proliferative intestinalized SPEM after only 3 days of treatment (Figure 7A). However, L635-treated IL33KO mice did not develop proliferative SPEM at the base of the glands (Figure 7B). Instead, L635-treated IL33KO mice showed Ki67-labeled mucus neck cells, indicative of mucus neck cell hyperplasia. We observed an occasional Ki67 and intrinsic factor double-positive cell in IL33KO mice treated with L635, which was not seen in wild-type untreated or control L635-treated mice, and may be indicative of the inability of chief cells to transdifferentiate into SPEM. Furthermore, quantitative PCR confirmed the lack of SPEM (*He4, Clu, Mmp12*) or intestinalized SPEM (*Cftr, Dmbt1, Etv5*) associated transcripts in L635-treated IL33KO mice (Figure 7C and 7D). Therefore, IL-33 is necessary for the induction of SPEM after acute parietal cell loss.

Loss of M2-polarized macrophages in L635-treated IL33KO mice

Our previous study determined that M2-like macrophages were key in developing intestinalized SPEM (Petersen et al., 2014). Since IL-33 does not prevent macrophage infiltration into the mucosa after L635-treatment (Figure 5D), we sought to determine if macrophage polarization was altered upon the loss of IL-33 using the M2 marker CD163. We observed that L635-treated IL33KO mice had a loss of CD163-positive macrophages within the mucosa compared to L635-treated control mice (Figure 8A). To identify if macrophages were polarizing towards M1, we immunolabeled with iNos and found an increase in iNos positive macrophages in IL33KO-L635-treated mice compared to L635-treated wild-type mice (Figure 8B). Quantitative PCR on RNA from whole corpus tissue revealed a significant decrease in only one M2 marker, Ym1, and confirmed upregulated M1 markers (Cd3 and Cxcl10) (Figure 8C and 8D). Ym1 and CD163 are both highly expressed in M2a macrophages specifically,

which may indicate that IL-33 may be important in inducing M2a macrophage polarization in the stomach.

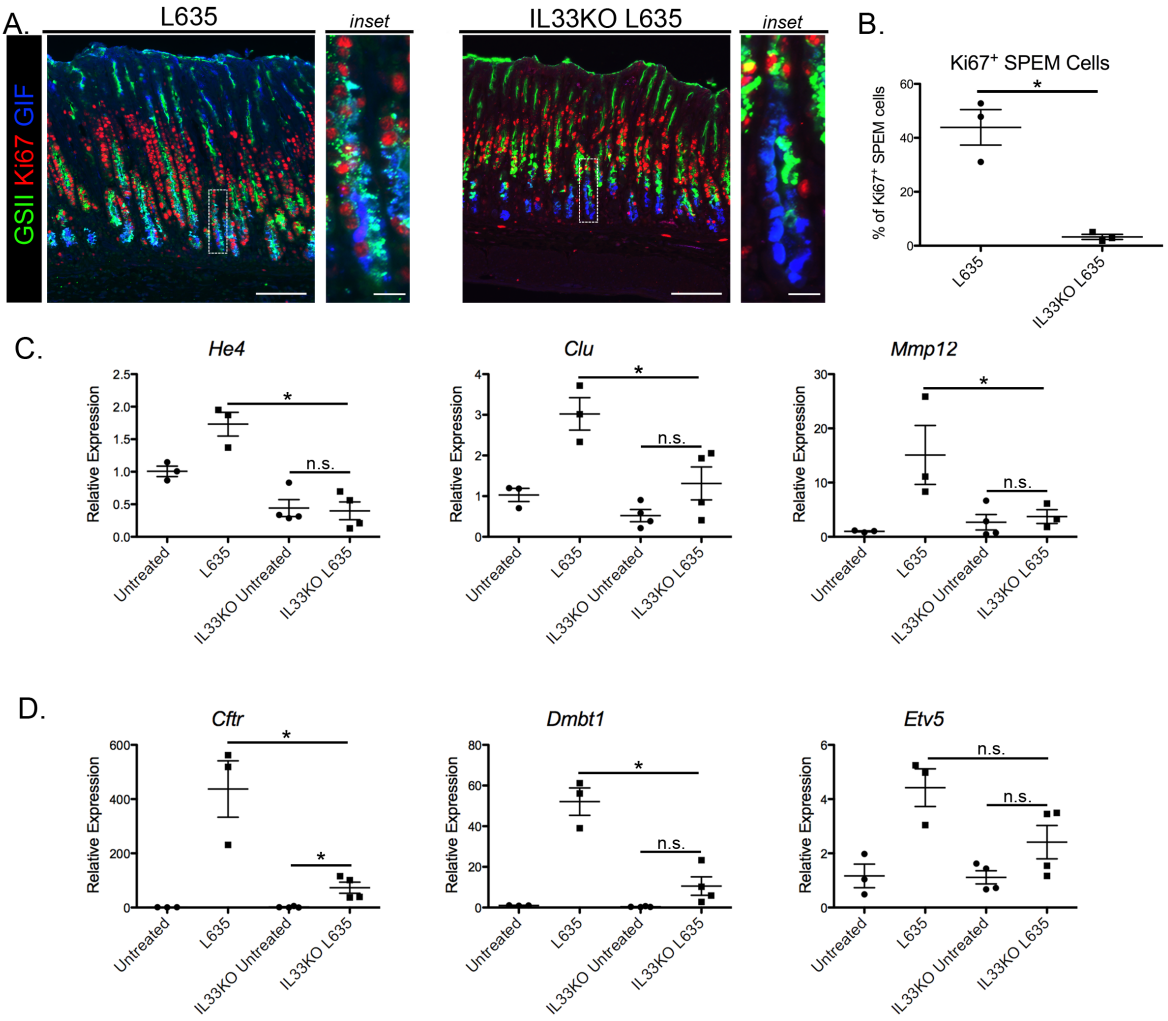

Figure 19. IL33KO mice treated with L635 do not develop proliferative or intestinalized SPEM after acute parietal cell loss. A. Immunofluorescence staining of GSII-lectin, Ki67 and GIF to identify proliferative SPEM. L635-treated wild-type mice develop proliferative SPEM at the base of the gland (triple positive for Ki67, GSII-lectin, GIF). L635-treated IL33KO have increased Ki67 positive GSII-lectin cells in the mucus neck cell region, but do not have proliferative SPEM cells at the base of the glands. Scale bars = 100 mm. White boxes are magnified in the insets, inset scale bars = 10mm. **B.** Quantitation of Ki67 positive SPEM cells. The percent of proliferating SPEM cells per 20x, n=3 mice. IL33KO mice treated with L635 have a significant reduction in proliferative SPEM present compared to L635-treated wild-type mice, p≥0.05. **C.** Quantitative RT-PCR of SPEM markers from whole corpus RNA. Increased SPEM markers (*He4*, *Clu*, *Mmp12*) are detected in wild-type mice after L635 treatment. IL33KO mice treated with L635 have significantly decreased SPEM transcripts compared to wild-type L635-treated mice, that do not significantly change compared to untreated IL33KO mice, p≥0.05. **D.** Quantitative RT-PCR of intestinalized SPEM markers from whole corpus RNA. Wild-type mice have increased intestinal transcripts (*Cftr*, *Dmbt1, Etv5*) after L635 treatment, p≥0.05. L635-treated IL33KO mice have significantly reduced *Cftr* and *Dmbt1* message compared to wild-type L635-treated mice, p≥0.05.

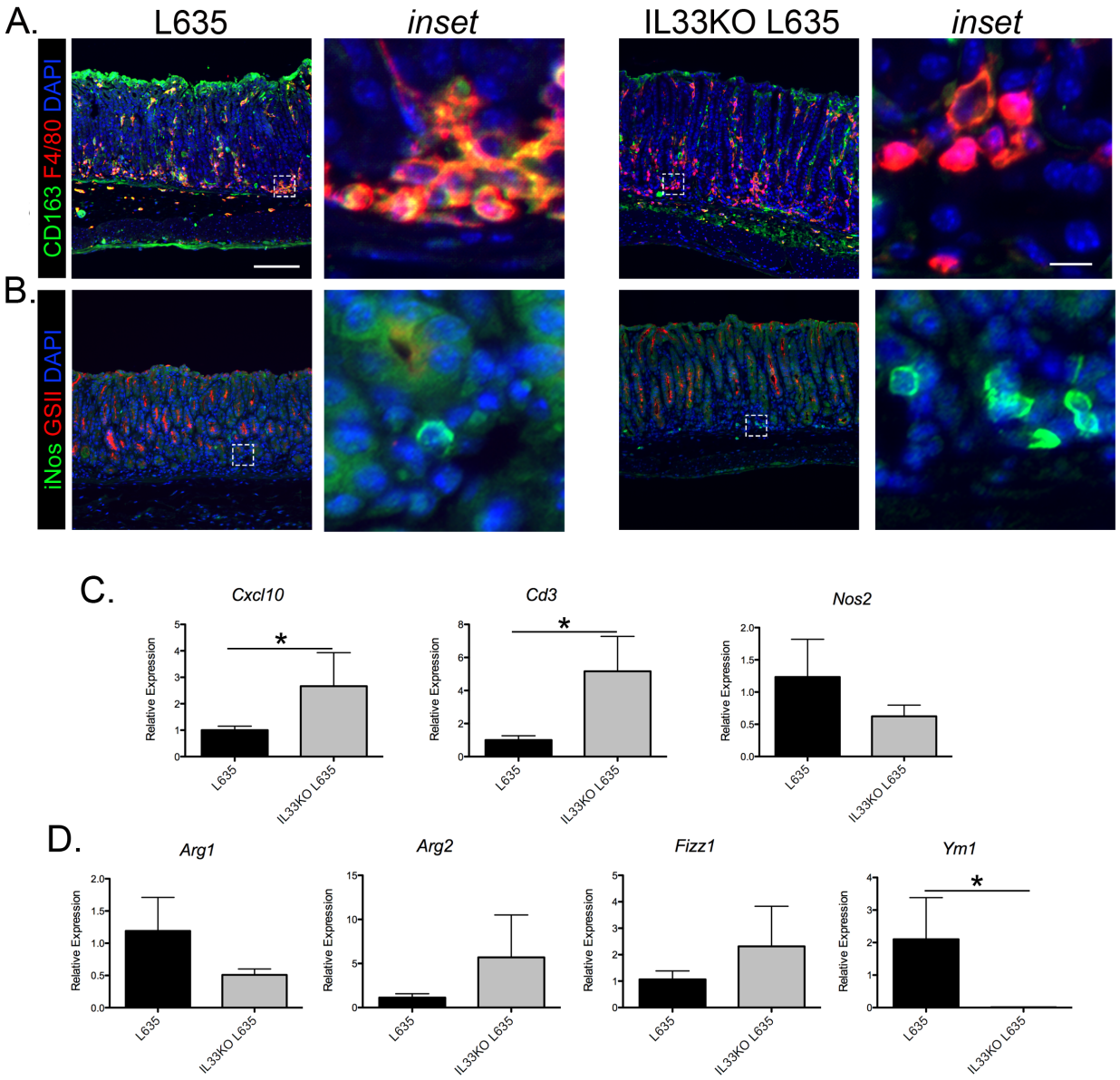

Figure 20. IL33 is required for macrophage M2 polarization after acute parietal cell loss. **A.** Immunofluorescence of M2 marker CD163, macrophage marker F4/80 and DAPI. F4/80 positive macrophages infiltrate into the mucosa after L635 treatment and are co-positive for CD163. L635-treated IL33KO mice have increased F4/80 positive macrophages after acute parietal cell loss, but are not positive for the M2 marker CD163. **B.** Immunofluorescence of M1 marker iNos, GSII-lectin and DAPI. L635-treated mice have very few iNos positive macrophages. Increased M1 macrophages are observed in L635-treated IL33KO mice. Scale bars are 100 mm. Insets are magnified regions, scale bars 10mm. **C.** Quantitative RT-PCR of M1 markers (*Cxcl10, Cd3* and *Nos2*) from whole corpus RNA. L635-treated IL33KO mice have a significant increase in *Cxcl10* and *Ccl3* message compared wild-type L635-treated mice, p≥0.05. **D.** Quantitative RT-PCR of M2 markers. Only *Ym1* was significantly reduced in L635-treated IL33KO mice compared to wild-type L635-treated mice, p≥0.05. No significant change detected in *Arg1*, *Arg2* or *Fizz1*.

We used a mouse specific cytokine and chemokine array to determine if M2a macrophage polarization or other cytokines/chemokines were altered in L635-treated IL33KO

mice. Two different categories of genes were down-regulated in L635-treated IL33KO mice compared to L635-treated wild-type mice: M2a macrophage-associated chemokines and Th2-related cytokines (Figure 9A and 9B). The alternatively activated macrophage M2a cytokine signature reflects high expression of Ccl11, Ccl17 and Ccl24, which were significantly decreased in L635-treated IL33KO mice compared to L635-treated wild-type mice (Figure 9A). Furthermore, Th2-related cytokines (IL4, IL5, IL9, IL13) were significantly decreased in L635-treated IL33KO mice (Figure 9B). Of note, IL-33 and Th2 cytokines were not necessary for macrophage recruitment upon acute parietal cell loss or for the regulation of other M2 genes (Arg2, Arg1, Fizz1) in infiltrating macrophages after parietal cell loss (Figure 4D and 3D).

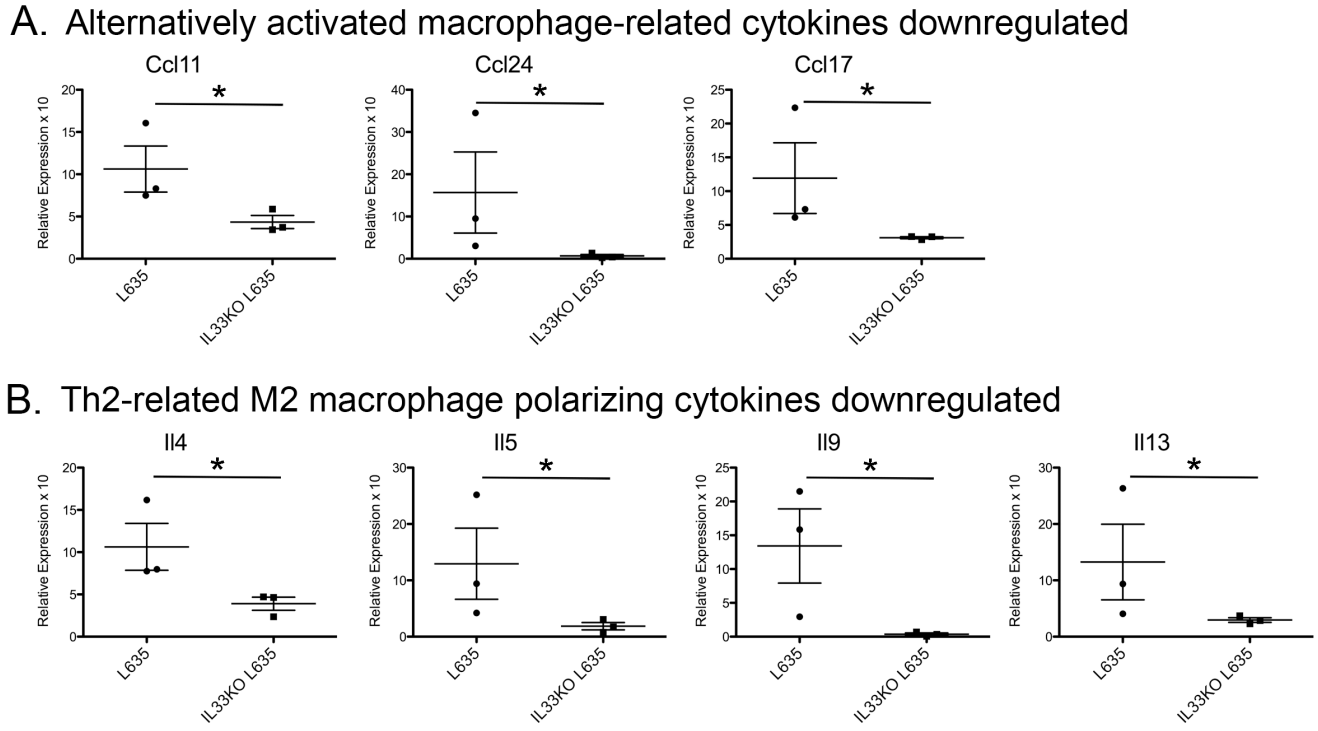

Figure 21. IL33 is required for M2a macrophage polarization and the production of Th2 cytokines. Mouse chemokine and cytokine array (Qiagen) for 84 different target genes on whole stomach corpus RNA from L635-treated mice and L635-treated IL33KO mice (n=3). Seven genes were significantly ($p \geq 0.05$) decreased L635-treated IL33KO mice compared to control L635-treated mice. Genes were grouped based on function. **A.** Alternatively activated macrophage-related chemokines (Ccl11, Ccl24 and Ccl17) and were all significantly decreased in L635-treated IL33KO mice. **B.** Th2-related M2 macrophage polarizing cytokines were significantly decreased in L635-treated IL33KO mice compared to L635-treated mice.

IL-33 positive macrophages in human SPEM and Intestinal Metaplasia

We investigated whether IL-33 was expressed in macrophages associated with SPEM and intestinal metaplasia in arrayed samples from human corpus (Leys et al., 2007). Our previous study determined that the majority of macrophages in metaplasia were M2 polarized (Petersen et al., 2014). We immunolabled for CD68 and IL-33 and determined that all macrophages associated with both SPEM and intestinal metaplasia in humans were IL-33 positive (Figure 10A and 10B). Therefore, IL-33 may have a role in metaplasia development, intestinalization and macrophage polarization in neoplastic progression within the human stomach.

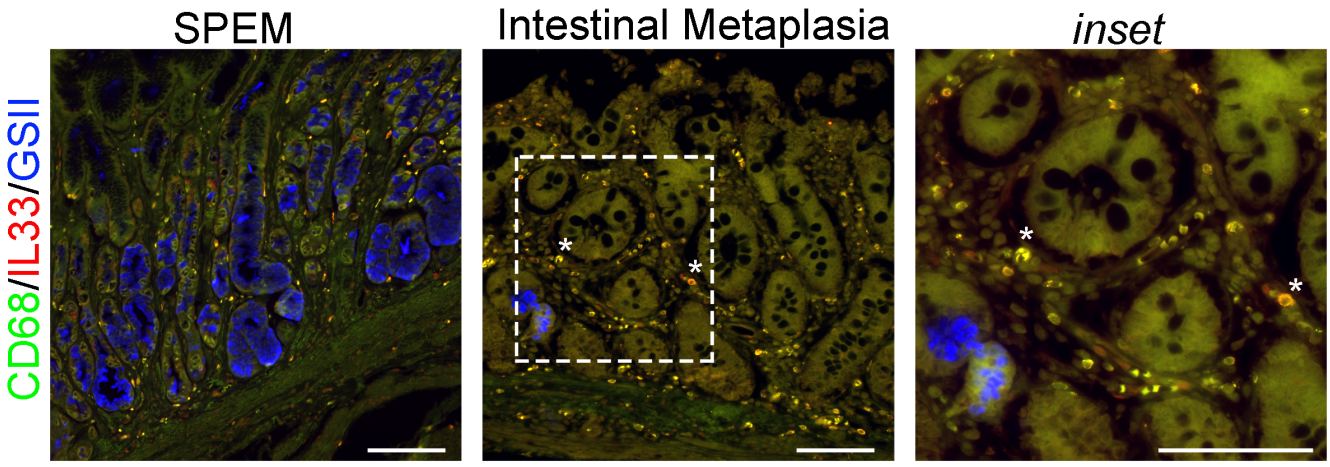

Figure 22. Macrophages associated with Human SPEM and Intestinal metaplasia are IL-33 positive. Immunofluorescence of macrophage marker CD68, IL-33, and SPEM marker GSII-lectin in human SPEM and Intestinal Metaplasia biopsy samples. A. Human SPEM has IL-33 positive macrophage infiltrating into the mucosa. B. Intestinal Metaplasia has CD68 positive macrophages that are co-positive for IL-33. Scale bars are 100 mm, inset scale bar is 20 mm. Asterisks in intestinal metaplasia denote similar area in the inset.

Discussion

In the current study, we establish that IL-33 is required for the development of metaplasia in the corpus of the stomach. IL-33 was necessary for the polarization of infiltrating macrophages towards M2 after acute parietal cell loss. In the absence of IL-33, chief cells were unable to transdifferentiate into SPEM, even in the presence of a substantial macrophage infiltration following L635 treatment. Our previous study showed that infiltrating M2 polarized macrophages were necessary for the intestinalization of metaplasia (Petersen et al., 2014). Here we found that IL-33 is required for the polarization of infiltrating macrophages towards M2a and the induction of SPEM. Investigations using our acute SPEM models provide an *in vivo* method to study the effects of inflammation on the metaplastic process, recapitulating the process observed in *Helicobacter* infection (Weis et al., 2012). The data presented here support a novel pathway for metaplasia induction, where IL-33 is a critical component in initiating metaplasia development and regulating the polarization of infiltrating macrophages towards M2a that subsequently drive the intestinalization of metaplasia in the stomach.

Our acute metaplasia model drug systems in the stomach are unique in respect to the ability to separate discrete inflammatory mechanisms in the progression of SPEM (Weis et al., 2012). Mice treated with DMP-777 develop SPEM after 10 days, whereas SPEM induced in L635-treated mice progresses in the setting of acute inflammation into a highly proliferative and intestinalized SPEM lineage in three days (Nam et al., 2010b). We identified differentially regulated genes that could promote the advancement of metaplasia by characterizing macrophages associated with SPEM (DMP-777-treated mice) and intestinalized SPEM (L635-treated mice). Both populations of macrophages in DMP-777 and L635-treated mice had similar expression patterns of M1 and M2 markers. However, markers typically used to classify the macrophage subclasses were not adequate to distinguish between the functionally distinct macrophage populations associated with SPEM versus intestinalized SPEM. Additionally, macrophage transcriptomes in the stomach after acute parietal cell loss revealed a general

profile indicative of mucosal injury repair, including genes involved with matrix remodeling, angiogenesis, chemokines/cytokines, and growth factors.

Previous studies have demonstrated the effect of specific cytokines on evoking inflammation to induce metaplasia in the stomach. Recombinant human IL-1b or IFNg expressed by parietal cells in transgenic mice is sufficient to induce gastric inflammation and dysplasia within the stomach (Syu et al., 2012; Tu et al., 2008). Administration of IL-11 also induces inflammation and metaplasia in the stomach (Howlett et al., 2012). Likewise the inhibition or ablation of different cytokines/chemokines can prevent macrophage infiltration and impact metaplasia. Ccl2 inhibition prevents macrophage infiltration and causes tumor regression in SPF-*Gan* mice (Oshima et al., 2011a). Il1b null mice infected with *Helicobacter pylori* have decreased macrophage and neutrophil recruitment into the mucosa that corresponded with reduced gastric pathology (Shigematsu et al., 2013). Therefore, stomach metaplasia progression or reversal directly relates to macrophage infiltration within the gastric mucosa. The work presented here identifies IL-33 as a key cytokine required to induce metaplasia separate from the induction of macrophage infiltration.

IL-33 was first reported in 2005 as the ligand to the orphan IL-1 receptor ST2 (Schmitz et al., 2005). IL-33 localizes to endothelial cells, epithelial cells, dendritic cells and activated macrophages in mice, and only activated dendritic cells and macrophages in humans (Kurowska-Stolarska et al., 2008; Schmitz et al., 2005). Administration of IL-33 is sufficient to induce hypertrophy and mucus metaplasia in the airway, stomach, and intestine, which is accompanied by an infiltration of myeloid cells and eosinophils (Buzzelli, 2015; Kurowska-Stolarska et al., 2008; Prefontaine et al., 2010; Schmitz et al., 2005; Stolarski et al., 2010). In this study, we investigated the requirement of IL-33 in the development and progression of metaplasia after finding it was upregulated over 6-fold in macrophages isolated from L635-treated mice compared to DMP-777-treated mice. IL-33 knockout mice treated with L635 showed parietal cell loss, nevertheless chief cells failed to transdifferentiate into SPEM or

progress to intestinalized SPEM. While loss of IL-33 did not impact the recruitment of macrophage infiltrates in the gastric mucosa after parietal cell loss, infiltrating macrophages were not M2 polarized. Thus indicating that IL-33 is critical for M2 polarization of recruited macrophages in the stomach.

Previous studies have focused on the role of IL-33 and inflammation in the context of allergic inflammation. In the airway, IL-33 upregulation promotes Th2 cytokine production by T helper cells, macrophages, and group 2 innate lymphoid cells (ILC2s) (Blom et al., 2011; Cayrol and Girard, 2014; Kurowska-Stolarska et al., 2009; Schmitz et al., 2005; Smith et al., 2015). The rapid release of IL-4 and IL-13 increase the M2a macrophage genes, CCL17 and CCL24 (Kurowska-Stolarska et al., 2009). In addition, Th2 cytokines IL-4, IL-9 and IL-13 can induce mucus production in the airway in response to allergen challenge (Dabbagh et al., 1999; Kurowska-Stolarska et al., 2008). We observed a similar phenotypic response after acute parietal cell loss and hypothesized that cytokines/chemokines downstream of IL-33 could impact the induction or progression of metaplasia. We found that IL33KO mice treated with L635 had decreased Th2 cytokines (IL4, IL5, IL9, IL13) and M2a-associated cytokines (CCL17, CCL22, CCL24) when compared to controls. Therefore IL-33 in the stomach is required to promote the expression of IL-4 and IL-13. The upregulation of IL-4, IL-9 and/or IL-13 is known to mucus production, which is a hallmark of chief cells transdifferentiating into a metaplastic mucus cell lineage (SPEM). Our previous study determined that M2 macrophages were necessary for the intestinalization of SPEM, but did not clarify the M2 subclass (M2a, M2b or M2c) (Petersen et al., 2014)'(Mantovani et al., 2004). Data presented here suggests that recruited macrophages polarize towards M2a after L635 treatment and that IL-33 necessary for macrophage polarization. Thus, we suggest that IL-33 is simultaneously driving metaplastic transition through downstream targets to upregulate mucus secretion in chief cells while potentiating the intestinalization of SPEM by polarizing recruited macrophages towards M2a. Another similarity between mucus metaplasia development in the airway and stomach is

the upregulation of TFF2 (Nikolaidis et al., 2003). IL-33 promotes TFF2 expression in asthma, and TFF2 expression is upregulated in chief cells transdifferentiating into SPEM after parietal cell loss (Schmidt et al., 1999a; Wills-Karp et al., 2012). This further suggests that key functions of inflammation in the airway (airway hyperactivity or allergic inflammation) parallel similar processes observed in SPEM regarding macrophage polarization and expansion of mucus-producing cell lineages. Allergic inflammation in the airway relies on the Th2 cytokines IL-4 and IL-13 through IL-33 to promote mucus cell metaplasia development and drive M2a polarization (Kurowska-Stolarska et al., 2008). We describe a similar process in the stomach, where IL-33 is necessary for metaplasia induction and intestinalization of SPEM. Future studies will be needed to understand further the roles of IL-13 and IL-4 in the induction and progression of metaplasia and macrophage function after acute parietal cell loss.

In summary, our investigation of the transcriptional profile of macrophages associated with intestinalized SPEM in L635-treated mice revealed the requirement of IL-33 in the development of SPEM. We further demonstrated that IL-33 is necessary to promote a Th2 inflammatory response and M2a polarization of recruited macrophages, which drives initialization of SPEM. The identification of IL-33 as a critical regulator of macrophage polarization and Th2 cytokine production suggests a central role for immune cell regulation of the epithelial response to acute injury. These observations provide a novel pathway and model for understanding the inflammatory response in the stomach after parietal cell loss. Furthermore, conclusions presented here suggest that therapeutic modalities currently used to treat inflammation in the airway could potentially modulate the inflammatory response in the stomach to prevent metaplasia progression towards gastric adenocarcinoma.

Chapter IV

CONCLUSIONS AND FUTURE DIRECTIONS

1. Conclusions

Inflammation is a key step in the development and progression of metaplasia in the stomach. In humans, *Helicobacter* infection occurs over years to incite oxyntic atrophy and chronic inflammation that predispose individuals to develop gastric cancer. Murine models of metaplasia have provided insights into the origin of metaplasia and cellular processes that progress metaplasia. To summarize, studies using immunodeficient murine models established that CD4+ T cells are necessary for *Helicobacter*-associated oxyntic atrophy (Eaton et al., 2001; Roth et al., 1999). After parietal cell loss, metaplasia develops from transdifferentiation of chief cells into spasmolytic polypeptide expression metaplasia (SPEM). SPEM can further progress to intestinalized metaplasia (intestinal metaplasia (IM) in humans, intestinalized SPEM in mice) in the presence of inflammation (Nam et al., 2010b; Yoshizawa et al., 2007). Whether SPEM or IM is the origin for gastric adenocarcinoma is still unknown. However, SPEM does not progress towards a more advanced intestinalized phenotype in mice without the influence of an inflammatory component (Weis et al., 2013a). The work presented here details the inflammatory mediators necessary for the induction and progression of SPEM, which could provide potential therapeutic targets.

Previous studies in our lab identified that while mice do not develop intestinal metaplasia, SPEM progresses to become more intestinalized over time. This progression is directly associated with the inflammatory response, as SPEM in L635-treated mice and *Helicobacter felis* infected mice has an increase in intestinal-associated transcripts (CFTR, DMBT1, ETV5 and GPX2) while non-inflammatory DMP-777-treated mice do not (Weis et al., 2013a). The first study, detailed in Chapter 2, sought to determine the inflammatory cells necessary for the

intestinalization and advancement of SPEM (Petersen et al., 2014). T cells, B cells, IFN gamma, neutrophils and macrophages are all associated with *Helicobacter* infection and were therefore were identified as potential targets that could contribute towards the progression of metaplasia. Therefore IFN gamma knock out mice, Rag1 knock out mice (lack T and B cells), neutrophil-depleted mice, and macrophage-depleted mice were all treated with L635 to determine if any of these cell types could solely prevent the progression of metaplasia. The results of this study revealed that only macrophages were necessary for the progression to intestinalized SPEM. Macrophage-depleted mice treated with L635 had decreased intestinalized transcripts, SPEM cells, and proliferation compared to control L635-treated mice. Further characterization of gastric macrophages present in L635-treated mice revealed a predominant M2 polarization (CD163, Ym1, Arg1, Arg2 positive), whereas macrophages in DMP-777-treated mice were not positive for M2 markers. Typically, M2-macrophages are associated with tumors and an anti-inflammatory response that is promoted by Th2 cytokines (Mills et al., 2000). M2 polarized macrophages are also implicated in driving the development of pancreatic acinar to ductal cell metaplasia (ADM), the neoplastic disease state prior to pancreatic ductal adenocarcinoma (PDAC) (Liou et al., 2013). Therefore the association of M2 macrophages in metaplastic tissues appears to promote cancer development. Nevertheless, the mechanism by which macrophages are promoting disease advancement is not well understood.

Our next aim was to further identify potential macrophage produced targets that could promote intestinalization of SPEM. Recent studies have identified diversity within macrophage populations according to the environmental niche (Davies et al., 2013; Martinez and Gordon, 2014). Therefore, our goal was not only to identify target genes, but also to characterize further gastric macrophages. Macrophages from the corpus of DMP-777 and L635-treated mice were isolated and RNA sequenced to compare SPEM-associated macrophages (DMP-777-treated mice) and intestinalized SPEM-associated macrophages (L635-treated mice). Isolating

macrophages from untreated wild-type mice was repeatedly unsuccessful. This is in part due to the low prevalence of tissue-resident macrophages in the stomach. Nevertheless, even with multiple mouse stomachs pooled together, RNA obtained from wild type macrophages had inadequate quality for RNA sequencing. One possibility is that macrophages associated with SPEM may be easier to remove from the epithelium because the mucosa in DMP-777-treated mice and L635-treated mice is damaged. The damaged mucosa may assist in tissue dissociation and therefore ease in the removal of macrophages. Macrophages within an undamaged wild-type stomach may be too well associated with epithelial cells to be removed without significant damage or death to the population. We therefore progressed with macrophage RNA from SPEM and intestinalized SPEM to be analyzed by HudsonAlpha (Huntsville, AL) and generated a list differentially expressed genes. Exactly 1641 genes were found to be significantly different (≥ 2 fold difference and $p \geq 0.01$) between the two groups. Of this, 811 genes were identified as being upregulated in macrophages isolated from DMP-777-treated mice, and 830 upregulated in L635-treated mouse macrophages. To determine potential targets, genes were classified into groups (cytokines, chemokines, matrix remodeling, angiogenic factors, cell adhesion) and genes with the greatest fold changes were examined first. The IL-1 family member IL-33 was the most significantly upregulated cytokine/chemokine in macrophages isolated from L635-treated mice compared to DMP-777-treated mice (6-fold increase). Using IL-33 knockout mice (IL33KO), we sought to identify whether IL-33 played a role in the development or progression of SPEM. IL33KO mice were treated with L635 and had typical parietal cell loss with had normal numbers macrophages recruited into the mucosa. This is of particular importance as our previous data shows macrophage depletion (or failure to recruit) would prevent the progression of SPEM. Thus the fact that IL-33 did not impact macrophage recruitment is critical to the study. Unexpectedly we found that L635-treated IL33KO mice did not develop SPEM or intestinalized SPEM in response to parietal cell loss. We anticipated that SPEM may not become intestinalized, and instead SPEM development

was prevented altogether. To determine how IL-33 could be impacting SPEM induction, we decided to do a cytokine array to see what other factors could potentially be differentially expressed. IL-4, IL-5, IL-9 and IL-13 (Th2 cytokines) were all found to be significantly reduced in L635-treated IL33KO mice compared to control L635-treated mice. The reduction of IL-4 and IL-13 are of particular interest as both have been shown to induce mucus metaplasia in the airway and intestine. Specifically IL-13 is required for the development of mucus metaplasia in those tissues. Thus, IL-33 in the stomach appears to induce IL-13 expression that could stimulate chief cells to transdifferentiate to SPEM cells and produce mucus. Further insight into this topic is discussed in future directions. Among other cytokines also decreased in L635-treated IL33KO mice were CCL11, CCL17 and CCL24, which are a signature of M2a polarized macrophages. Other M1 and M2 cytokines were assessed and we determined that the recruited macrophages in L635-treated IL33KO mice did not polarize towards M2a. Taken together, these data show that IL-33 is necessary for M2a macrophage polarization, Th2 cytokine induction in the stomach, and transdifferentiation of chief cells into SPEM cells. While previous studies show that exogenous administration of IL-33 is able to induce mucus metaplasia in the airway, stomach and intestine, (Buzzelli, 2015; Kurowska-Stolarska et al., 2009; Prefontaine et al., 2010) our data suggest that IL-33 is required for metaplasia development and macrophage polarization to induce intestinalization. In summary, our studies investigating the role of the immune system in the development and progression of SPEM identified M2 macrophages and IL-33 as key regulators for M2a macrophage polarization and chief cell transdifferentiation into SPEM. These findings parallel key inflammatory responses observed in allergic inflammation and airway hyperactivity. Thus a unified paradigm has developed illustrating that the inflammatory response to injury in the airway and stomach promote a similar processes of inducing Th2-driven mucus metaplasia that is associated with M2a polarized macrophages.

2. Future Directions

The studies detailed here identify specific aspects of the immune system that directly regulate metaplasia development and progression in the murine stomach. Further studies should focus on investigating the mechanisms by which these immune components influence the induction of metaplasia and the progression of metaplastic lesions. Specifically, there are three different categories that contain follow-up questions: IL-33-related studies, Th2 cytokines in the induction and intestinalization in SPEM, and other immune targets to explore.

IL-33-related studies.

Chapter 3 details the identification of IL-33 as a critical factor for macrophage polarization and SPEM induction. The resulting questions pertain to how IL-33 induces these responses. Buzzelli et al. described that IL-33 acted as stomach alarmin by exogenously administering recombinant IL-33 into mice, resulting in SPEM accompanied by an inflammatory response (Buzzelli, 2015). Scientists typically use two definitions to designate a specific cytokine/chemokine as an alarmin (Haraldsen et al., 2009). First, is the ability to alert other cell types to damage (i.e. a danger signal), which is synonymous to the definition of DAMP (damage-associated molecular pattern) (Foell et al., 2007). Therefore a second more specific definition was imposed to only include factors released by damaged/injured/infected cells that attract the immune system in effort to amount an inflammatory response (Oppenheim et al., 2007; Oppenheim and Yang, 2005). For example, HMGB1 is a protein located in the nucleus that aids in the binding of transcription factors to DNA, and when released from apoptotic or necrotic cells causes a strong inflammatory response (Scaffidi et al., 2002). IL-33 is normally expressed in the nucleus of surface epithelial cells in the corpus and recruited macrophages after parietal cell loss (Schmitz et al., 2005). Nevertheless, neither macrophages nor the surface epithelial cells undergo apoptosis or necrosis during *Helicobacter* infection or acute

parietal cell loss using the drugs L635 or DMP-777. Thus, while exogenously administered IL-33 does act as an alarmin in the stomach by recruiting inflammatory cells, it is unlikely that endogenous IL-33 functions through this mechanism. Instead is it plausible that IL-33 is acting as a transcription factor to affect downstream signaling instead of acting as an alarmin. The role of IL-33 in the nucleus is still not well described; however, IL-33 is thought to effect transcription by associating with heterochromatin (Carriere et al., 2007). Ali et al were the first to describe that nuclear IL-33 is able to repress NF-kB signaling by associating with p65 (Ali et al., 2011). Therefore, accessing the downstream factors mediated by IL-33 in the inflamed stomach in both surface epithelial cells and infiltrating macrophages through a method such as ChIP-sequencing would identify novel IL-33 target genes. Determining how IL-33 is being differentially regulated depending on the source cell would also determine how epithelial cell associated IL-33 differs in gene transcription regulation compared to IL-33 associated with macrophages. A similar follow up question is how IL-33 from different cell sources impacts the overall metaplastic phenotype. A potential approach would be a bone marrow transplantation experiment, where IL33 knock out mouse bone marrow would be transplanted into a wild-type C57Bl/6 mouse ($WT^{IL33koBM}$) and IL-33 knock out mouse would receive wild-type bone marrow ($IL33KO^{wtBM}$). Acute parietal cell loss could be induced using L635 in both models and the phenotype accessed to determine how the source of IL-33 in the stomach effects metaplasia development. It could be that IL-33 solely from macrophages is important in both inducing the production of IL-13 from ILC2 cells to promote mucus production and macrophage polarization. Finally, to ensure that IL-33 is important in a more natural setting of metaplasia development, IL-33 knock out mice should be infected with *Helicobacter felis*.

Th2 cytokines in the induction and intestinalization in SPEM.

The aim of the study detailed in Chapter 3 was to determine how infiltrating M2 macrophages were intestinalizing metaplasia. We identified IL-33 as a factor important in both

metaplasia induction and macrophage polarization. Further studies are needed to separate the two effects to better understand how IL-33 is preventing chief cells from transdifferentiating into SPEM cells and how the lack of M2 polarized macrophages affects SPEM development and progression. To approach these two questions, a few different methods could be employed. First, one potential explanation for the changes observed is the significant reduction of Th2 cytokines in the stomach of IL33KO mice treated with L635 compared to control L635-treated mice. Exogenous treatment of Th2 cytokines IL-4, IL-13 and IL-9 are able to induce mucus metaplasia in the airway in mice through IL-33 (Dabbagh et al., 1999; Kurowska-Stolarska et al., 2008). Therefore understanding how the loss of different Th2 cytokines impacts the development of SPEM is an imperative question. It is a viable hypothesis that if Th2 cytokines can induce mucus metaplasia, perhaps in their absence metaplasia development is prevented. An approach would be to use genetic knock out mouse models for the ligands and receptors (all mice are viable and available) and treat each with L635. The cytokine IL-13 is of specific interest, as other studies detailed that manipulations within IL-13 signaling through deletion of the IL-13 receptor, IL4ra, or of IL-13 itself abrogates mucus production in the intestine (von Moltke et al., 2015). While IL-4 is important for immune cell recruitment, IL-4 is not required for mucus production in the airway or intestine (Cohn et al., 1997). Another approach could be administering exogenous Th2 cytokines to L635-treated IL-33 knock out mice to see which parts of the phenotype are ameliorated. On a similar note, DMP-777 treated mice could be administered different cytokine cocktails (IL-33, IL-4, IL-13, IL-9) to push an intestinalized SPEM phenotype or macrophage polarization. After each cytokine administration, mice should be checked for SPEM intestinalization and macrophage polarization to determine the effect of cytokines on the metaplastic progression and immune infiltrate.

IL-25 and innate lymphoid cells (ILCs).

In effort to expand the immunological studies of SPEM progression in the stomach, new cytokines and immune populations should be explored that have yet to be evaluated. Specifically, the cytokine IL-25 and the innate lymphoid cell population (ILCs) could be of importance in Th2 cytokine regulation and expansion of different cell types during inflammation. The IL-17 family member IL-25 is of specific interest due to its role in allergic inflammation and promoting a Th2 cytokine response (Hongjia et al., 2014). Data presented in Chapter 3 indicate that the inflammatory response to acute parietal cell loss in the stomach parallels the Th2 cytokine and M2a signature observed in allergic airway inflammation (Kurowska-Stolarska et al., 2009). Mice infused with IL-25 have induced expression of IL-4, IL-5 and IL-13, causing eosinophilia and pathological changes in the GI tract. Specifically, IL-25 administration caused stomach changes in the corpus described as “a vacuolation of stomach mucus cells” that appear to be similar to the appearance of SPEM cells (Fort et al., 2001). IL-25 is also expressed in the stomach under normal conditions in DLCK1-positive tuft cells that expand in response to parietal cell loss (Saqui-Salces et al., 2011; von Moltke et al., 2015). Thus, perhaps tuft cell expansion during atrophic gastritis may be in part to increased IL-25 production. IL-25 functions to activate and expand tissue resident ILC2 cells that are a significant producer of type 2 cytokines (IL-4, IL-13) (Licona-Limon et al., 2013). In the absence of IL-25, IL-33 also activates ILC2 cells to produce type 2 cytokines that evoke mucus metaplasia. However, the converse is not true, IL-25 cannot replace the function of IL-33. Nevertheless, the key downstream regulator is IL-13, where in the absence of IL-13 neither IL-25 nor IL-33 are unable to induce mucus metaplasia in the airway or intestine. Thus further adding evidence to the IL-13 null mouse or administrations of IL-13 to IL-33 knock out mice in the experiments detailed above. IL-25 expression should be studied in our acute parietal cell

loss models (L635 and DMP-777) along with chronic infection with *Helicobacter felis* at different time points in context with tuft cell expansion and function.

In conclusion, it appears that in response to acute parietal cell loss there are several immuno-epithelia circuits synergizing to promote SPEM. While the timing of these processes is unclear, parietal cell loss induces the expansion of tuft cells (increased IL-25) and surface epithelial cells (increased IL-33). These two cytokines working through IL-9 would most likely function to activate the tissue resident ILC2 populations that in turn produce IL-13 (among other Th2/type 2 cytokines). IL-13 may then induce chief cells to transdifferentiate into SPEM cells through an unknown mechanism. Simultaneously, macrophages infiltrating into the mucosa in response to parietal cell loss are polarizing towards M2a in the Th2 cytokine environment. M2a polarized macrophages expressing IL-33 are then able to promote the intestinalization of SPEM that progresses metaplasia towards adenocarcinoma.

REFERENCES

Ali, S., A. Mohs, M. Thomas, J. Klare, R. Ross, M.L. Schmitz, and M.U. Martin. 2011. The dual function cytokine IL-33 interacts with the transcription factor NF-kappaB to dampen NF-kappaB-stimulated gene transcription. *Journal of immunology* 187:1609-1616.

Appelmelk, B.J., I. Simoons-Smit, R. Negrini, A.P. Moran, G.O. Aspinall, J.G. Forte, T. De Vries, H. Quan, T. Verboom, J.J. Maaskant, P. Ghiara, E.J. Kuipers, E. Bloemena, T.M. Tadema, R.R. Townsend, K. Tyagarajan, J.M. Crothers, Jr., M.A. Monteiro, A. Savio, and J. De Graaff. 1996. Potential role of molecular mimicry between Helicobacter pylori lipopolysaccharide and host Lewis blood group antigens in autoimmunity. *Infection and immunity* 64:2031-2040.

Beales, I.L., and J. Calam. 1998. Interleukin 1 beta and tumour necrosis factor alpha inhibit acid secretion in cultured rabbit parietal cells by multiple pathways. *Gut* 42:227-234.

Benjamini, Y.a.H., Y. 1995. Controlling the False Discovery Rate: A Practical and Powerful Approach to Multiple Testing. *Journal of the Royal Statistical Society. Series B (Methodological)* 57:12.

Beuscher, H.U., C. Gunther, and M. Rollinghoff. 1990. IL-1 beta is secreted by activated murine macrophages as biologically inactive precursor. *Journal of immunology* 144:2179-2183.

Blaser, M.J. 1992. Hypotheses on the pathogenesis and natural history of Helicobacter pylori-induced inflammation. *Gastroenterology* 102:720-727.

Blaser, M.J., and J. Parsonnet. 1994. Parasitism by the "slow" bacterium Helicobacter pylori leads to altered gastric homeostasis and neoplasia. *The Journal of clinical investigation* 94:4-8.

Blom, L., B.C. Poulsen, B.M. Jensen, A. Hansen, and L.K. Poulsen. 2011. IL-33 induces IL-9 production in human CD4+ T cells and basophils. *PloS one* 6:e21695.

Bronte, V., and P. Zanovello. 2005. Regulation of immune responses by L-arginine metabolism. *Nature reviews. Immunology* 5:641-654.

Buzzelli, J.N., Chalinor, H.V., Pavlic, D.I., Sutton, P., Menheniott, T.R., Giraud, A.S., Judd, L.M. 2015. IL33 is a Stomach Alarmin that initiates a Skewed Th2 response to Injury and Infection. In CMGH. 19.

Cancer Genome Atlas Research, N. 2014. Comprehensive molecular characterization of gastric adenocarcinoma. *Nature* 513:202-209.

Carriere, V., L. Roussel, N. Ortega, D.A. Lacorre, L. Americh, L. Aguilar, G. Bouche, and J.P. Girard. 2007. IL-33, the IL-1-like cytokine ligand for ST2 receptor, is a chromatin-associated nuclear factor in vivo. *Proceedings of the National Academy of Sciences of the United States of America* 104:282-287.

Cayrol, C., and J.P. Girard. 2014. IL-33: an alarmin cytokine with crucial roles in innate immunity, inflammation and allergy. *Current opinion in immunology* 31:31-37.

Chang, N.C., S.I. Hung, K.Y. Hwa, I. Kato, J.E. Chen, C.H. Liu, and A.C. Chang. 2001. A macrophage protein, Ym1, transiently expressed during inflammation is a novel mammalian lectin. *The Journal of biological chemistry* 276:17497-17506.

Choi, E., A.M. Hendley, J.M. Bailey, S.D. Leach, and J.R. Goldenring. 2015. Expression of Activated Ras in Gastric Chief Cells of Mice Leads to the Full Spectrum of Metaplastic Lineage Transitions. *Gastroenterology*

Chow, A., B.D. Brown, and M. Merad. 2011. Studying the mononuclear phagocyte system in the molecular age. *Nature reviews. Immunology* 11:788-798.

Cohn, L., R.J. Homer, A. Marinov, J. Rankin, and K. Bottomly. 1997. Induction of airway mucus production By T helper 2 (Th2) cells: a critical role for interleukin 4 in cell recruitment but not mucus production. *The Journal of experimental medicine* 186:1737-1747.

Correa, P. 1988. A human model of gastric carcinogenesis. *Cancer Res.* 48:3554-3560.

Correa, P., and M.B. Piazuelo. 2012. The gastric precancerous cascade. *Journal of digestive diseases* 13:2-9.

Dabbagh, K., K. Takeyama, H.M. Lee, I.F. Ueki, J.A. Lausier, and J.A. Nadel. 1999. IL-4 induces mucin gene expression and goblet cell metaplasia in vitro and in vivo. *Journal of immunology* 162:6233-6237.

Daley, J.M., A.A. Thomay, M.D. Connolly, J.S. Reichner, and J.E. Albina. 2008. Use of Ly6G-specific monoclonal antibody to deplete neutrophils in mice. *Journal of leukocyte biology* 83:64-70.

Davies, L.C., S.J. Jenkins, J.E. Allen, and P.R. Taylor. 2013. Tissue-resident macrophages. *Nature immunology* 14:986-995.

de Martel, C., J. Ferlay, S. Franceschi, J. Vignat, F. Bray, D. Forman, and M. Plummer. 2012. Global burden of cancers attributable to infections in 2008: a review and synthetic analysis. *The lancet oncology* 13:607-615.

Dempsey, P.J., J.R. Goldenring, C.J. Soroka, I.M. Modlin, R.W. McClure, C.D. Lind, D.A. Ahlquist, M.R. Pittelkow, D.C. Lee, E.P. Sandgren, and et al. 1992a. Possible role of transforming growth factor alpha in the pathogenesis of Menetrier's disease: supportive evidence form humans and transgenic mice. *Gastroenterology* 103:1950-1963.

Dempsey, P.J., J.R. Goldenring, C.J. Soroka, I.M. Modlin, R.W. McClure, C.D. Lind, D.A. Ahlquist, M.R. Pittlekow, D.C. Lee, E.P. Sandgren, D.L. Page, and R.J. Coffey. 1992b. Possible role of TGFa in the pathogenesis of Menetrier's Disease: Supportive evidence from humans and transgenic mice. *Gastroenterology.* 103:1950-1963.

Deng, N., L.K. Goh, H. Wang, K. Das, J. Tao, I.B. Tan, S. Zhang, M. Lee, J. Wu, K.H. Lim, Z. Lei, G. Goh, Q.Y. Lim, A.L. Tan, D.Y. Sin Poh, S. Riahi, S. Bell, M.M. Shi, R. Linnartz, F. Zhu, K.G. Yeoh, H.C. Toh, W.P. Yong, H.C. Cheong, S.Y. Rha, A. Boussioutas, H. Grabsch, S. Rozen, and P. Tan. 2012. A comprehensive survey of genomic alterations in gastric cancer reveals systematic patterns of molecular exclusivity and co-occurrence among distinct therapeutic targets. *Gut* 61:673-684.

Dockray, G.J., A. Varro, R. Dimaline, and T. Wang. 2001. The gastrins: their production and biological activities. *Annual review of physiology* 63:119-139.

Eaton, K.A., M. Mefford, and T. Thevenot. 2001. The role of T cell subsets and cytokines in the pathogenesis of Helicobacter pylori gastritis in mice. *Journal of immunology* 166:7456-7461.

Eidt, S., G. Oberhuber, A. Schneider, and M. Stolte. 1996. The histopathological spectrum of type A gastritis. *Pathology, research and practice* 192:101-106.

El-Zimaity, H.M., H. Ota, D.Y. Graham, T. Akamatsu, and T. Katsuyama. 2002. Patterns of gastric atrophy in intestinal type gastric carcinoma. *Cancer* 94:1428-1436.

Evans, D.J., Jr., D.G. Evans, T. Takemura, H. Nakano, H.C. Lampert, D.Y. Graham, D.N. Granger, and P.R. Kvietys. 1995. Characterization of a Helicobacter pylori neutrophil-activating protein. *Infection and immunity* 63:2213-2220.

Fehlings, M., L. Drobbe, V. Moos, P. Renner Viveros, J. Hagen, M. Beigier-Bompadre, E. Pang, E. Belogolova, Y. Churin, T. Schneider, T.F. Meyer, T. Aebischer, and R. Ignatius. 2012. Comparative analysis of the interaction of Helicobacter pylori with human dendritic cells, macrophages, and monocytes. *Infection and immunity* 80:2724-2734.

Ferenbach, D.A., T.A. Sheldrake, K. Dhaliwal, T.M. Kipari, L.P. Marson, D.C. Kluth, and J. Hughes. 2012. Macrophage/monocyte depletion by clodronate, but not diphtheria toxin, improves renal ischemia/reperfusion injury in mice. *Kidney international* 82:928-933.

Foell, D., H. Wittkowski, and J. Roth. 2007. Mechanisms of disease: a 'DAMP' view of inflammatory arthritis. *Nature clinical practice. Rheumatology* 3:382-390.

Fort, M.M., J. Cheung, D. Yen, J. Li, S.M. Zurawski, S. Lo, S. Menon, T. Clifford, B. Hunte, R. Lesley, T. Muchamuel, S.D. Hurst, G. Zurawski, M.W. Leach, D.M. Gorman, and D.M. Rennick. 2001. IL-25 induces IL-4, IL-5, and IL-13 and Th2-associated pathologies in vivo. *Immunity* 15:985-995.

Fox, J.G., M. Blanco, J.C. Murphy, N.S. Taylor, A. Lee, Z. Kabok, and J. Pappo. 1993. Local and systemic immune responses in murine Helicobacter felis active chronic gastritis. *Infection and immunity* 61:2309-2315.

Fox, J.G., X. Li, R.J. Cahill, K. Andrutis, A.K. Rustgi, R. Odze, and T.C. Wang. 1996. Hypertrophic gastropathy in Helicobacter felis-Infected wild type C57BL/6 mice and p53 hemizygous transgenic mice. *Gastroenterology.* 110:155-166.

Fox, J.G., and T.C. Wang. 2007. Inflammation, atrophy, and gastric cancer. *The Journal of clinical investigation* 117:60-69.

Fox, J.G., T.C. Wang, A.B. Rogers, T. Poutahidis, Z. Ge, N. Taylor, C.A. Dangler, D.A. Israel, U. Krishna, K. Gaus, and R.M. Peek, Jr. 2003. Host and microbial constituents influence Helicobacter pylori-induced cancer in a murine model of hypergastrinemia. *Gastroenterology* 124:1879-1890.

Gautier, E.L., T. Shay, J. Miller, M. Greter, C. Jakubzick, S. Ivanov, J. Helft, A. Chow, K.G. Elpek, S. Gordonov, A.R. Mazloom, A. Ma'ayan, W.J. Chua, T.H. Hansen, S.J. Turley, M. Merad, G.J. Randolph, and C. Immunological Genome. 2012. Gene-expression profiles and

transcriptional regulatory pathways that underlie the identity and diversity of mouse tissue macrophages. *Nature immunology* 13:1118-1128.

Goldenring, J.R., and K.T. Nam. 2010. Oxyntic atrophy, metaplasia, and gastric cancer. *Progress in molecular biology and translational science* 96:117-131.

Goldenring, J.R., K.T. Nam, T.C. Wang, J.C. Mills, and N.A. Wright. 2010. Spasmolytic polypeptide-expressing metaplasia and intestinal metaplasia: time for reevaluation of metaplasias and the origins of gastric cancer. *Gastroenterology* 138:2207-2210, 2210 e2201.

Goldenring, J.R., and S. Nomura. 2006. Differentiation of the gastric mucosa III. Animal models of oxyntic atrophy and metaplasia. *Am J Physiol Gastrointest Liver Physiol* 291:G999-1004.

Goldenring, J.R., G.S. Ray, R.J. Coffey, P.C. Meunier, P.J. Haley, T.B. Barnes, and B.D. Car. 2000a. Reversible drug-induced oxyntic atrophy in rats. *Gastroenterology* 118:1080-1093.

Goldenring, J.R., G.S. Ray, R.J. Coffey, P.C. Meunier, P.J. Haley, T.B. Barnes, and B.D. Car. 2000b. Reversible drug-induced oxyntic atrophy in rats. *Gastroenterology.* 118:1080-1093.

Goldenring, J.R., G.S. Ray, C.J. Soroka, J. Smith, I.M. Modlin, K.S. Meise, and R.J. Coffey, Jr. 1996. Overexpression of transforming growth factor-alpha alters differentiation of gastric cell lineages. *Dig Dis Sci* 41:773-784.

Halldorsdottir, A.M., M. Sigurdardottir, J.G. Jonasson, M. Oddsdottir, J. Magnusson, J.R. Lee, and J.R. Goldenring. 2003. Spasmolytic polypeptide expressing metaplasia (SPEM) associated with gastric cancer in Iceland. *Dig.Dis.Sci.* 48:431-441.

Haraldsen, G., J. Balogh, J. Pollheimer, J. Sponheim, and A.M. Kuchler. 2009. Interleukin-33 - cytokine of dual function or novel alarmin? *Trends in immunology* 30:227-233.

Hashimoto, D., A. Chow, C. Noizat, P. Teo, M.B. Beasley, M. Leboeuf, C.D. Becker, P. See, J. Price, D. Lucas, M. Greter, A. Mortha, S.W. Boyer, E.C. Forsberg, M. Tanaka, N. van Rooijen, A. Garcia-Sastre, E.R. Stanley, F. Ginhoux, P.S. Frenette, and M. Merad. 2013. Tissue-resident macrophages self-maintain locally throughout adult life with minimal contribution from circulating monocytes. *Immunity* 38:792-804.

Hattori, T., B. Helpap, and P. Gedigk. 1982. The morphology and cell kinetics of pseudopyloric glands. *Virchows Arch B Cell Pathol Incl Mol Pathol* 39:31-40.

Hayashi, D., A. Tamura, H. Tanaka, Y. Yamazaki, S. Watanabe, K. Suzuki, K. Suzuki, K. Sentani, W. Yasui, H. Rakugi, Y. Isaka, and S. Tsukita. 2012. Deficiency of claudin-18 causes paracellular H+ leakage, up-regulation of interleukin-1beta, and atrophic gastritis in mice. *Gastroenterology* 142:292-304.

Heusinkveld, M., and S.H. van der Burg. 2011. Identification and manipulation of tumor associated macrophages in human cancers. *Journal of translational medicine* 9:216.

Hongjia, L., Z. Caiqing, L. Degan, L. Fen, W. Chao, W. Jinxiang, and D. Liang. 2014. IL-25 promotes Th2 immunity responses in airway inflammation of asthmatic mice via activation of dendritic cells. *Inflammation* 37:1070-1077.

Houghton, J., C. Stoicov, S. Nomura, A.B. Rogers, J. Carlson, H. Li, X. Cai, J.G. Fox, J.R. Goldenring, and T.C. Wang. 2004. Gastric cancer originating from bone marrow-derived cells. *Science* 306:1568-1571.

Howlett, M., H.V. Chalinor, J.N. Buzzelli, N. Nguyen, I.R. van Driel, K.M. Bell, J.G. Fox, E. Dimitriadis, T.R. Menheniott, A.S. Giraud, and L.M. Judd. 2012. IL-11 is a parietal cell cytokine that induces atrophic gastritis. *Gut* 61:1398-1409.

Hsieh, C.S., S.E. Macatonia, A. O'Garra, and K.M. Murphy. 1995. T cell genetic background determines default T helper phenotype development in vitro. *The Journal of experimental medicine* 181:713-721.

Hsu, L.S., C.P. Chan, C.J. Chen, S.H. Lin, M.T. Lai, J.D. Hsu, K.T. Yeh, and M.S. Soon. 2013. Decreased Kruppel-like factor 4 (KLF4) expression may correlate with poor survival in gastric adenocarcinoma. *Med Oncol* 30:632.

Huh, W.J., S.S. Khurana, J.H. Geahlen, K. Kohli, R.A. Waller, and J.C. Mills. 2012. Tamoxifen induces rapid, reversible atrophy, and metaplasia in mouse stomach. *Gastroenterology* 142:21-24 e27.

Ismail, H.F., J. Zhang, R.G. Lynch, Y. Wang, and D.J. Berg. 2003. Role for complement in development of Helicobacter-induced gastritis in interleukin-10-deficient mice. *Infection and immunity* 71:7140-7148.

Jain, R.N., A.A. Al-Menhali, T.M. Keeley, J. Ren, M. El-Zaatari, X. Chen, J.L. Merchant, T.S. Ross, C.S. Chew, and L.C. Samuelson. 2008. Hip1r is expressed in gastric parietal cells and is required for tubulovesicle formation and cell survival in mice. *J Clin Invest* 118:2459-2470.

Jenkins, S.J., D. Ruckerl, P.C. Cook, L.H. Jones, F.D. Finkelman, N. van Rooijen, A.S. MacDonald, and J.E. Allen. 2011. Local macrophage proliferation, rather than recruitment from the blood, is a signature of TH2 inflammation. *Science* 332:1284-1288.

Jones, T.R., I.H. Kang, D.B. Wheeler, R.A. Lindquist, A. Papallo, D.M. Sabatini, P. Golland, and A.E. Carpenter. 2008. CellProfiler Analyst: data exploration and analysis software for complex image-based screens. *BMC bioinformatics* 9:482.

Kang, J.M., B.H. Lee, N. Kim, H.S. Lee, H.E. Lee, J.H. Park, J.S. Kim, H.C. Jung, and I.S. Song. 2011. CDX1 and CDX2 expression in intestinal metaplasia, dysplasia and gastric cancer. *J Korean Med Sci* 26:647-653.

Kang, W., S. Rathinavelu, L.C. Samuelson, and J.L. Merchant. 2005. Interferon gamma induction of gastric mucous neck cell hypertrophy. *Laboratory investigation; a journal of technical methods and pathology* 85:702-715.

Katz, J.P., N. Perreault, B.G. Goldstein, L. Actman, S.R. McNally, D.G. Silberg, E.E. Furth, and K.H. Kaestner. 2005. Loss of Klf4 in mice causes altered proliferation and differentiation and precancerous changes in the adult stomach. *Gastroenterology* 128:935-945.

Kozol, R., A. Domanowski, R. Jaszewski, R. Czanko, B. McCurdy, M. Prasad, B. Fromm, and R. Calzada. 1991. Neutrophil chemotaxis in gastric mucosa. A signal-to-response comparison. *Digestive diseases and sciences* 36:1277-1280.

Kurowska-Stolarska, M., P. Kewin, G. Murphy, R.C. Russo, B. Stolarski, C.C. Garcia, M. Komai-Koma, N. Pitman, Y. Li, W. Niedbala, A.N. McKenzie, M.M. Teixeira, F.Y. Liew, and D. Xu. 2008. IL-33 induces antigen-specific IL-5+ T cells and promotes allergic-induced airway inflammation independent of IL-4. *Journal of immunology* 181:4780-4790.

Kurowska-Stolarska, M., B. Stolarski, P. Kewin, G. Murphy, C.J. Corrigan, S. Ying, N. Pitman, A. Mirchandani, B. Rana, N. van Rooijen, M. Shepherd, C. McSharry, I.B. McInnes, D. Xu, and F.Y. Liew. 2009. IL-33 amplifies the polarization of alternatively activated macrophages that contribute to airway inflammation. *Journal of immunology* 183:6469-6477.

Langmead, B., C. Trapnell, M. Pop, and S.L. Salzberg. 2009. Ultrafast and memory-efficient alignment of short DNA sequences to the human genome. *Genome biology* 10:R25.

Lawrence, T., and G. Natoli. 2011. Transcriptional regulation of macrophage polarization: enabling diversity with identity. *Nature reviews. Immunology* 11:750-761.

Lee, M.P., J.D. Ravenel, R.J. Hu, L.R. Lustig, G. Tomaselli, R.D. Berger, S.A. Brandenburg, T.J. Litzi, T.E. Bunton, C. Limb, H. Francis, M. Gorelikow, H. Gu, K. Washington, P. Argani, J.R. Goldenring, R.J. Coffey, and A.P. Feinberg. 2000. Targeted disruption of the Kvlqt1 gene causes deafness and gastric hyperplasia in mice. *J Clin Invest* 106:1447-1455.

Lennerz, J.K.M., S. Kim, E.L. Oates, W.J. Huh, J.M. Dherty, X. Tian, A.J. Bredemeyer, J.R. Goldenring, G.Y. Lauwers, G.Y. Shin, and J.C. Mills. 2010. The transcription factor MIST1 is a novel human gastric chief cell marker whose expression is lost in metaplasia, dysplasia and carcinoma. . *Amer. J. Pathol.* 177:1514-1533.

Leys, C.M., S. Nomura, B.J. LaFleur, S. Ferrone, M. Kaminishi, E. Montgomery, and J.R. Goldenring. 2007. Expression and prognostic significance of prothymosin-alpha and ERp57 in human gastric cancer. *Surgery* 141:41-50.

Li, H., B. Handsaker, A. Wysoker, T. Fennell, J. Ruan, N. Homer, G. Marth, G. Abecasis, R. Durbin, and S. Genome Project Data Processing. 2009. The Sequence Alignment/Map format and SAMtools. *Bioinformatics* 25:2078-2079.

Licona-Limon, P., L.K. Kim, N.W. Palm, and R.A. Flavell. 2013. TH2, allergy and group 2 innate lymphoid cells. *Nature immunology* 14:536-542.

Liou, G.Y., H. Doppler, B. Necela, M. Krishna, H.C. Crawford, M. Raimondo, and P. Storz. 2013. Macrophage-secreted cytokines drive pancreatic acinar-to-ductal metaplasia through NF-kappaB and MMPs. *The Journal of cell biology* 202:563-577.

Liu, Z., E.S. Demitrack, T.M. Keeley, K.A. Eaton, M. El-Zaatari, J.L. Merchant, and L.C. Samuelson. 2012. IFNgamma contributes to the development of gastric epithelial cell metaplasia in Huntingtin interacting protein 1 related (Hip1r)-deficient mice. *Laboratory investigation; a journal of technical methods and pathology* 92:1045-1057.

Lopez-Diaz, L., K.L. Hinkle, R.N. Jain, Y. Zavros, C.S. Brunkan, T. Keeley, K.A. Eaton, J.L. Merchant, C.S. Chew, and L.C. Samuelson. 2006. Parietal cell hyperstimulation and autoimmune gastritis in cholera toxin transgenic mice. *American journal of physiology. Gastrointestinal and liver physiology* 290:G970-979.

Lu, H., K.R. Clauser, W.L. Tam, J. Frose, X. Ye, E.N. Eaton, F. Reinhardt, V.S. Donnenberg, R. Bhargava, S.A. Carr, and R.A. Weinberg. 2014. A breast cancer stem cell niche supported by juxtacrine signalling from monocytes and macrophages. *Nature cell biology* 16:1105-1117.

Mai, U.E., G.I. Perez-Perez, L.M. Wahl, S.M. Wahl, M.J. Blaser, and P.D. Smith. 1991. Soluble surface proteins from Helicobacter pylori activate monocytes/macrophages by lipopolysaccharide-independent mechanism. *The Journal of clinical investigation* 87:894-900.

Mantovani, A., A. Sica, S. Sozzani, P. Allavena, A. Vecchi, and M. Locati. 2004. The chemokine system in diverse forms of macrophage activation and polarization. *Trends in immunology* 25:677-686.

Martinez, F.O., and S. Gordon. 2014. The M1 and M2 paradigm of macrophage activation: time for reassessment. *F1000prime reports* 6:13.

Maywald, R.L., S.K. Doerner, L. Pastorelli, C. De Salvo, S.M. Benton, E.P. Dawson, D.G. Lanza, N.A. Berger, S.D. Markowitz, H.J. Lenz, J.H. Nadeau, T.T. Pizarro, and J.D. Heaney. 2015. IL-33 activates tumor stroma to promote intestinal polyposis. *Proceedings of the National Academy of Sciences of the United States of America* 112:E2487-2496.

Meining, A., A. Morgner, S. Miehlke, E. Bayerdorffer, and M. Stolte. 2001. Atrophy-metaplasia-dysplasia-carcinoma sequence in the stomach: a reality or merely an hypothesis? *Best practice & research. Clinical gastroenterology* 15:983-998.

Merchant, J.L. 2005. Inflammation, atrophy, gastric cancer: connecting the molecular dots. *Gastroenterology* 129:1079-1082.

Mills, C.D., K. Kincaid, J.M. Alt, M.J. Heilman, and A.M. Hill. 2000. M-1/M-2 macrophages and the Th1/Th2 paradigm. *Journal of immunology* 164:6166-6173.

Minegishi, Y., H. Suzuki, M. Arakawa, Y. Fukushima, T. Masaoka, T. Ishikawa, N.A. Wright, and T. Hibi. 2007. Reduced Shh expression in TFF2-overexpressing lesions of the gastric fundus under hypochlorhydric conditions. *J Pathol* 213:161-169.

Mombaerts, P., J. Iacomini, R.S. Johnson, K. Herrup, S. Tonegawa, and V.E. Papaioannou. 1992. RAG-1-deficient mice have no mature B and T lymphocytes. *Cell* 68:869-877.

Mueller, A., D.S. Merrell, J. Grimm, and S. Falkow. 2004. Profiling of microdissected gastric epithelial cells reveals a cell type-specific response to Helicobacter pylori infection. *Gastroenterology* 127:1446-1462.

Murray, P.J., and T.A. Wynn. 2011. Protective and pathogenic functions of macrophage subsets. *Nature reviews. Immunology* 11:723-737.

Nair, M.G., I.J. Gallagher, M.D. Taylor, P. Loke, P.S. Coulson, R.A. Wilson, R.M. Maizels, and J.E. Allen. 2005. Chitinase and Fizz family members are a generalized feature of nematode infection with selective upregulation of Ym1 and Fizz1 by antigen-presenting cells. *Infection and immunity* 73:385-394.

Nam, K.T., H.-J. Lee, J.F. Sousa, V.G. Weis, R.L. O'Neal, P.E. Finke, J. Romero-Gallo, G. Shi, J.C. Mills, R.M. Peek, S.F. Konieczny, and J.R. Goldenring. 2010a. Mature chief cells are cryptic progenitors for metaplasia in the stomach. *Gastroenterology* 139:2028-2037.

Nam, K.T., H.J. Lee, H. Mok, J. Romero-Gallo, J.E. Crowe, Jr., R.M. Peek, Jr., and J.R. Goldenring. 2009. Amphiregulin-deficient mice develop spasmolytic polypeptide expressing metaplasia and intestinal metaplasia. *Gastroenterology* 136:1288-1296.

Nam, K.T., H.J. Lee, J.F. Sousa, V.G. Weis, R.L. O'Neal, P.E. Finke, J. Romero-Gallo, G. Shi, J.C. Mills, R.M. Peek, Jr., S.F. Konieczny, and J.R. Goldenring. 2010b. Mature chief cells are cryptic progenitors for metaplasia in the stomach. *Gastroenterology* 139:2028-2037 e2029.

Nam, K.T., R. O'Neal, Y.S. Lee, Y.C. Lee, R.J. Coffey, and J.R. Goldenring. 2012. Gastric tumor development in Smad3-deficient mice initiates from forestomach/glandular transition zone along the lesser curvature. *Lab Invest* 92:883-895.

Nam, K.T., A. Varro, R.J. Coffey, and J.R. Goldenring. 2007. Potentiation of oxyntic atrophy-induced gastric metaplasia in amphiregulin-deficient mice. *Gastroenterology* 132:1804-1819.

Nguyen, T.L., S.S. Khurana, C.J. Bellone, B.J. Capoccia, J.E. Sagartz, R.A. Kesman, Jr., J.C. Mills, and R.J. DiPaolo. 2013. Autoimmune gastritis mediated by CD4+ T cells promotes the development of gastric cancer. *Cancer research* 73:2117-2126.

Nikolaidis, N.M., N. Zimmermann, N.E. King, A. Mishra, S.M. Pope, F.D. Finkelman, and M.E. Rothenberg. 2003. Trefoil factor-2 is an allergen-induced gene regulated by Th2 cytokines and STAT6 in the lung. *American journal of respiratory cell and molecular biology* 29:458-464.

Nomura, S., T. Baxter, H. Yamaguchi, C. Leys, A.B. Vartapetian, J.G. Fox, J.R. Lee, T.C. Wang, and J.R. Goldenring. 2004. Spasmolytic polypeptide expressing metaplasia to preneoplasia in H. felis-infected mice. *Gastroenterology* 127:582-594.

Nomura, S., S.H. Settle, C.M. Leys, A.L. Means, R.M. Peek, Jr., S.D. Leach, C.V. Wright, R.J. Coffey, and J.R. Goldenring. 2005a. Evidence for repatterning of the gastric fundic epithelium associated with Menetrier's disease and TGFalpha overexpression. *Gastroenterology* 128:1292-1305.

Nomura, S., H. Yamaguchi, M. Ogawa, T.C. Wang, J.R. Lee, and J.R. Goldenring. 2005b. Alterations in gastric mucosal lineages induced by acute oxyntic atrophy in wild-type and gastrin-deficient mice. *American journal of physiology. Gastrointestinal and liver physiology* 288:G362-375.

Nozaki, K., M. Ogawa, J.A. Williams, B.J. Lafleur, V. Ng, R.I. Drapkin, J.C. Mills, S.F. Konieczny, S. Nomura, and J.R. Goldenring. 2008a. A molecular signature of gastric metaplasia arising in response to acute parietal cell loss. *Gastroenterology* 134:511-522.

Nozaki, K., M. Ogawa, J.A. Williams, B.J. LaFleur, V. Ng, R.I. Drapkin, J.C. Mills, S.F. Konieczny, S. Nomura, and J.R. Goldenring. 2008b. A molecular signature of gastric metaplasia arising in response to acute parietal cell loss. *Gastroenterology.* 511-521.

Ogawa, M., S. Nomura, A. Varro, T.C. Wang, and J.R. Goldenring. 2006. Altered metaplastic response of waved-2 EGF receptor mutant mice to acute oxyntic atrophy. *Am J Physiol Gastrointest Liver Physiol* 290:G793-804.

Oppenheim, J.J., P. Tewary, G. de la Rosa, and D. Yang. 2007. Alarmins initiate host defense. *Advances in experimental medicine and biology* 601:185-194.

Oppenheim, J.J., and D. Yang. 2005. Alarmins: chemotactic activators of immune responses. *Current opinion in immunology* 17:359-365.

Oshima, H., K. Hioki, B.K. Popivanova, K. Oguma, N. Van Rooijen, T.O. Ishikawa, and M. Oshima. 2011a. Prostaglandin E(2) signaling and bacterial infection recruit tumor-promoting macrophages to mouse gastric tumors. *Gastroenterology* 140:596-607 e597.

Oshima, H., B.K. Popivanova, K. Oguma, D. Kong, T.O. Ishikawa, and M. Oshima. 2011b. Activation of epidermal growth factor receptor signaling by the prostaglandin E(2) receptor EP4 pathway during gastric tumorigenesis. *Cancer science* 102:713-719.

Oshima, M., H. Oshima, A. Matsunaga, and M.M. Taketo. 2005. Hyperplastic gastric tumors with spasmolytic polypeptide-expressing metaplasia caused by tumor necrosis factor-alpha-dependent inflammation in cyclooxygenase-2/microsomal prostaglandin E synthase-1 transgenic mice. *Cancer research* 65:9147-9151.

Pastorelli, L., C. De Salvo, M. Vecchi, and T.T. Pizarro. 2013. The role of IL-33 in gut mucosal inflammation. *Mediators of inflammation* 2013:608187.

Petersen, C.P., V.G. Weis, K.T. Nam, J.F. Sousa, B. Fingleton, and J.R. Goldenring. 2014. Macrophages promote progression of spasmolytic polypeptide-expressing metaplasia after acute loss of parietal cells. *Gastroenterology* 146:1727-1738 e1728.

Poynter, D., S.A. Selway, S.A. Papworth, and S.R. Riches. 1986. Changes in the gastric mucosa of the mouse associated with long lasting unsurmountable histamine H2 blockade. *Gut* 27:1338-1346.

Prefontaine, D., J. Nadigel, F. Chouiali, S. Audusseau, A. Semlali, J. Chakir, J.G. Martin, and Q. Hamid. 2010. Increased IL-33 expression by epithelial cells in bronchial asthma. *The Journal of allergy and clinical immunology* 125:752-754.

Quiding-Jarbrink, M., S. Raghavan, and M. Sundquist. 2010. Enhanced M1 macrophage polarization in human helicobacter pylori-associated atrophic gastritis and in vaccinated mice. *PloS one* 5:e15018.

Ray, G.S., M.W. Jackson, and J.R. Goldenring. 1996. Foveolar hyperplasia following partial gastrectomy results from expansion of surface mucous cell compartment. *Digestive diseases and sciences* 41:2016-2024.

Robinson, M.D., and A. Oshlack. 2010. A scaling normalization method for differential expression analysis of RNA-seq data. *Genome biology* 11:R25.

Roth, K.A., S.B. Kapadia, S.M. Martin, and R.G. Lorenz. 1999. Cellular immune responses are essential for the development of Helicobacter felis-associated gastric pathology. *Journal of immunology* 163:1490-1497.

Saqui-Salces, M., T.M. Keeley, A.S. Grosse, X.T. Qiao, M. El-Zaatari, D.L. Gumucio, L.C. Samuelson, and J.L. Merchant. 2011. Gastric tuft cells express DCLK1 and are expanded in hyperplasia. *Histochemistry and cell biology* 136:191-204.

Scaffidi, P., T. Misteli, and M.E. Bianchi. 2002. Release of chromatin protein HMGB1 by necrotic cells triggers inflammation. *Nature* 418:191-195.

Schmidt, P.H., J.R. Lee, V. Joshi, R.J. Playford, R. Poulsom, N.A. Wright, and J.R. Goldenring. 1999a. Identification of a metaplastic cell lineage associated with human gastric adenocarcinoma. *Laboratory investigation; a journal of technical methods and pathology* 79:639-646.

Schmidt, P.H., J.R. Lee, V. Joshi, R.J. Playford, R. Poulsom, N.A. Wright, and J.R. Goldenring. 1999b. Identification of a metaplastic cell lineage associated with human gastric adenocarcinoma. *Lab.Invest.* 79:639-646.

Schmitz, J., A. Owyang, E. Oldham, Y. Song, E. Murphy, T.K. McClanahan, G. Zurawski, M. Moshrefi, J. Qin, X. Li, D.M. Gorman, J.F. Bazan, and R.A. Kastelein. 2005. IL-33, an interleukin-1-like cytokine that signals via the IL-1 receptor-related protein ST2 and induces T helper type 2-associated cytokines. *Immunity* 23:479-490.

Shibata, W., H. Ariyama, C.B. Westphalen, D.L. Worthley, S. Muthupalani, S. Asfaha, Z. Dubeykovskaya, M. Quante, J.G. Fox, and T.C. Wang. 2013. Stromal cell-derived factor-1 overexpression induces gastric dysplasia through expansion of stromal myofibroblasts and epithelial progenitors. *Gut* 62:192-200.

Shigematsu, Y., T. Niwa, E. Rehnberg, T. Toyoda, S. Yoshida, A. Mori, M. Wakabayashi, Y. Iwakura, M. Ichinose, Y.J. Kim, and T. Ushijima. 2013. Interleukin-1beta induced by Helicobacter pylori infection enhances mouse gastric carcinogenesis. *Cancer letters* 340:141-147.

Shinohara, M., M. Mao, T.M. Keeley, M. El-Zaatari, H.J. Lee, K.A. Eaton, L.C. Samuelson, J.L. Merchant, J.R. Goldenring, and A. Todisco. 2010. Bone morphogenetic protein signaling regulates gastric epithelial cell development and proliferation in mice. *Gastroenterology* 139:2050-2060 e2052.

Sica, A., and A. Mantovani. 2012. Macrophage plasticity and polarization: in vivo veritas. *J Clin Invest* 122:787-795.

Silva, M.T. 2010. When two is better than one: macrophages and neutrophils work in concert in innate immunity as complementary and cooperative partners of a myeloid phagocyte system. *Journal of leukocyte biology* 87:93-106.

Smith, S.G., A. Gugilla, M. Mukherjee, K. Merim, A. Irshad, W. Tang, T. Kinoshita, B. Watson, J.P. Oliveria, M. Comeau, P.M. O'Byrne, G.M. Gauvreau, and R. Sehmi. 2015. Thymic stromal lymphopoietin and IL-33 modulate migration of hematopoietic progenitor cells in patients with allergic asthma. *The Journal of allergy and clinical immunology* 135:1594-1602.

Smythies, L.E., K.B. Waites, J.R. Lindsey, P.R. Harris, P. Ghiara, and P.D. Smith. 2000. Helicobacter pylori-induced mucosal inflammation is Th1 mediated and exacerbated in IL-4, but not IFN-gamma, gene-deficient mice. *Journal of immunology* 165:1022-1029.

Solcia, E., G. Rindi, R. Fiocca, L. Villani, R. Buffa, L. Ambrosiani, and C. Capella. 1992. Distinct patterns of chronic gastritis associated with carcinoid and cancer and their role in tumorigenesis. *The Yale journal of biology and medicine* 65:793-804; discussion 827-799.

Sousa, J.F., A.J. Ham, C. Whitwell, K.T. Nam, H.J. Lee, H.K. Yang, W.H. Kim, B. Zhang, M. Li, B. LaFleur, D.C. Liebler, and J.R. Goldenring. 2012. Proteomic profiling of paraffin-embedded

samples identifies metaplasia-specific and early-stage gastric cancer biomarkers. *The American journal of pathology* 181:1560-1572.

Stoger, J.L., M.J. Gijbels, S. van der Velden, M. Manca, C.M. van der Loos, E.A. Biessen, M.J. Daemen, E. Lutgens, and M.P. de Winther. 2012. Distribution of macrophage polarization markers in human atherosclerosis. *Atherosclerosis* 225:461-468.

Stolarski, B., M. Kurowska-Stolarska, P. Kewin, D. Xu, and F.Y. Liew. 2010. IL-33 exacerbates eosinophil-mediated airway inflammation. *Journal of immunology* 185:3472-3480.

Suganami, T., J. Nishida, and Y. Ogawa. 2005. A paracrine loop between adipocytes and macrophages aggravates inflammatory changes: role of free fatty acids and tumor necrosis factor alpha. *Arteriosclerosis, thrombosis, and vascular biology* 25:2062-2068.

Syu, L.J., M. El-Zaatari, K.A. Eaton, Z. Liu, M. Tetarbe, T.M. Keeley, J. Pero, J. Ferris, D. Wilbert, A. Kaatz, X. Zheng, X. Qiao, M. Grachtchouk, D.L. Gumucio, J.L. Merchant, L.C. Samuelson, and A.A. Dlugosz. 2012. Transgenic expression of interferon-gamma in mouse stomach leads to inflammation, metaplasia, and dysplasia. *The American journal of pathology* 181:2114-2125.

Takabayashi, H., M. Shinohara, M. Mao, P. Phaosawasdi, M. El-Zaatari, M. Zhang, T. Ji, K.A. Eaton, D. Dang, J. Kao, and A. Todisco. 2014. Anti-inflammatory activity of bone morphogenetic protein signaling pathways in stomachs of mice. *Gastroenterology* 147:396-406 e397.

Tan, I.B., T. Ivanova, K.H. Lim, C.W. Ong, N. Deng, J. Lee, S.H. Tan, J. Wu, M.H. Lee, C.H. Ooi, S.Y. Rha, W.K. Wong, A. Boussioutas, K.G. Yeoh, J. So, W.P. Yong, A. Tsuburaya, H. Grabsch, H.C. Toh, S. Rozen, J.H. Cheong, S.H. Noh, W.K. Wan, J.A. Ajani, J.S. Lee, M.S. Tellez, and P. Tan. 2011. Intrinsic subtypes of gastric cancer, based on gene expression pattern, predict survival and respond differently to chemotherapy. *Gastroenterology* 141:476-485, 485 e471-411.

Tatematsu, M., T. Tsukamoto, and T. Toyoda. 2007. Effects of eradication of Helicobacter pylori on gastric carcinogenesis in experimental models. *J Gastroenterol* 42 Suppl 17:7-9.

Todisco, A., M. Mao, T.M. Keeley, W. Ye, L.C. Samuelson, and K.A. Eaton. 2015. Regulation of gastric epithelial cell homeostasis by gastrin and bone morphogenetic protein signaling. *Physiol Rep* 3:

Trapnell, C., L. Pachter, and S.L. Salzberg. 2009. TopHat: discovering splice junctions with RNA-Seq. *Bioinformatics* 25:1105-1111.

Tu, S., G. Bhagat, G. Cui, S. Takaishi, E.A. Kurt-Jones, B. Rickman, K.S. Betz, M. Penz-Oesterreicher, O. Bjorkdahl, J.G. Fox, and T.C. Wang. 2008. Overexpression of interleukin-1beta induces gastric inflammation and cancer and mobilizes myeloid-derived suppressor cells in mice. *Cancer cell* 14:408-419.

Tu, S.P., M. Quante, G. Bhagat, S. Takaishi, G. Cui, X.D. Yang, S. Muthuplani, W. Shibata, J.G. Fox, D.M. Pritchard, and T.C. Wang. 2011. IFN-gamma inhibits gastric carcinogenesis by inducing epithelial cell autophagy and T-cell apoptosis. *Cancer research* 71:4247-4259.

van Amerongen, M.J., M.C. Harmsen, N. van Rooijen, A.H. Petersen, and M.J. van Luyn. 2007. Macrophage depletion impairs wound healing and increases left ventricular remodeling after myocardial injury in mice. *The American journal of pathology* 170:818-829.

Varon, C., P. Dubus, F. Mazurier, C. Asencio, L. Chambonnier, J. Ferrand, A. Giese, N. Senant-Dugot, M. Carlotti, and F. Megraud. 2012. Helicobacter pylori infection recruits bone marrow-derived cells that participate in gastric preneoplasia in mice. *Gastroenterology* 142:281-291.

Verreck, F.A., T. de Boer, D.M. Langenberg, L. van der Zanden, and T.H. Ottenhoff. 2006. Phenotypic and functional profiling of human proinflammatory type-1 and anti-inflammatory type-2 macrophages in response to microbial antigens and IFN-gamma- and CD40L-mediated costimulation. *Journal of leukocyte biology* 79:285-293.

von Moltke, J., M. Ji, H.E. Liang, and R.M. Locksley. 2015. Tuft-cell-derived IL-25 regulates an intestinal ILC2-epithelial response circuit. *Nature*

Wada, T., T. Ishimoto, R. Seishima, K. Tsuchihashi, M. Yoshikawa, H. Oshima, M. Oshima, T. Masuko, N.A. Wright, S. Furuhashi, K. Hirashima, H. Baba, Y. Kitagawa, H. Saya, and O. Nagano. 2013. Functional role of CD44v-xCT system in the development of spasmolytic polypeptide-expressing metaplasia. *Cancer science* 104:1323-1329.

Wang, T.C., C.A. Dangler, D. Chen, J.R. Goldenring, T. Koh, R. Raychowdhury, R.J. Coffey, S. Ito, A. Varro, G.J. Dockray, and J.G. Fox. 2000a. Synergistic interaction between hypergastrinemia and Helicobacter infection in a mouse model of gastric cancer. *Gastroenterology* 118:36-47.

Wang, T.C., C.A. Dangler, D. Chen, J.R. Goldenring, T. Koh, R. Raychowdhury, R.J. Coffey, S. Ito, A. Varro, G.J. Dockray, and J.G. Fox. 2000b. Synergistic interaction between hypergastrinemia and Helicobacter infection in a mouse model of gastric cancer. *Gastroenterology* 118:36-47.

Wang, T.C., J.R. Goldenring, C. Dangler, S. Ito, A. Mueller, W.K. Jeon, T.J. Koh, and J.G. Fox. 1998. Mice lacking secretory phospholipase A2 show altered apoptosis and differentiation with Helicobacter felis infection. *Gastroenterology.* 114:675-689.

Watanabe, H., K. Numata, T. Ito, K. Takagi, and A. Matsukawa. 2004. Innate immune response in Th1- and Th2-dominant mouse strains. *Shock* 22:460-466.

Wei, D., W. Gong, M. Kanai, C. Schlunk, L. Wang, J.C. Yao, T.T. Wu, S. Huang, and K. Xie. 2005. Drastic down-regulation of Kruppel-like factor 4 expression is critical in human gastric cancer development and progression. *Cancer Res* 65:2746-2754.

Weis, V.G., C.P. Petersen, J.C. Mills, P.L. Tuma, R.H. Whitehead, and J.R. Goldenring. 2014. Establishment of novel in vitro mouse chief cell and SPEM cultures identifies MAL2 as a marker of metaplasia in the stomach. *AMer. J. Physiol.: GI & Liver Physiol.* Revised submission under review.:

Weis, V.G., J.F. Sousa, B.J. Lafleur, K.T. Nam, J.A. Weis, P.E. Finke, N.A. Ameen, J.G. Fox, and J.R. Goldenring. 2012. Heterogeneity in mouse spasmolytic polypeptide-expressing metaplasia lineages identifies markers of metaplastic progression. *Gut*

Weis, V.G., J.F. Sousa, B.J. LaFleur, K.T. Nam, J.A. Weis, P.E. Finke, N.A. Ameen, J.G. Fox, and J.R. Goldenring. 2013a. Heterogeneity in mouse spasmolytic polypeptide-expressing metaplasia lineages identifies markers of metaplastic progression. *Gut* 62:1270-1279.

Weis, V.G., J.F. Sousa, B.J. LaFleur, K.T. Nam, J.A. Weis, P.E. Finke, N.A. Ameen, J.G. Fox, and J.R. Goldenring. 2013b. Heterogeneity in mouse SPEM lineages identifies markers of metaplastic progression. *Gut* 62:1270-1279.

Wills-Karp, M., R. Rani, K. Dienger, I. Lewkowich, J.G. Fox, C. Perkins, L. Lewis, F.D. Finkelman, D.E. Smith, P.J. Bryce, E.A. Kurt-Jones, T.C. Wang, U. Sivaprasad, G.K. Hershey, and D.R. Herbert. 2012. Trefoil factor 2 rapidly induces interleukin 33 to promote type 2 immunity during allergic asthma and hookworm infection. *The Journal of experimental medicine* 209:607-622.

Wright, N.A., C. Pike, and G. Elia. 1990. Induction of a novel epidermal growth factor-secreting cell lineage by mucosal ulceration in human gastrointestinal stem cells. *Nature.* 343:82-85.

Wroblewski, L.E., R.M. Peek, Jr., and K.T. Wilson. 2010. Helicobacter pylori and gastric cancer: factors that modulate disease risk. *Clinical microbiology reviews* 23:713-739.

Yamaguchi, H., J.R. Goldenring, Kaminishi.M., and J.R. Lee. 2001. Identification of spasmolytic polypeptide expressing metaplasia (SPEM) in remnant gastric cancer and surveillance postgastrectomy biopsies. *Dig.Dis.Sci.* 47:573-578.

Yoshizawa, N., Y. Takenaka, H. Yamaguchi, T. Tetsuya, H. Tanaka, M. Tatematsu, S. Nomura, J.R. Goldenring, and M. Kaminishi. 2007. Emergence of spasmolytic polypeptide-expressing metaplasia in Mongolian gerbils infected with Helicobacter pylori. *Laboratory investigation; a journal of technical methods and pathology* 87:1265-1276.

Zaynagetdinov, R., T.P. Sherrill, V.V. Polosukhin, W. Han, J.A. Ausborn, A.G. McLoed, F.B. McMahon, L.A. Gleaves, A.L. Degryse, G.T. Stathopoulos, F.E. Yull, and T.S. Blackwell. 2011. A critical role for macrophages in promotion of urethane-induced lung carcinogenesis. *Journal of immunology* 187:5703-5711.

Zhu, Y., J.A. Richardson, L.F. Parada, and J.M. Graff. 1998. Smad3 mutant mice develop metastatic colorectal cancer. *Cell* 94:703-714.